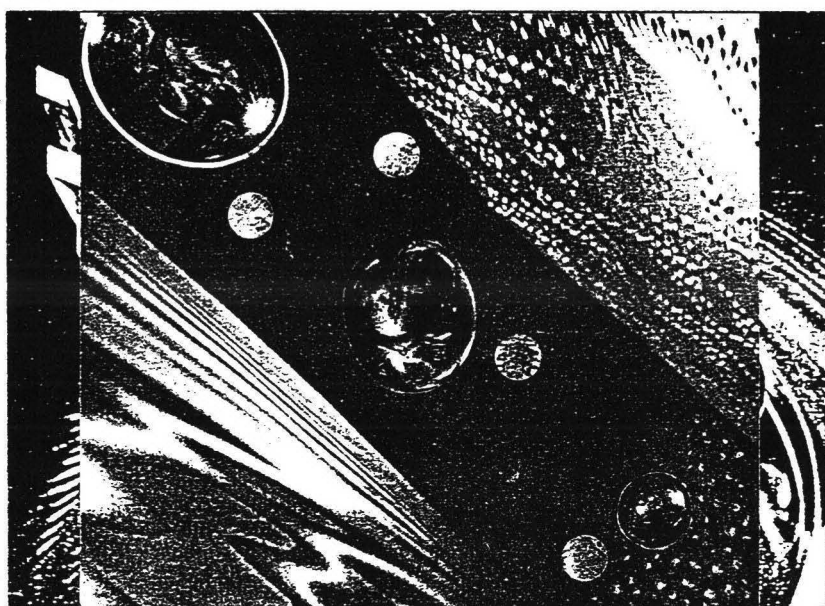




第2回年次総会・学術シンポジウム

講演要旨集



1990. 12. 13 - 14 川崎市 KSP

日 本 M R S
The Materials Research Society of Japan

協賛 財団法人神奈川科学技術アカデミー



第2回年次総会・学術シンポジウム 講演要旨集

- ・このシンポジウムは、（財）神奈川科学技術アカデミーの平成2年度学協会等研究集会助成金をうけております。
- ・また、第3シンポジウムは、（社）ニューガラスフォーラムと共催です。

本要旨集の内容の一部あるいは全部を無断で複製すると著作権および出版権侵害となることがありますのでご注意ください。

日 本 M R S
The Materials Research Society of Japan

先進材料科学・技術研究会より改称
[Advanced Materials Science and Engineering Society]

事務局 川崎市高津区坂戸100-1 西304 〒213
株式会社ケイエスピー内
TEL. 044(819)2001 FAX. 044(819)2009

日 本 M R S
第2回年次総会・学術シンポジウム

MRS-Japan
The 2nd Annual Meeting and Symposia

< 日 時 > 1990年12月13日(木)、14日(金) 10:00 ~
December 13(Thur.)、14(Fri.) 10:00 ~

< 場 所 > 川崎市高津区かながわサイエンスパーク
西棟3F・KSPホール/ギャラリー, 7F・701/708/709
West 3F・KSP Hall/Gallery, 7F・701/708/709
Kanagawa Science Park, Kawasaki City

内 容	12月13日(木)	12月14日(金)
年次総会 Annual Meeting	3F・KSPホール(曙) 13:00-13:30 総会 Annual Meeting 13:30-15:00 記念講演 Lecture	
シンポジウム Symposia 第1シンポジウム 先進材料 Advanced Materials	3F・KSPホール(曙) 10:00-11:30 講演 Lecture 15:30-17:30 " "	7F・708 10:00-16:40 講演 Lecture
第2シンポジウム センサー材料 Sensor Materials	3F・KSPホール(光) 10:00-12:00 講演 Lecture 15:20-17:30 " "	7F・709 10:20-17:30 講演 Lecture
第3シンポジウム シリカ系非晶質材料の 不完全構造 Structural Imperfections in SiO ₂ -Based Amorphous Materials	7F・701 10:00-17:20 講演 Lecture	7F・701 9:40-17:50 講演 Lecture
「ポスター」による研究 成果発表 Poster Session	3F・ギャラリー 10:00-19:00 展示 Exhibition 7F・708 10:30-13:00 口頭発表 Oral 15:30-16:30 Presentation	3F・ギャラリー 10:00-15:00 展示 Exhibition
先進材料・製品の解説紹介 Exhibition	3F・ギャラリー 10:00-19:00 展示 Exhibition	3F・ギャラリー 10:00-19:00 展示 Exhibition
懇親会 Party	3F・ギャラリー 17:30-19:00 懇親会 Party 「ポスター」表彰 Awards	

記 念 講 演

日時 1990年12月13日 (木) 13:30～15:00
場所 かながわサイエンスパーク 西3F KSPホール (曙)

- (1) ウラン濃縮技術と材料の進歩
 武田邦彦 (旭化成工業)
- (2) 有機非線型光学材料研究における最近の進展
 中西八郎 (工業技術院繊維高分子材料研究所)

- (1) Uranium Enrichment Technology and the Progress of its Materials
 Kennichi Takeda
 (Uranium Enrichment Laboratory
 Asahi Chemical Industry Co., Ltd.)
- (2) Recent Progress in Organic Materials for Nonlinear Optics (in Japan)
 Hachiro Nakanishi
 (Research Institute for Polymers and Textiles)

Uranium Enrichment Technology and the Progress of its Materials

Kunihiko Takeda

Uranium Enrichment Laboratory
Asahi Chemical Industry Co., Ltd.
1-1 Takeshima, Hyuga, Miyazaki 883

In this anniversary lecture, an overview of the materials used in uranium enrichment equipment is given, as well as, the present status of the chemical method, which has been developed by Asahi Chemical as Japan's own contribution to uranium enrichment technology.

Uranium enrichment itself is the operation that enriches uranium-235 isotope to a state higher than found in nature, and is one of the most difficult of all the separation technologies. At present there are several methods of uranium enrichment which are either in use or development. Gaseous diffusion and gas centrifuge are being used in plants under operation. Nozzle process, chemical, atomic vapor laser and others are either in development. Since each enrichment method is based on quite a different separation principle, the methods needed in equipment construction are extremely diverse. Furthermore, in technology requiring high performance, equipment material must exist in and around exceedingly harsh environments.

In the case of gaseous diffusion, the barrier material requires not only pore diameters of less than 30nm, but also uniformly in pore size, as well as, a material which is stable and chemically inert to corrosive UF_6 . The gas centrifuge method requires a high tensile material with acceptable resistance to UF_6 corrosion. The nozzle process calls for the installation of elaborate equipment on the micron-order. The chemical method demands adsorbent and materials which are anti-corrosive in hydrochloric acid at high temperature. In the atomic vapor laser process, the equipment is subjected temperatures of nearly 3000 °C.

Each of these methods uses materials radically diverse to each other yet common in the characteristic of high stability in difficult environments.

Recent progress in organic materials for nonlinear optics (in Japan)

Hachiro NAKANISHI

Research Institute for Polymers and Textiles

1-1-4 Higashi, Tsukuba 305, Japan

Brief introduction to the Japanese activities in the field of organic and polymeric nonlinear optical materials will be given under comparison with world-wide activities, followed by the somewhat detailed description about our preparative studies.

More than fifty groups from universities, governmental institutes, and industries have already made any presentations at the academic meetings of this field. A lot of efforts have been paid for the survey of 2nd order organic crystals with both large d_{11} and transparency to blue light. By use of such crystals in a cored-fibre configuration, frequency-doubling of semiconductor-laser to a blue laser is coming close to the real application. Several interesting phase-matchable crystals as well have been found and their performance upon frequency-doubling and wave-mixing has been investigated, partly in combination with semiconductor lasers. Noteworthy progress has been brought in the polar-structured LB films as well. On the contrary, so-far less results have been presented on poled-polymers. As for third-order materials, studies are in more academic stage and less efforts have been made around conjugated polymers, chromophore-containing polymers, dye-stuffs and so on. Remarkable contributions have been made also from the theoretical and analytical sides.

Aiming at the enlarged $\chi^{(3)}$, we have been synthesizing a lot of new polydiacetylenes on the basis of crystal engineering technique to have aromatic- or acetylene-substituted diacetylene monomers crystallized in a solid-state polymerizable stack. Ionic dye - polymer ion composites and phthalocyanines have also been studied to have fundamental understanding on structure - $\chi^{(3)}$ relationship. p-Toluenesulfonate complexes of cationic dyes gave a lot of noncentrosymmetric crystals, including those with d_{11} greater than that of MNA. Representative data of these studies will be presented.

「ポスター」による研究発表

Poster Session

テーマ 先進材料 (Advanced Materials) に関する研究

区分 A. 先進材料 (B, Cを除く)

B. センサー材料

C. 非品質シリカ

展示/Exhibition

日時 1990年12月13日 (木) 10:00～19:00

12月14日 (金) 10:00～17:00

場所 かながわサイエンスパーク 西3F ギャラリー

口頭発表/Oral Presentation

日時 1990年12月13日 (木) 10:30～13:00

15:30～16:30

場所 かながわサイエンスパーク 西7F 708

発表は、A,B,C 各区分合同で、学士課程・修士課程・博士課程・
一般のグループに分け、それぞれ発表者のアルファベット順に
行なう予定です。

表彰/Awards

日時 1990年12月13日 (木) 17:30～

場所 かながわサイエンスパーク 西3F ギャラリー

「ポスター」による研究発表(1) 学士課程

No.	テーマ Theme	発表者・所属 Name
B-1 C	Analysis of Bonding State in Pure Silica Glass from Paramagnetic Defects Induced by Mechanical Fracture	○道口信行 外 早稲田大 ○ N. Dohguchi, S. Munekuni, M. Kitagawa, H. Nishikawa, K. Nagasawa*, Y. Ohki, Y. Hama Waseda Univ., * Shonan Institute of Technology
B-2 A	Hydrogels with High Water Content	○笠原章玄、星道昭、吉田泰彦、 山下忠孝 東洋大学 ○ F. Kasahara, M. Hoshi, Y. Yoshida, T. Yamashita Toyo Univ.
B-3 A	アルミナ粉体の振動ボールミル粉砕 Vibration Ball Milling of Al_2O_3 Powders	○菊池真哉、伴隆幸、岡田清、 大津賀望 東京工大 ○ S. Kikuchi, T. Ban, K. Okada, N. Otsuka, T. Hayashi* Tokyo Inst. of Technology * Nish-Tokyo Univ.
B-4 B	パセリの種子を用いたアミノ酸センサー Amid Acid and Urea Sensors Using Parsley Seeds as Catalytic Material	○牧野哲也 外 神奈川大 ○ T. Makino, K. Kobayakawa, Y. Sato Kanagawa Univ.
B-5 A	反応焼結による微構造制御アパタイト複合 体の作製 Preparation of Microstructure-Controlled Apatite Composite by Reaction Sintering	○村上猛、伊熊泰郎、井奥洪二、 吉村昌弘 神奈川工科大 ○ T. Murakami, Y. Ikuma, K. Ioku*, M. Yoshimura** Kanagawa Inst. of Tech., * Kochi Univ., ** Tokyo Inst. of Tech.

No.	テーマ Theme	発表者・所属 Name
B-6 A	フッ素原子を含む縮合系芳香族高分子の合成とそれらの特性 Preparation and Characterization of Fluorine-Containing Aromatic Condensation Polymers	○酒井大介 外 神奈川大 ○ D. Sakai, Y. Saegusa, M. Kuriki, S. Nakamura Kanagawa Univ.
B-7 A	圧電複合材料を用いた機械的ダンパー Mechanical Damper Using Piezo. electric Composites	○鈴木洋二 外 上智大 ○ Y. Suzuki, K. Uchino, H. Gouda*, M. Fumita* Sophia Univ. * Tokyo Inst. of Technology
B-8 B	光ファイバーを用いた温度センサー Studies on the Development of an Optical Fiber Sensor for Thermochemical Analysis	○富岡祥子、角田文、金子明子、藤江忠男、高井信治*、平井利志*、内山秀文*、福井康裕**、佐久間一郎**、長岡昭二***、田口一宏*** 共立薬大、*東大生研、**東京電機大、***東レ ○ Y. Tomioka, A. Tsunoda, N. Takai*, H. Hirai*, I. Sakuma**, Y. Fukui**, A. Kaneko, T. Fujie, S. Nagaoka***, K. Taguchi*** Kyoritsu College of Pharmacy, *Univ. of Tokyo, ** Tokyo Denki Univ., *** Toray Co.
B-9 B	光ファイバーを用いた免疫センサー Immunological detection system by using optical fiber sensor	○角田文、富岡祥子、金子明子、藤江忠男、高井信治*、内山秀文*、福井康裕**、佐久間一郎**、長岡昭二***、田口一宏***、平井利志*、熊谷善博**** 共立薬大、*東大生研、**東京電機大、***東レ、****バイオマテリアル研究所 ○ A. Tsunoda, Y. Tomioka, A. Kaneko, T. Fujie, N. Takai*, H. Uchiyama*, Y. Fukui**, I. Sakuma**, S. Nagaoka***, K. Taguchi***, T. Hirai*, Y. Kumagai**** Kyoritsu College of Pharmacy, *Univ. of Tokyo, ** Tokyo Denki Univ., *** Toray Co., ****Biomaterial Research Inst.
B-10 A	チッ化けい素粉末中での炭化けい素ウiskerのIn-Situ合成とその複合焼結体 IN-SITU Preparation of Silicon Carbide Whiskers in Silicon Nitride Powder	○阿部秀明 外 東京工大 ○ H. Abe, S. Yamada*, E. Yasuda**, T. Iida, T. Kawasaki Tokai Univ. * NishTokyo Univ. ** Tokyo Inst. of Technology

「ポスター」による研究発表(2) 修士課程

No.	テーマ Theme	発表者・所属 Name
M-1 A	Cu基板上のFe超薄膜の成長課程 Process of Epitaxial Growth of Fe Ultr Thin Film on Cu Substrate	○土井一英 外 名古屋大 ○ K. Doi, S. Mitani, H. Toyoda, M. Matsui, M. Doyama* Nagoya Univ. * Nishi-Tokyo Univ.
M-2 A	New Conducting Polymer Composites	○韓峻熙 外 東京農工大 ○ J.H. Han, T. Motobe, Y.E. Whang, S. Miyata Tokyo Univ. of Agriculture and Technology
M-3 A	Low Temperature Growth of β -SiC Films on Si Substrate by Direct Carbonization Method	○平野恭章 法政大 ○ Y. Hirano Hosei Univ.
M-4 B	Molecular Recognition through Selective Intermolecular Hydrogen Bonding for a New Functional Liquid Crystalline System	○広田憲史 外 東京大 ○ N. Hirota, T. Kato, A. Fujisha, J.M.J. Frechet* Univ. of Tokyo, * Cornell Univ.
M-5 A	Structures and Mechanical Properties of Squeeze Cast SiCw Reinforced Al-Li Metal Matrix Composites	○洪性吉 東京工大 ○ Tokyo Inst. of Technology
M-6 A	ダイヤモンド-Co系粉末の超高压焼結 High Pressure Sintering of Diamond-Cobalt System	○飯塚誠 外 東京工大 ○H. Iizuka, H. Hirai Tokyo Inst. of Technology
M-7 A	$\text{YBa}_2\text{Cu}_4\text{O}_{8-x}$ の合成と物性 Synthesis and properties of $\text{YBa}_2\text{Cu}_4\text{O}_{8-x}$	○岩間宏 外 東京工大 ○ H. Iwama, N. Ohashi, H. Ikawa, O. Fukunaga Tokyo Inst. of Technology
M-8 A	Rapid Thermal Annealing for High-Energy Ion-Implanted Si	○岩崎広之 法政大学 ○H. Iwasaki Hosei Univ.

No.	テーマ Theme	発表者・所属 Name
M-9 A	側鏡に増感基と基質結合基を有する複合機能型高分子増感剤を用いたノルボルナジエン誘導体の光原子価異性化反応 Photochemical Valence Isomerization of Norbornadiene Derivative Using Multifunctional Polymeric Photosensitizers	○川島辰雄 外 神奈川大 ○T. Kawashima, K. Inomata, T. Nishubo Kanagawa Univ.
M-10 A	Precursor of the 74 Gauss Doublet in a-SiO ₂	○喜多川学 外 早稲田大 ○M. Kitagawa, S. Munekuni, H. Nishikawa, K. Nagasawa*, Y. Ohki, Y. Hama Waseda Univ. * Shonan Inst. of Technology
M-11 A	エレクトロクロミックな銅酸化物薄膜の電解析出 Electrochromic Copper Oxide Film by Electrodeposition	○小嶋健 外 東京都立大 ○T. Kojima, T. Yoshio, N. Baba Tokyo Metropolitan Univ.
M-12 A	A New Fabrication Technique for Oxide/Metal Composites by Controlled Directed Oxidation	○小久保信作 東京工大 ○ S. Kokubo Tokyo Inst. of Technology
M-13 A	New Microporous Glass-Ceramics Composed of CaTi ₄ (PO ₄) ₆ Skeleton and Their Application to Carriers for Immobilization of Enzymes	○前浪洋輝 外 名古屋工大 ○H. Maenami, T. Naruse, H. Hosono, Y. Abe, T. Suzuki*, M. Toriyama Nagoya Inst. of Technology, * Government Industrial Research Inst.
M-14 A	ゾルーゲル法によって生成したアルミナを誘電体に用いた分散型ACEL素子の作成 Preparation of Powder ACEL Device Using Alumina Dielectrics Formed by Sol-Gel Method	○森正澄 外 東京都立大学 ○M. Mori, T. Yoshino, S. Norisaki, N. Baba Tokyo Metropolitan Univ.
M-15 A	9Al ₂ O ₃ ・2B ₂ O ₃ ウイスキーカーへの加熱分解反応と複合体の試作 Thermal Decomposition of 9Al ₂ O ₃ ・2B ₂ O ₃ Whiskers into Al ₂ O ₃ Whiskers and Preparation of its Composites	○武藤晴文、岡田清、大津賀望、矢野豊彦 東京工大 ○H. Mutoh, K. Okada, N. Otsuka, T. Yano Tokyo Inst. of Technology

No.	テーマ Theme	発表者・所属 Name
M-16 A	$\text{Fe}_{73.5}\text{Cu}_1\text{Nb}_3\text{Si}_{13.5}\text{B}_9$ の超微細析出磁性相のメスbauer効果 Mossbauer Effect of Magnetic Phases with Ultra Fine Structure of $\text{Fe}_{73.5}\text{Cu}_1\text{Nb}_3\text{Si}_{13.5}\text{B}_9$	○中林久直 外 名古屋大 ○H. Nakabayash M. Doi, M. Matsui, Y. Yoshizawa*, K. Yamaguchi Nagoya Univ., * Hitachi Metals Ltd.
M-17 B	Saccharide Recognition of Ultrafine Platinum Particle-Modified Concanavalin A	○中川聡 外 東京大 ○ S. Nakagawa, N. Toshima, Y. Saito Univ. of Tokyo
M-18 C	Photon Energy Dependence of Defect Photogeneration in a - SiO_2	○中村龍太 外 早稲田大 ○ R. Nakamura, H. Nishikawa, K. Nagasawa*, Y. Hoki, Y. Hama Waseda Univ. * Shonan Inst. of Technology
M-19 A	電気化学法に寄るバリウムフェレート(BaFeO_4)薄膜の作製 Preparation of Barium Ferrate (BaFeO_4) fioms by Electrochemical Method	○中津雅治、柳承乙、石沢伸夫、吉村昌弘 東京工大 ○M. Nakatsu, S.E. Yoo, N. Ishizawa, M. Yoshimura Tokyo Inst. of Technology
M-20 A	Strong Photoluminescence from Si Fine Particles	○折原豊 外 電気通信大 ○Y. Orihara, H. Gomyoh, F.W. Ping Univ. of Electro-Communications
M-21 A	2-フェニル-1,3,4-オキサジアゾリン-S-オンのアニオン開環重合による新規な1-ナイロンの合成とその性質 Preparation and Characterization of Novel 1-Nylon by Anionic Ring-Opoening Polymerization of Z-Phenyl-1,3,4-Oxadiazolin-5-One	○尾関康宏 神奈川大学 ○Y. Ozeki, Y. Saegusa, S. Nakamura Kanagawa Univ.
M-22 A	肝細胞特異性材料の設計とDDSへの応用 Design of Polymeric Micelle Recognizable by Hepatic Perenchymal Cells and its Application to Drug Delivery System (DDS)	○斉藤和宏 東京工大/神奈川科学技術アカデミー ○K. Saito, M. Goto*, A. Kobayashi*, S. Tobe*, K. Kobayashi**, T. Akaike Tokyo Inst. of Technology, * Kanagawa Academy of Science and Technology, ** Nagoya Univ.

No.	テーマ Theme	発表者・所属 Name
M-23 A	不斉中心にトリフルオロメチル基をもつ強誘電性液晶の合成とその物性評価 Synthesis and Properties of the Ferroelectric Liquid Crystals with a Trifluoromethyl group at the Asymmetric Center	○境川亮 外 埼玉大 ○A. Sakaigawa, H. Nohira Saitama Univ.
M-24 A	亀裂や切欠きを有するFRP平板の破壊力学 The Fracture Mechanics of FRP Plate with Cracks and Notches	○佐藤和彦 外 東海大学 ○ K. Sato, Y. Yasni, S. Narasethaspon*, H. Kasuga Tokai Univ., * KMITL
M-25 A	Joining of Silicon Nitride with Copper Using Filler Alloys	○佐藤直治、岸本信也、金井正善 大阪大 ○N. Satoh, N. Iwamoto, M. Kanai Osaka Univ.
M-26 A	アルミナ／板状アルミナ混合粉体の成型性と焼結性 Formability and Sinterability of Alumina-Playty Alumina Mixed Powders	○高木保宏、岡田清、大津賀望、樽田誠一*、北島罔夫*、田草川信夫* 東京工大、*信州大 ○Y. Takagi, K. Okada, N. Otsuka, S. Taruda*, K. Kitajima*, N. Takasugawa Tokyo Inst. of Technology, * Shinshu Univ.
M-27 A	Fabrication and Evaluation of Natural Mullite/SiC Nanocomposites by Pressureless Reaction-sintering	○高田寛 大阪大学 ○H. Takada, K. Niihara Osaka Univ.
M-28 A	Susceptibility of Cobalt(II)-Alginate Complex Films to Moisture	○高橋圭 外 東京理科大 ○K. Takahashi, H. Yajima, T. Miyamoto, R. Endo, S. Furuya* Science Univ. of Tokyo, * Research Inst. for Polymers and Textile
M-29 A	ムライト ウィスカーの合成と評価 Synthesis and Characterization of Mullite Whiskers	○田中章裕、岡田清、大津賀望 東京工大 ○A. Tanaka, K. Okada, N. Otsuka Tokyo Inst. of Technology

No.	テーマ Theme	発表者・所属 Name
M-30 A	The Synthesis of High-purity Ceramics by Alkoxy-based Preparation	○谷田正道、岩本信也、金井正善 大阪大 ○M. Tanida, N. Iwamoto, M. Kanai Osaka Univ.
M-31 A	電子ビーム精練法を用いたTiの新製法 New Way to Produce Titanium by Electron Beam Remelting	○八幡稔文 東京大 ○T. Yahata Univ. of Tokyo
M-32 A	Ti-40% Al合金における α 相の分解 Decomposition of Alpha Phase in Titan Alloy	○山辺容子 外 東京工大 ○Y. Yamabe, M. Kikuchi Tokyo Inst. of Technology
M-33 A	Ta基板上へのLiTaO ₃ 薄膜の水熱反応 Hydrothermal Synthesis of LiTaO ₃ Thin Film on Substrate	○山口英將、石沢伸夫、吉村昌弘 東京工大 ○H. Yamaguchi, N. Ishizawa, M. Yoshimura Tokyo Inst. of Technology
M-34 A	非中心対称構造構築のための新しい分子設計法；SHG用の Λ 型分子 New molecular design method for noncentrosymmetric crystal structure Lambda(Λ) shape molecules for frequency doubling	○山本弘信 外 東京農工大 ○H. Yamamoto, S. Katogi, T. Watanabe, H. Sato, S. Miyata, T. Hosomi* Tokyo Univ. of Agriculture and Technology, * Sumitomo Bakelite
M-35 A	気相法ダイヤモンド合成における基板の効果 Effect of the substrate on diamond synthesis in gas phase	○矢崎陽一 東京工大 ○Y. Yazaki, H. Hirai, H. Ikawa, O. Fukunaga Tokyo Inst. of Technology
* D-6 A M-36	Electrical Properties of ZrO ₂ -TiO ₂ -Y ₂ O ₃ System	○内藤均 東北大 ○H. Naito, H. Arashi Tohoku Univ.

「ポスター」による研究発表(3) 博士課程

No.	テーマ Theme	発表者・所属 Name
D-1 A	イオン打ち込みによるFe膜の磁気光学効果の増大 Enhancement of the Magneto-optical Rotation of Fe Films due to Ion implantation	○青柳淳 横浜国立大 ○ K. Aoyagi Yokohama National Univ.
D-2 A	Ag/Cu multilayered films prepared by different vapor deposition method	○狭間克樹 外 東京工大 ○K. Hazama, J. Kozaki, K. Hachiyama, O. Nitono Tokyo Inst. of Technology
D-3 A	フォトクロミック スピロベンゾチオピラン ポリマーの合成 Synthesis of New Photochromic Spirobenzothiopyran Polymers	○平野雅文 外 埼玉大 ○M. Hirano, A. Miyashita, H. Nohira Saitama Univ.
D-4 A	Y-TZPセラミックスにおける欠陥の評価および欠陥分布と強度特性との関係 Characterization of Defect and Relation between Defect Size Distribution and Fracture Strength in Y-TZP ceramics	○金鎮映 外 長岡技術科学大 ○J.Y. Kim, Z. Kato, N. Uchida, K. Uematsu, K. Saito Nagaoka Univ. of Technology
D-5 A	Difference in High Temperature Creep Behaviors Between As-Cast TiAl and Homogenized TiAl	○貝明会 外 東京工大 ○M. Koo, T. Matsuo, M. Kikuchi Tokyo Inst. of Technology
D-6 A * M-36	Electrical Properties of ZrO_2 - TiO_2 - Y_2O_3 System	○内藤均 東北大 ○H. Naito, H. Arashi Tohoku Univ.
D-7 A	Solid Solution Strengthening due to Chromium and Molybdenum in High Temperature Creep in an Austenitic Single Phase Alloy --Effect of Dislocation Substructure Formation	○中島要 外 東京工大 ○ K. Nakajima, T. Matsuo, M. Kikuchi Tokyo Inst. of Technology
D-8 A	Seを含むスピロピランの側鎖型逆フォトクロミックポリマーの合成 Synthesis of New Reverse - photo - chromic Spirobenzo - selenazolinobenzopyran Polymers	○中野真二 外 埼玉大 ○ S. Nakano, A. Miyashita, H. Nohira Saitama Univ.

No.	テーマ Theme	発表者・所属 Name
D-9 C	Chlorine - and Oxygen - Related Paramagnetic Centers in Vuv - Irradiated High - Purity Silicas	○西川宏之 早稲田大 ○H. ishikawa, R. Nakamura, K. Nagasawa*, Y. Oki, Y. Hama Waseda Univ. * Shonan Inst. of Technology
D-10 A	Morphological Evolution and Amorphization of Ti-Cu Powder Particles during Vibratory Ball Milling	○朴容浩 外 東北大 ○Y.H. Par, H. Hashimoto, R. Watanabe Tohoku Univ.
D-11 A	Deformation behavior in dispersion strengthened Al-8 mass% Fe Alloy at high temperatures	○桜井喜宣 東京工大 ○Y. Sakurai Tokyo Inst. of Technology
D-12 A	Super structure of Rare-Earth Tantalum oxides R_3TaO_7 (R=Ho, Y, Yb)	○田中大介 外 東京工大 ○T. Tanaka, Y. Tabira, N. Ishizawa, F. Marumo, N. Yoshimura Tokyo Inst. of Technology
D-13 B	固定化水銀還元酵素を用いた水銀センサー Mercuric Sensor with Immobilized Mercurit Reductase on Porous Glass	○宇屋基弘 外 東京大 ○M. Uo, M. Numata*, E. Tamiya, I. Karube, A. Makishima Univ. of Tokyo, * Dowa Mining Co., Ltd
D-14 A	A Theoretical Estimation of Ceramic Strength at High Temperatures	○曾健任 外 大阪大 ○J.R. Zeng, K. Nuhara Osaka Univ.

No.	テーマ Theme	発表者・所属 Name
S-1 A	共沈法によるウォラストナイト粉末の合成 Preparation of wollastonite powder by co-precipitation method	○林滋夫、岡田清、大津賀望 東京工大 ○ S. Hayashi, K. Okada, N. Otsuka Tokyo Inst. of Technology
S-2 A	接着基質材料設計による肝細胞の分化・脱分化の制御 Design and Evaluation of Materials for Controlling the Differentiation of Hepatocytes	○小林明 外 神奈川科学技術アカデミー ○O.A. Kobayash, Y. Takei, S. Tobe, M. Goto, T. Sekine*, A. Masumoto**, N. Yamamoto**, K. Kobayashi***, T. Akaike**** Kanagawa Academy of Science and Technology, * Tokyo Univ. of Agri. and Tech., ** Kitazato Univ. *** Nagoya Univ., **** Tokyo Inst. of Technology
S-3 A	Mn置換超磁歪合金とその応用 Mn-Substituted Giant Magnet-ostrictive RFe ₂ and Its Application	○小林忠彦 外 東芝総研 ○T. Kobayashi, T. Funayama, I. Sakai, M. SahashToshiba Corp.
S-4 A	Photoelectrochemical Information Recording Using the Newly-Found Hybrid Process of Azobenzene System	○劉忠範 外 東京大 ○Z.F. Liu, K. Hashimoto, A. Fujishma Univ. of Tokyo
S-5 A	Improvement of Mechanical Properties for Al ₂ O ₃ /SiC Nanocomposites	○中平敦 外 大阪大 ○A. Nakahira, K. Niihara Osaka Univ.
S-6 B >35	2,5-ジスチルピラジン誘導体のEL挙動 Electroluminescent Behavior of 2,5-Distyrylpyrazine Derivatives	○野原正雄 東京大 ○M. Nohara, M. Hasegawa, C. Hosokawa*, H. Tokailin*, T. Kusumoto* Univ. of Tokyo, * Idemitsu Kosan Co., Ltd.
S-7 A	ホウ化物複合セラミックスの機械的性質 Mechanical Properties and Micro-structure of Boride Based Composite Ceramics	○尾形知彦 外 東レ ○T. Ogata, H. Kuwajima Toray Industries Inc.

No.	テーマ Theme	発表者・所属 Name
S-8 A	β -シクロデキストリンによる分子認識機構 The Mechanism of molecular recognition by β -Cyclodextrin -- Application of molecular dynamics simulation to the design of molecular recognition materials	○岡崎秀美 外 ○H. Okazaki, T. Yamashita, T. Yasukawa, T. Akaike Kanagawa Academy of Science and Technology
S-9 A >35	窒素原子を含むセルロース誘導体の合成と重金属イオンの吸着挙動 Preparation of Nitrogen-Containing Cellulose Derivatives and their Adsorption Behavior of Heavy Metal Ions	○三枝康男 外 神奈川大学 ○Y. Saegusa, S. Nakamura, M. Amano Kanagawa Univ.
S-10 A	ZrO_2 発熱体の特性評価 Evaluation of the Zirconia Form as a Heating Element	○佐伯恒信 品川白煙瓦 ○T. Saeki Sinagawa Refractories Co., Ltd.
S-11 A	小型冷凍機用極低温蓄冷材R3T系化合物 The Properties of R3T Compounds as a Heat Regenerator Matrix Used in Small Size Helium Refrigerator	○東海陽一 外 東芝総研 ○Y. Tokai, M. SahashTosha Corp.
S-12 A	先端デバイス用エポキシ封止材 Epoxy Molding Compound for Advanced Semiconductor Devices -- Stress Reduction Technology with Silicone polymer	○土屋貴史 信越化学工業 ○T. Tsuchiya Shin-Etsu Chemical Co., Ltd.

ANALYSIS OF BONDING STATE IN PURE SILICA GLASS FROM
PARAMAGNETIC DEFECTS INDUCED BY MECHANICAL FRACTURE

Nobuyuki Dohguchi, Shuji Munekuni, Manabu Kitagawa,
Hiroyuki Nishikawa, Kaya Nagasawa*, Yoshimichi Ohki,
Yoshimasa Hama

Waseda University

3-4-1 Ohkubo, Shinjuku-ku, Tokyo, 169 Japan

*Shonan Institute of Technology

1-1-25 Tsujido-Nishi-kaigan, Fujisawa, Kanagawa 251, Japan

Due to the advancement in technology, production of α -SiO₂ that is virtually defect-free and stoichiometric is now possible. Therefore, most of the recent studies regarding α -SiO₂ and its physical properties are usually carried out by first creating defects, then analyzing and characterizing the induced defect. Some of the most commonly used method for defect creations are radiations such as gamma and X rays, UV and VUV photons, and diffusion of gases such as oxygen and hydrogen into the sample.

In the present study, defect formation is done by applying mechanical stress to, and fracturing the α -SiO₂ samples. Unlike radiation or UV photons, which selectively severs the weak unstable bonding states, mechanical fracturing is found to cut practically all bonds, even the normal Si-O bond in the glass network. Therefore, the induced paramagnetic defect reflects the chemical bonding state within the glass. From this, it can be stated that mechanical fracturing is a good technique for elucidating existing chemical bond and interstitials in the samples, and by comparing induced paramagnetic defect with the sample manufacturing method, impurity content, and pre-existing absorption band, defect formation mechanism and eventually insights into improvement in manufacturing method may be obtained.

Also, in the present report, the difference of induced paramagnetic centers between glass preform samples and those which have been drawn into optical fibers is compared. From the comparison, the effect of fiber drawing on chemical bonding within the glass is discussed. Finally, the existence of strained bond, or the unstable Si-O-Si bonding state is demonstrated.

Nobuyuki Dohguchi

Waseda University

Dept. of Electr. Eng., Ohki Laboratory

3-4-1 Ohkubo, Shinjuku-ku, Tokyo, 169 Japan

Tel:03-203-4141 ext. 73-3167

Fax:03-200-2567

Hydrogels with High Water Content

F. Kasahara*, M. Hoshi*, Y. Yoshida* and T. Yamashita*

Faculty of Engineering, Toyo University, Kawagoe, Saitama 350,

(1) The purpose of this study is to develop the advanced materials capable of using at the intraoperative examination of the real-time echocardiography. These advanced materials are expected to be used directly on the cardiac surface at operations as the contact surface material between the ultrasonic transducer surface and the cardiac surface. This examination can provide the useful information on the correct position and the degree of the cardiac lesion. We have reported that the hydrogels having the convenient elastic property and the excellent ultrasonic characteristics were useful as the soft contact surface material attached on the ultrasonic transducer. In this paper, we reports the preparation and the physical property of various hydrogels with the high water contents, which are prepared by γ -ray or electron beam irradiation.

(2) The hydrogels of the polyvinyl alcohol (PVA)/ polyvinylpyrrolidone (PVP)/ water solution were prepared by γ -ray or electron beam (EB) irradiation. The physical properties of hydrogels were measured by using the rheometer .

(3) Figs. 1 and 2 show the effects of the irradiation strength and the mixture ratios of PVA/PVP on the hardness of hydrogels of PVA/PVP (Water content : 95%) obtained by γ -ray and EB irradiation, respectively. The hardness of PVA/PVP hydrogel increased with the increase of the absorbed dose by γ -ray or EB irradiation. The hardness of the γ -ray irradiated hydrogel was larger than that of EB irradiated hydrogel. The γ -ray irradiation to PVA/PVP water solution was easy to form the elastic hydrogel, compared with EB irradiation. In the case of EB irradiated hydrogel, the mixture ratio of PVA/PVP in the hydrogel had no very effect on the hardness. The hardness of γ -ray irradiated hydrogel, however, varied with the ratio PVA/PVP in the hydrogel.

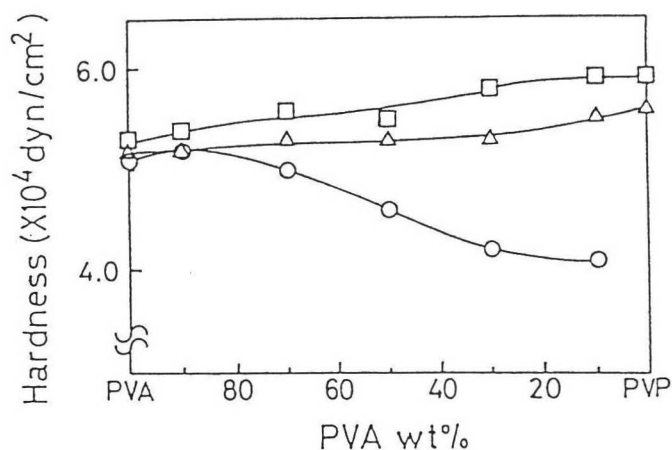
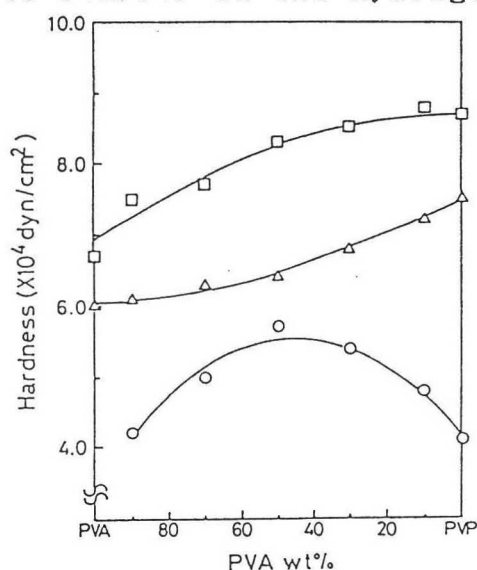


Fig.1. Hardness of PVA/PVP hydrogel obtained by γ -ray irradiation. (PVA: Mw 1.33×10^5 , PVP: Mw 3.6×10^5) (○ : 2 Mrad, △ : 3 Mrad □ : 5 Mrad)

Fig.2. Hardness of PVA/PVP hydrogel obtained by EB irradiation. (PVA: Mw 1.33×10^5 , PVP: Mw 3.6×10^5) (○ : 2 Mrad, △ : 3 Mrad □ : 5 Mrad)

Vibration Ball Milling of Al_2O_3 Powders

○ Shinya KIKUCHI, Takayuki BAN, Kiyoshi OKADA, Nozomu OTSUKA
 Department of Inorganic Materials, Tokyo Institute of Technology
 and Tsuyoshi HAYASHI
 The Nishi-Tokyo University

Three kinds of Al_2O_3 powders with the different preparation methods (Bayer and electrofused aluminas) and average particle sizes ($0.6\mu\text{m}$, $3.9\mu\text{m}$, and $22\mu\text{m}$) were ground by a dry and a wet vibration ball mill. Variation of particle size distribution, specific surface area, crystallite size, lattice strain, effective temperature factor and lattice deformation was measured against milling time up to 300 h. Various parameters were found to differ between the dry and the wet milling. An average particle size of the specimen ($3.9\mu\text{m}$) decreased only a little to $3.52\mu\text{m}$ after 300 h milling in the dry milling, in which size was even a little larger than that of the specimen ($22\mu\text{m}$), i.e., $3.39\mu\text{m}$. On the other hand, it dropped down largely to $1.35\mu\text{m}$ in the wet milling. The particle sizes of both the dry and wet milled specimens ($0.6\mu\text{m}$) decreased a little. The particle size change in the wet milled specimen saturated more quickly than that in the dry milled specimen. As shown in Fig. 1, the crystallite size of the specimen ($3.9\mu\text{m}$) in the wet milling decreased more rapidly than that in dry milling while the crystallite size of the specimen ($0.6\mu\text{m}$) in the wet and the dry milling showed opposite correlation. There observed a large difference in lattice strain for the dry and wet milled specimens as shown in Fig. 2. The lattice strain of the dry milled specimen ($0.6\mu\text{m}$) was very large but was small in the wet milled specimen. On the other hand, the lattice strain of the dry milled specimen ($3.9\mu\text{m}$) was much smaller than that of the wet milled specimen.

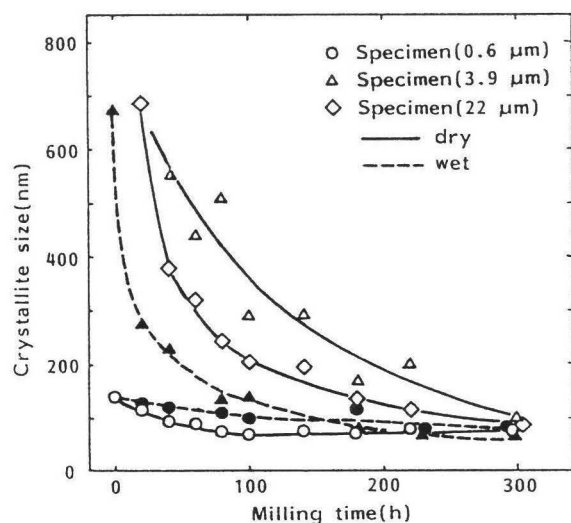


Fig. 1 Crystallite size vs milling time.

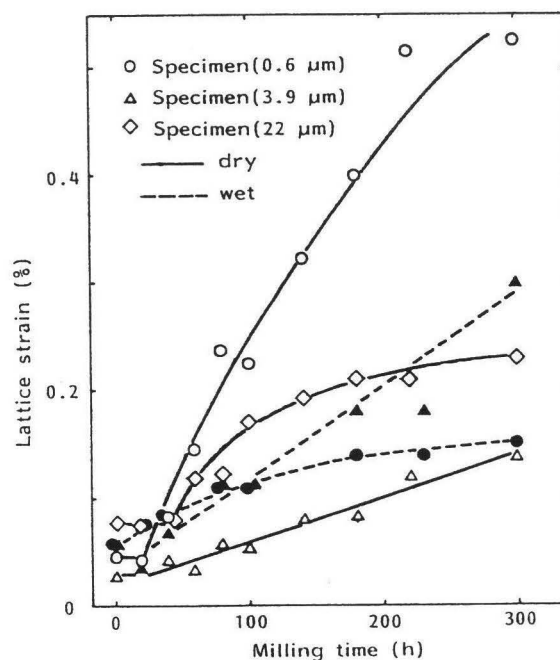


Fig. 2 Lattice strain vs milling time.

Amino Acid and Urea Sensors Using Parsley Seeds as Catalytic Material

°Tetsuya MAKINO, Koichi KOBAYAKAWA and Yuichi SATO

Department of Applied Chemistry, Faculty of Engineering,
Kanagawa University, Rokkakubashi, Kanagawa-ku, Yokohama 221

Introduction : Plant substances have been used as biocatalytic layers coupled with potentiometric or amperometric techniques. In this paper, we report the minced parsley(*Petroselinum Crispum*) seeds coupled with potentiometric ammonia gas sensing electrode show effective biocatalytic activity, i.e. selective deamination responses for certain amino acids and urea, and can be usable as biosensor for these substances.

Experimental : An Orion Model 95-10 ammonia gas electrode was used in the construction of the biosensors. Parsley minced seeds of 1~10mg were attached to the surface of ammonia electrode covered by dialysis membrane and set by O-ring. The parsley immobilized electrode was dipped in $0.1\text{mol}\cdot\text{dm}^{-3}$ Tris-HCl buffer solution. To find out the response on this electrode, various sorts of amino acid were added to buffer solution and the potential change due to NH_3 liberated from amino acid by the catalytic action of the enzyme contained in parsley was followed.

Results and Discussion : Figure 1 shows a typical example of calibration curve for L-asparagine with a slope of 51mV per decade in the 6×10^{-5} - $7\times 10^{-4}\text{mol}\cdot\text{dm}^{-3}$ range.

The activity of this electrode immediately after the immobilization of minced tissue was not so high, but it showed the highest value after a few times measuring and was kept for more than forty days. This parsley immobilized electrode also showed a good response at pH 7.4 for L-glutamine, L-serine, L-threonine and for urea. Though the selectivity of this electrode is not so good, it is usable as a biosensor for above substances. This simple technique also offers a very useful method for enzyme screening in plant substances.

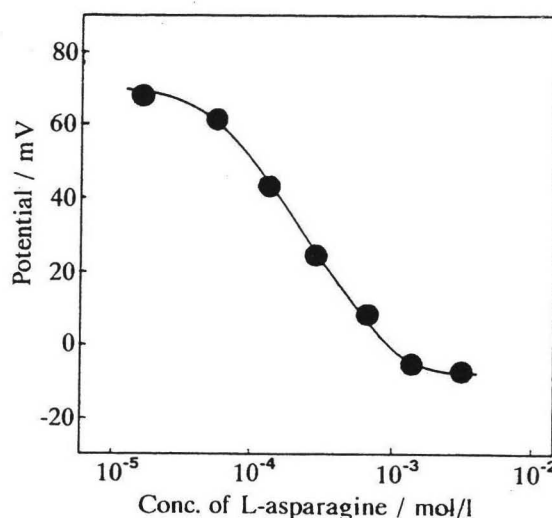


Fig. 1 Calibration curves for L-asparagine using 6.3mg immobilized minced parsley seeds electrode in 0.1M Tris-HCl buffer at pH 7.4, 30°C.

Preparation of Microstructure - Controlled Apatite Composite by Reaction Sintering

Takeshi MURAKAMI*, Yasuro IKUMA*, Koji IOKU,** and Masahiro Yoshimura***

* Kanagawa Institute of Technology

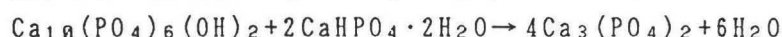
** Kochi University

*** Tokyo Institute of Technology

【Introduction】

Since Hydroxyapatite $\text{Ca}_{10}(\text{PO}_4)_6(\text{OH})_2$; (HAp) and Tricalcium phosphate $\text{Ca}_3(\text{PO}_4)_2$; (TCP) are excellent biocompatible ceramics, they have been used for artificial teeth and bone implant materials. Such bioceramics are said to require more than 70% porosity with larger pores than $200\mu\text{m}$ in size, because they must allow bone-bearing cells to enter and to fill up by new bones. Those ceramics, however, would be too weak to be used as the implants to load-bearing bones. To overcome these problems, microstructure-controlled ceramic composites which consist of HAp and TCP grains are designed. Since the latter dissolve twice faster than the former, it will give larger pores in vivo during the substitution by new bones.

The present study aims to prepare those composites by the reaction sintering from HAp and Brushite ($\text{CaHPO}_4 \cdot 2\text{H}_2\text{O}$) as follows:



【Experimental】

HAp and Brushite powders were mixed, pressed into pellets, and then sintered at 900°C for 3h. TG-DTA and TMA (Thermal Mechanical Analysis) were performed to study the reaction and thermal shrinkage of powder compacts. The sintered samples were examined by X-ray diffraction (XRD) and SEM.

【Results】

According to TG-DTA and XRD, the formation of β -TCP starts at about 800°C . A sintered compact with 46% porosity with the pores of $5\sim 10\mu\text{m}$ in diameter was obtained (Fig.1). The addition of Brushite enhanced the formation of TCP nonlinearly (Fig.2), and accelerate the sintering of HAp in this system.

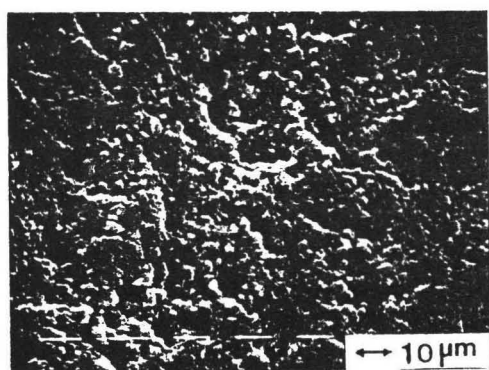


Fig.1 SEM photograph of the fracture surface of HAp-TCP composite.

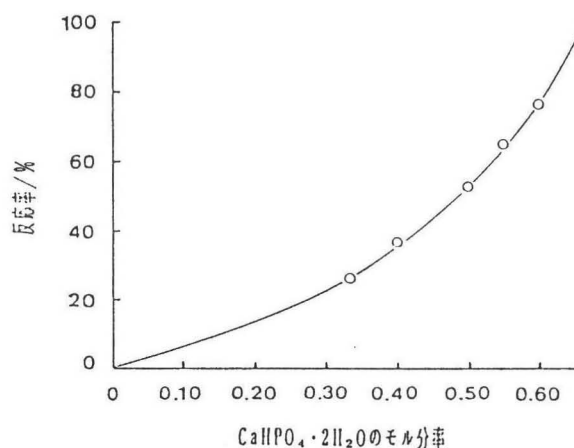


Fig.2 Relationship between mole fraction of Brushite and reaction rate.

PREPARATION AND CHARACTERIZATION OF
FLUORINE-CONTAINING AROMATIC CONDENSATION POLYMERS

Yasuo SAEGUSA, Minoru KURIKI, Daisuke SAKAI, and Shigeo NAKAMURA
Department of Applied Chemistry, Faculty of Engineering,
Kanagawa University, Kanagawa-ku, Yokohama 221, JAPAN

Recently, much interest has been focused on the synthesis of fluorine-containing polymers because of their unique properties and high performance. However, the studies on the preparation of fluorine-containing aromatic condensation polymers are rather few. The purpose of this investigation is therefore to synthesize a variety of novel fluorine-containing aromatic condensation polymers, polyketones (I), polybenzimidazoles (II), polybenzothiazoles (III), polyformal (IV), polycarbonate (V), polyazomethines (VI) and/or the respective copolymers, and to elucidate their properties with relation to the fluorine contents.

Polyketones and copolyketones, polybenzimidazoles and polybenzothiazoles were synthesized by the direct polycondensation of 2,2-bis(4-carboxyphenyl)-1,1,1,3,3,3-hexafluoropropane and/or 2,2-bis(4-carboxyphenyl)propane with diphenyl compounds, aromatic tetramines and bis-o-aminothiophenols, respectively, at elevated temperature above 80°C using polyphosphoric acid or Eaton reagent as condensing agent and solvent. Polyformal and copolyformals were synthesized by the solution polycondensation of 2,2-bis(4-hydroxyphenyl)-1,1,1,3,3,3-hexafluoropropane (BPAF) and/or 2,2-bis(4-hydroxyphenyl)propane (BPA) with dichloromethane at 75°C in NMP in the presence of potassium hydroxide. Polycarbonate and copolycarbonates were synthesized by the phase-transfer-catalyzed polycondensation of BPAF and/or BPA with trichloromethyl chloroformate at ambient temperature in the two-phase of aqueous sodium hydroxide and 1,2-dichloroethane using tetra-n-butylammonium bromide as catalyst. Polyazomethines and copolyazomethines were synthesized by the solution polycondensation of 2,2-bis[4-(4'-aminophenoxy)phenyl]- and 2,2-bis(4-aminophenyl)-1,1,1,3,3,3-hexafluoropropane and/or 2,2-bis[4-(4'-aminophenoxy)phenyl]- and 2,2-bis(4-aminophenyl)propane with aromatic dialdehydes mainly at room temperature in m-cresol.

Moderate- to high-molecular-weight fluorine-containing polymers with reduced viscosities up to in the order 0.37, 1.15, 1.55, 4.62, 0.54 and 0.41 dL/g were successfully obtained under the conditions. The yields of these polymers were mostly quantitative.

The most remarkable difference in properties was observed in solubility and mechanical and thermal behavior. Most of the fluorine-containing polymers, particularly homopolymers, were easily soluble in polar aprotic media and even in common organic solvents at room temperature, in which the homopolymers without fluorine were insoluble. Clear, tough and flexible films of the polymers, except polyketones, could be cast from their solutions. From the mechanical measurements of the films, the introduction of fluorine atom into the benzimidazole, carbonate and azomethine polymers was found to increase considerably the pliability of the films. In polymers I, IV and V, the differences in surface properties such as contact angle (θ) formed by water and/or critical surface tension (γ) and/or in optical properties such as refractive index (n) were also so clear. The θ , γ and n of BPAF-based homopolycarbonate were 91°, ca. 20 dyn/cm and 1.426, respectively, at 25°C, whereas BPA-based homopolycarbonate with no fluorine atom had the respective values of 84°, 42 dyn/cm and 1.585. Thermal stability of polymers I, V and VI was clearly improved by introducing fluorine atom and increased monotonously with the increase in fluorine content. Fluorine-containing ketone, benzimidazole, benzothiazole and azomethine (homo)polymers showed high thermal stability, the weight residue at 500°C in air all being more than 90%. The glass transition temperatures of the copolyformals decreased monotonically between those of the two homopolymers as BPAF component was increased, whereas those of the copolycarbonates increased.

Mechanical Damper Using Piezoelectric Composites

Y. SUZUKI and K. UCHINO, Department of Physics Sophia University, 7-1 Kioicho, Chiyoda-ku, Tokyo 102 and
H. GOUDA and M. SUMITA, Department of Textile and Polymeric Materials Tokyo Institute of Technology 2-12-1 Ookayama, Meguro-ku, Tokyo 152

A new mechanical damper using piezoelectric flexible composites is proposed in this paper.

The principle of the piezoelectric damper is converting the mechanical vibration energy to electrical energy, and this electrical energy is consumed to heat by resistance. When the piezoelectric material is vibrated by stress, electric charge is induced on the surface, and the vibration is sustained by this induced field. If this electrical energy is dissipated through an external resistance before this energy is transformed back into mechanical vibration energy through the piezoelectric effect again, it can be expected to have an effect on the damping. The previous paper¹⁾ reported that piezoelectric ceramics are applicable to a damper, but those have some problems in flexibility and durability.

We have newly investigated flexible mechanical dampers using piezoelectric composites. This damper consists of polymer containing piezoelectric ceramic powder and carbon black instead of an external resistance. (See Fig. 1) Piezoelectricity and conductivity can be controlled by volume fraction of ceramic powder and carbon black. Figure 2 shows the damping time constant τ change with fraction of carbon black x . Drastic decrease of τ is observed around $x=0.074$.

This type composite damper will be applicable to equipments mounted on a car or audios apparatus.

Reference

- 1) T.Ishi and K.Uchino : J.Jpn.Ceram.Soc. 96[8]863-67(1988)

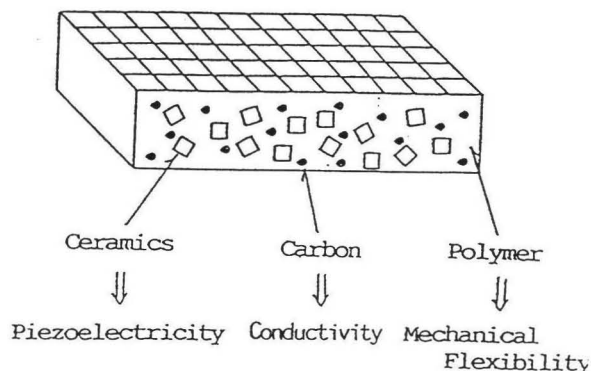


Fig.1 Piezo-ceramic : polymer : carbon composites for mechanical damper.

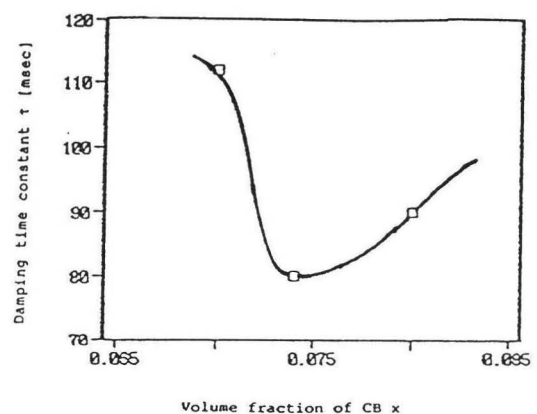
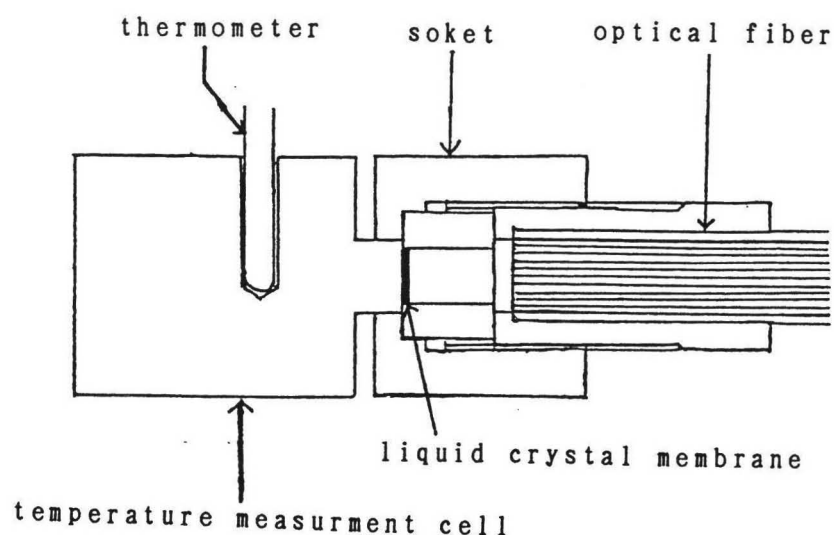


Fig.2 Damping time constant vs. volume fraction of CB.

STUDIES ON THE DEVELOPEMENT OF AN OPTICAL FIBER SENSOR FOR THERMOCHEMICAL ANALYSIS

Y.TOMIOKA(1), A.TSUNODA(1), N.TAKAI(2), T.HIRAI(2), I.SAKUMA(3),
Y.FUKUI(3), A.KANEKO(1), T.FUJIE(1), S.NAGAOKA(4), K.TAGUCHI(4)
(1) Kyoritsu College of Pharmacy (1-5-30, Shibakoen, Minato-ku,
Tokyo, 105 JAPAN)
(2) Inst. of Industrial Science , The Univ. of Tokyo (7-22-1, .
Roppongi, Minato-ku, Tokyo, 106 JAPAN)
(3) Dept. of Applied Electronics, Fac. of Science and Engineering,
Tokyo Denki Univ. (Ishizaka, Hatoyama-machi, Hiki-gun, Saitama,
350-03 JAPAN)
(4) TORAY Co. (2-2, Muromachi, Nihonbashi, Chuo-ku, Tokyo, 103
JAPAN)

For in vivo monitoring of various kinds of temperature in the human body, several kinds of themal sensors have been developed mainly using temperature detection system. In this study, we made a fundamental research for the development of themal sensors based on spectroscopic detection with liquid crystal membrane. The sensor system consists of an optical fiber, membrane of which spectroscopic characteristics change according to the temperature, and a spectrophotometer. By attaching the membrane at the tip of the optical fiber, we can measure the changes in its optical properties such as reflection spectra. The optical fiber and the spectrometer was connected with a specially prepared optical system and a xenon lamp was used as a light source.



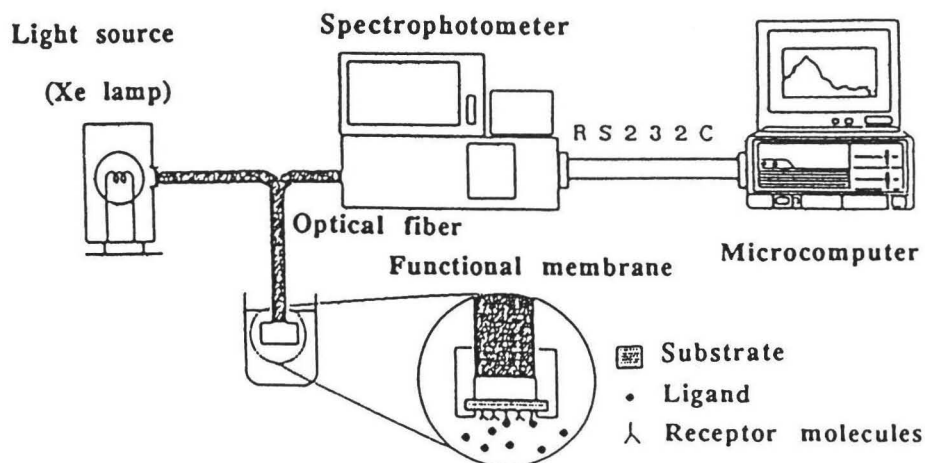
measurment of temperature system

Immunological detection system by using optical fiber sensor

Aya Tsunoda*, Yoshiko Tomioka*, Akiko Kaneko*, Tadao Fujie*, Nobuharu Takai**, Hidefumi Uchiyama**, Yasuhiro Fukui[‡], Ichiro Sakuma[‡], Shoji Nagaoka[‡], Kazuhiro Taguchi[‡], Toshiyuki Hirai**, and Yoshihiro Kumagai***
(Kyoritsu College of Pharmacy*, Institute of Industrial Science, University of Tokyo**, Tokyo Denki University[‡], Toray[‡], and Biomaterial Research Institute***)

The ligand-receptor interactions like antigen-antibody, enzyme-substrate, hormon-receptor etc., which have key roles in living bodies, are based on the specific recognition of counterpart molecules. The versatility of immunological recognition capacity of antibodies are used for many research and diagnostic purposes. Especially, the monoclonal antibodies are sensitive and useful probes to detect versatile target substances. The fixed monoclonal antibodies on the artificial membrane can be used as recognition elements of antigens by converting the antibody-antigen reaction to the detectable signals. This study has been aiming at the construction of antibody-utilized immune sensor by detecting the optically converted signals from antigen-antibody interaction.

The model system to assay the concentration of human serum albumin (HSA) was designed by setting the hardware as shown below. The actual sandwich detection of HSA was facilitated by using two monoclonal anti-HSA antibodies which recognize different epitopes each other. The quantity of HSA recognized by membrane bound antibodies was detected by biotin-coupled second monoclonal antibodies and peroxidase-labelled avidin, and finally converted to the enzyme/substrate reaction. This system enables us to detect the nanogram-quantity of HSA in the body fluid. The further improved system to measure the bound antigen directly is now underway.



IN-SITU PREPARATION OF SILICON CARBIDE WHISKERS IN SILICON NITRIDE POWDER

S. YAMADA (The Nishi Tokyo Univ.)

E. YASUDA, Y. TANABE (RLEM, Tokyo Inst. Tech.)

T. IIDA, T. KAWASAKI, H. ABE (Tokai Univ.)

A preliminary research work¹⁾ concerning in-situ preparation of silicon carbide whiskers (SiC-w) in silicon nitride powder (Si_3N_4 -p), suggested that the density of hot-pressed body derived from the mixture containing in-situ prepared SiC-w was improved; whereas the diameter of thus formed SiC-w were found to be thinner than of industrial product SiC-w, and the strength of the hot-pressed specimens was not superior to that of the physically mixed derivatives.

An approach was further made to improve the diameter, resulting in the thicker whiskers than that of the industrial²⁾. However, the procedure to get the thicker ones, needed the pressure, being higher than normal. It is not always convenient to apply to the continuous process in industry.

In this article, a new catalyzer, iron oxide powder, having a certain range of diameter, to obtain thicker SiC-w in-situ in Si_3N_4 -p under normal pressure was described. Efforts were made to improve the strength as well as fracture toughness, but the homogeneity of hot-pressed specimens was found not to be good enough yet to give the superiority to the physically mixed derivatives. As a result of the detailed observation of a physically mixed specimen, having shown the highest strength and toughness, its homogeneity was still superior to that of the in-situ prepared, i.e. chemically mixed ones. Details of the flexural strength and fracture toughness, determined by SENB-method, are presented, in comparison with those of physically mixed specimens. It was consequently made clear that the in-situ preparation procedure is not enough to improve the homogeneity. Any additional idea must be needed for further improvement.

1) S. YAMADA et al., J. Mater. Research, 3, 538-544 (1988).

2) S. YAMADA et al., Ceramic Transactions, 1, 269-276 (1988).

PROCESS OF EPITAXIAL GROWTH OF Fe ULTRA THIN FILM ON Cu SUBSTRATE

K. Doi, S. Mitani, H. Toyoda, M. Matsui and M. Doyama[#]

Dept. of Materials Science and Engineering, Nagoya Univ., Nagoya

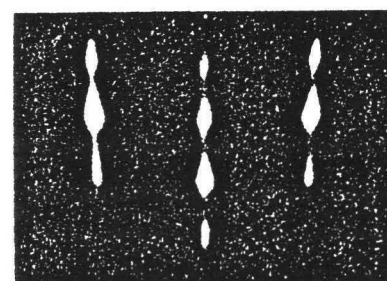
[#]Dept. of Materials Science, Nishi Tokyo Univ., Uenohara, Yamanashi

At room temperature, the stable crystal structure of iron is the bcc structure, while fcc structure can be stabilized as a precipitate in supersaturated CuFe alloy and as a thin film on Cu substrate. From band structure calculations, magnetic behavior of fcc-Fe is predicted to be strongly dependent on the lattice constant. Recently we reported the ferromagnetic properties of multilayered fcc-Fe/Cu thin films grown on a Cu(001) single crystal substrate by MBE. Now we tried to get the epitaxial growth of Fe on Cu(111) substrate under the same conditions of Cu(001), but it became the bcc structure. To investigate the difference of growing process, we prepared the samples under the various conditions by the MBE method.

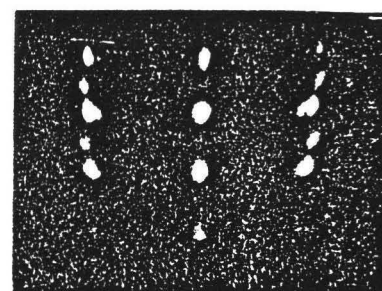
We prepared [2.8~10 ML Fe/Cu(001)] and [2~10 ML Fe/Cu(111)] multilayers. The samples were grown under the vacuum better than 2×10^{-11} Torr. The evaporation rate was about 1Å/min and the substrate temperature was about 50°C. Furthermore we prepared Fe/Cu(111) overlayers under the various evaporation conditions. Structure of films was studied by RHEED and X-ray diffraction. Magnetic properties were studied by SQUID and VSM.

The RHEED patterns of Fe layer in the film on Cu(001) are in good agreement with that of Cu substrate before growth. It means that Fe layer is grown on Cu(001) epitaxially with layer by layer fcc structure. The fcc-Fe showed ferromagnetism whose magnetic moment is $2.0 \pm 0.1 \mu_B$. Fig.1 shows the RHEED patterns of (a) Cu(111) substrate before growth, (b) Fe layer (3ML) grown on Cu(111) under a pressure of 2×10^{-11} Torr and (c) Fe layer (3ML) on Cu(111) under a pressure of 8×10^{-10} Torr. Analyzing the RHEED pattern of Fig.1(b) we found that island-like bcc-Fe was grown on Cu(111) substrate. The direction relationship at the interface between bcc-Fe and Cu substrate is satisfied by both of K-S and N-W relationships. On the other hand Fig.1(c) shows fcc-Fe structure, where the pressure is higher than Fig.1(b). It should be noted that crystal structure of the Fe films is dependent on the pressure.

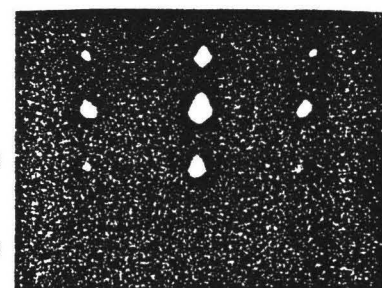
We tried a computer simulation of these process of the epitaxial growth using a pair potential.



(a)



(b)



(c)

Fig. 1

NEW CONDUCTING POLYMER COMPOSITES

J.H. HAN, T. MOTOBE, Y.E. WHANG and S. MIYATA

Department of Materials Systems Engineering, Tokyo University of Agriculture and Technology.

We have developed highly electrically conducting polymer-composites of polypyrrole and poly(vinyl acetate) using chemical oxidation polymerization. The most attractive feature of this method lies on that the polymerization of pyrrole follows after fabrication.

After controlling an oxidation potential by dissolving poly(vinyl acetate) and FeCl_3 in methanol, pyrrole was added with stirring. When the mixture solution is casted on the substrates, polymerization immediately proceeds with solvent evaporation which causes an increase in the oxidation potential. The electrical conductivity of solution-casted composite depends on the initial oxidation potential of the solution as well as on the incubation time in solution state before casting. When kept in solution state for a long time, phase separation of poly(vinyl acetate) and polypyrrole occurs which results into very low conductivity. When casted within specified time, the polymerization of pyrrole progresses close to the optimum oxidation potential condition due to the evaporation of solvent. If the initial oxidation potential of the solution is either too low or too high, the prepared solution-casted composites show poor electrical conductivities. The optimum range of initial oxidation potential of the solution is 480~560mV(vs. SCE). The electrical conductivity shows percolation behavior in the vicinity of about 3wt.% of monomer ratio and it reaches 10S/cm when only 5wt.% of pyrrole monomer is incorporated under optimum condition. Moreover, the composites show a good environmental stability.

Based on the above techniques, we also tried to fabricate conducting polymer composite fibers. Conducting polymer fibers can be prepared by a conventional solution spinning technique from the mixture of pyrrole monomer with poly(styrene) or poly(acrylonitrile). The mixture was extruded into non-solvent solution containing oxidizer. The conducting composite fibers exhibit an electrical conductivity as high as 20S/cm.

Low Temperature Growth of β -SiC Films on Si Substrate
by Direct Carbonization Method.

Yasuaki Hirano

Master Course, Graduate School of Engineering, Hosei University
Kajino-cho, Koganei, Tokyo 184

β -SiC is an attractive material since it is a wide band-gap semiconductor with a high breakdown voltage, a high saturation velocity, and a high electron mobility. It is an interesting material which is applicable to an emitter of a high-speed, hetero-bipolar transistor. Recently, the hetero-epitaxial growth of a β -SiC film on Si has been studied by using a CVD technique. The previous work has shown that the epitaxial temperature is in a range of 1300-1400°C when the film is formed by CVD. The epitaxial temperature is too high to apply the film growth to a conventional Si device process. In other words, low temperature growth of a β -SiC film on Si is strongly required to fabricate the hetero-bipolar transistors in integrated circuits.

In this work, the hetero-epitaxial growth of a β -SiC film on Si has been examined by a new technique. The growth is made by a thermal reaction between the substrate and carbon atoms sublimated from a high purity graphite. The growth temperature is ranged from 800 to 1100°C. The atomic composition of the film grown is analyzed by a RBS method. The crystalline properties of the film are examined by XRD and RHEED methods and also by channeling measurements. It has been demonstrated that film properties depend strongly upon the substrate temperature during carbon deposition. It is found that the epitaxial growth initiates when the deposition is done at 900°C. Great improvement of the crystalline state can be achieved in the film grown at 1100°C, as shown in Fig.1. The hetero-epitaxial growth of a β -SiC film on Si will be discussed based on the data of properties of films grown under various conditions.

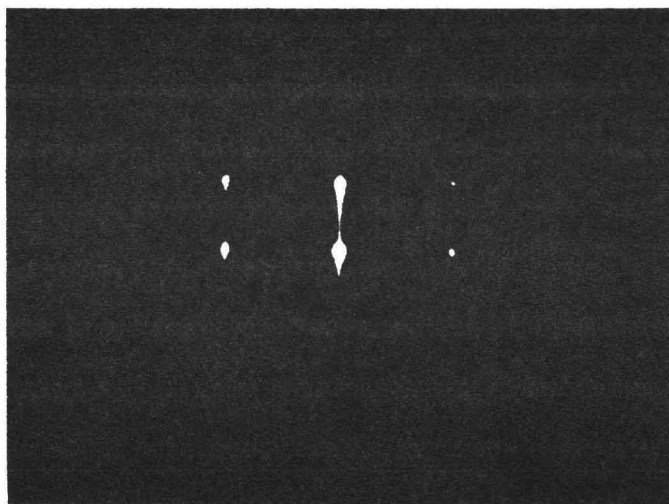


Fig.1 The RHEED pattern of a β -SiC film grown on (111)Si at 1100°C.

Molecular Recognition through Selective Intermolecular Hydrogen
Bonding for a New Functional Liquid Crystalline System

Norifumi Hirota, Takashi Kato, Akira Fujishima and Jean M. J. Fréchet⁺

Department of Synthetic Chemistry, Faculty of Engineering,
The University of Tokyo, Hongo, Bunkyo-ku, Tokyo 113, Japan.

⁺Department of Chemistry, Baker Laboratory, Cornell University,
Ithaca, New York 14853-1301, U.S.A.

A new type of photoresponsive liquid crystalline (LC) polymeric system has been built through selective intermolecular hydrogen bonding between a liquid crystalline polymer matrix and the photo-responsive molecule. The liquid crystalline copolyacrylate containing the pyridyl group which is H-bond acceptor moiety has been complexed with the azobenzene derivative containing the carboxyl group which is H-bond donor. This hydrogen-bonded binary polymeric material formed by intermolecular hydrogen bonding showed a nematic phase, which was highly homogeneous. Photoirradiation to the hydrogen-bonded LC complex at 366 nm light caused the trans→cis photoisomerization of the azobenzene molecule, which induced the nematic→isotropic isothermal phase transition of the matrix. The photoinduced phase transition was not clearly observed for a simple mechanical mixture. This shows that the intermolecular hydrogen bonding between the LC host and the photoresponsive molecule is much effective for the photochemical phase transition. The hydrogen-bonded LC polymeric material is a new type of functional host-guest system and seems to have great potential for advanced materials.

Structures and Mechanical Properties of Squeeze Cast SiCw Reinforced Al-Li Metal Matrix Composites

* S.K.Hong

Abstract

The increasing need for light-weight, high-strength and cost-effective materials for structural applications has resulted in significant improvement and development of new advanced materials such as Al-Li alloys, MMC and Ti alloys. Lithium additions to an aluminium are known to provide the greatest density reduction and increase in elastic modulus of any known alloying element. It is considered that the most variable MMC with high specific strength and high specific elastic modulus can be obtained by combination Al-Li alloys and SiCw. However, it has been well known that sound Al-Li alloys cast ingots are very difficult to obtain using conventional cast technique. Thus, in this study, the sound MMC ingots have been successfully fabricated by specially designed squeeze casting under open atmosphere. This study has investigated age hardening behavior, mechanical properties and interfacial reaction behavior between reinforcement and matrix for castings and hot-extruded materials. In general, MMC based on Al alloys has not shown prominent age hardening effect because the the formation of G.P zone was delayed and metastable precipitation phase was preferentially precipitated on defects. But SiCw/Al-Li MMC has shown prominent age hardening phenomenon resulted in precipitation of δ' (Al_3Li) during quench after the solution treatment at 793K for 10 minutes. The coarsening phenomenon was accelerated in MMC compared to matrix alloys. MMC obtained by melting process and squeeze casting in this work has not shown an obvious interfacial reaction products between SiCw /matrix interface.

High Pressure Sintering of Diamond-Cobalt System

Makoto IIZUKA, Hisako HIRAI^A, Hiroyuki IKAWA and Osamu FUKUNAGA

Faculty of Engineering, Tokyo Institute of Technology, Meguro, Tokyo

^A Research Laboratory of Engineering Materials, T.I.T., Yokohama

Sintered diamond compact was prepared using mixed powder of diamond and cobalt powder at a temperature of 1550 °C under a pressure of 5.5 GPa. Mixed powder was prepared by the precipitation method of cobalt solution.

Microstructure of diamond-cobalt powders was observed by SEM to clear the dispersion condition of cobalt. Fig.1 shows the BEI of diamond-cobalt mixed powders. The figure shows that fine cobalt particles (0.3 μm dia) was dispersed around the surface of diamond powders. Such homogeneous mixture could be obtained when we use $\text{Co}(\text{OH})_2$ precipitation method at low reduction temperature (400 °C). Fig.2 shows BEI of the fractured surfaces of sintered compacts. From the figure it can be observed that using fine cobalt dispersed powder was sintered well.

Dispersion experiment of commercial synthetic diamond powder (2-3 μm) into the organic solvents was studied to improve dispersion of diamond powder. Diamond powder was dispersed well in a 2-Ethyl hexanol. This result suggests that surface of synthetic diamond polarized slightly.

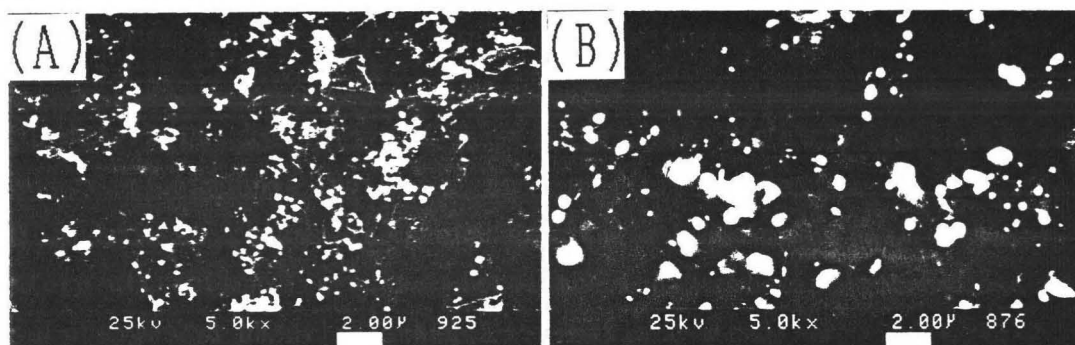


Fig.1 BEI of diamond-cobalt powder. $\text{Co}(\text{OH})_2$ precipitation method. Reduction Temperature: (A); 400 °C (Co 12.5 vol%), (B) 800 °C (Co: 22.6 vol%).

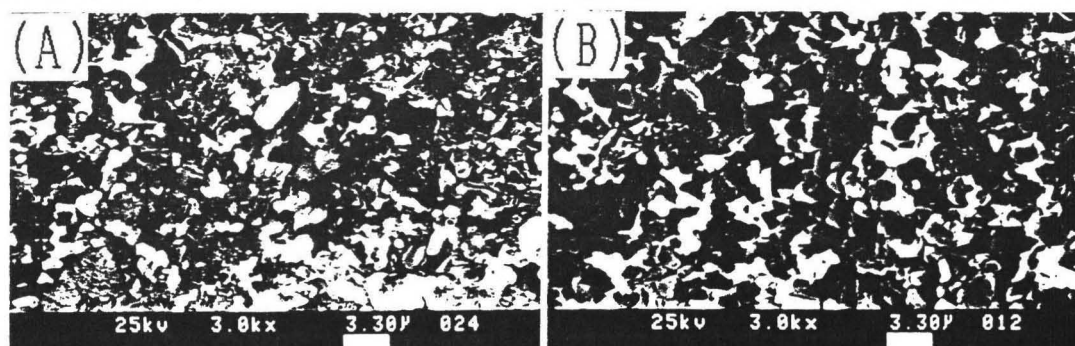


Fig.2 BEI of fractured surface of sintered diamond. (A); $\text{Co}(\text{OH})_2$ precipitation method. Reduction Temp. : 400 °C. (Co: 12.5 vol%), (B) CoCl_2 precipitation method. Reduction Temp. : 800 °C. (Co: 13 vol%).

[Synthesis and properties of $\text{YBa}_2\text{Cu}_4\text{O}_{8-x}$]

Hiroshi Iwama, Naoki Ohasi, Hisako Hirai^a, Hiroyuki IKAWA and Osamu FUKUNAGA

Faculty of Engineering, Tokyo Institute of Technology, Meguro-ku, Tokyo

Research Laboratory of Engineering Materials, Tokyo Institute of Technology

The well-known 90K superconductor $\text{YBa}_2\text{Cu}_3\text{O}_{7-x}$ (123) was discovered in 1986. There are another superconducting phases $\text{YBa}_2\text{Cu}_4\text{O}_{8-x}$ (124), $\text{Y}_2\text{Ba}_4\text{Cu}_7\text{O}_{15-x}$ (247), and they differ from 123 in T_c , number of Cu-O chains.

Unlike the 123 compound, especially, 124 is more stable phase at high temperature. The 123 phase is very sensitive compound by oxygen defect and 124 is much more stable against high temperature than that of 123.

It was said that 124 phase was only synthesized at 1000°C, high oxygen pressure (100-200bar). But recently, 124 is synthesized at 1 bar oxygen pressure.

We synthesized 124 compound by two starting materials, "123+CuO"; "Starting mixture ratio Y:Ba:Cu=1:2:4" and oxygen pressure, $P_{\text{O}_2} \ll 10\text{bar}$.

Properties were measured by powder X-ray diffraction pattern (XRD), T_c Measurement, magnetization measurements (SQUID), TEM.

@ Results

1. The 124 phase can be synthesized from "123+CuO" "Starting mixture ratio Y:Ba:Cu=1:2:4" at 1 bar oxygen pressure. The 124 phase could be obtained easily by the former method.
2. High oxygen pressure is more effective to "123+CuO" method.
3. The present results suggested that 124 synthesized by the process.

Mixture materials \rightarrow 123+impurity (CuO) \rightarrow 124

Micro structure of 124 phase will be reported to confirm above process.

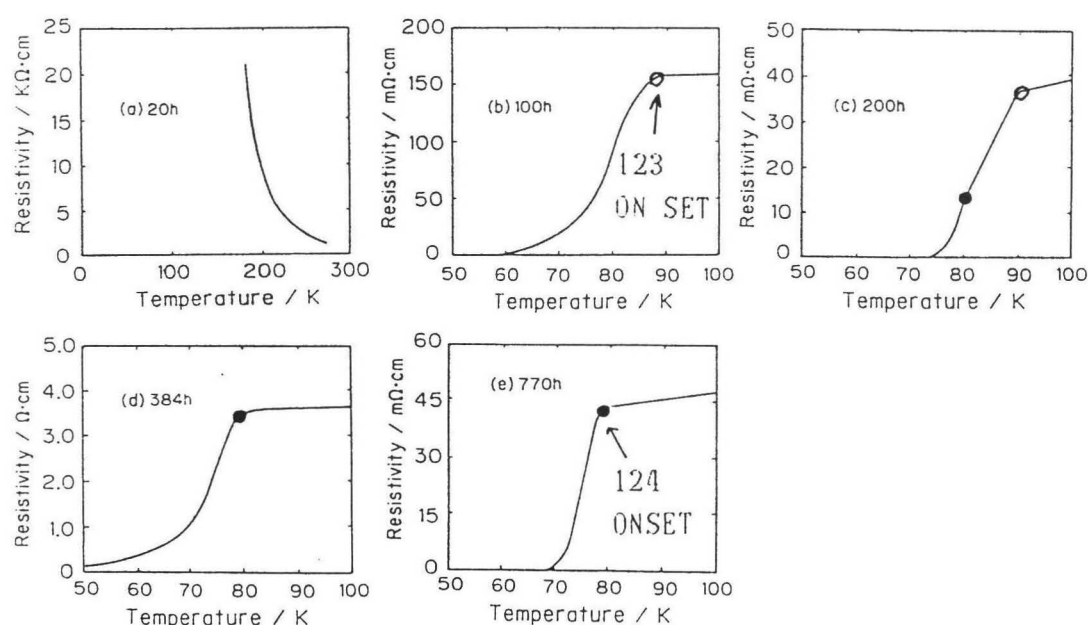


Fig.1 Resistivity as a function of temperature for various annealing time

Starting materials " $\text{Y}_2\text{O}_3:\text{BaCO}_3:\text{CuO}=1:2:4$ "

800°C, $P_{\text{O}_2}=1\text{bar}$ (a)20h(b)100h(c)200h(d)384h(e)700h

Rapid Thermal Annealing for High-Energy Ion-Implanted Si

Hiroyuki Iwasaki

Master Course, Graduate School of Engineering, Hosei University

Kajino-cho, Koganei, Tokyo 184

Recently, high energy ion implantation in Si substrates has been widely studied as a means of forming novel device structures such as a retrograde well for CMOS latch-up protection, a buried layer for soft error reduction of dynamic RAMs and a subcollector of bipolar transistors. The previous work, however, has shown that annealing process in Si implanted with high energy ions in a MeV region is much complicated as compared with low energy implants. For example, a high density of secondary defects grow in Si substrates when they are processed through furnace annealing.⁽¹⁾ This is why the applications of high energy implantation to a silicon device fabrication process are limited at the present time.

In order to search for an annealing technique which is useful to high energy implantation, the effects of rapid thermal annealing (RTA) on the annealing characteristics and electrical properties of As-implanted layers in Si has been studied. Arsenic implantation is carried out at incident energy of 1MeV to a dose of $1 \times 10^{15} / \text{cm}^2$. Annealing process is examined by RBS measurements and by XTEM observations. Electrical properties for As-implanted layers are evaluated by electrical measurements. It has clearly shown that the growth of secondary defects can be effectively suppressed by using RTA, as shown in Fig.1. From the results obtained in this work, it is concluded that RTA is useful for annealing of high-energy ion-implanted Si as compared with conventional furnace annealing.

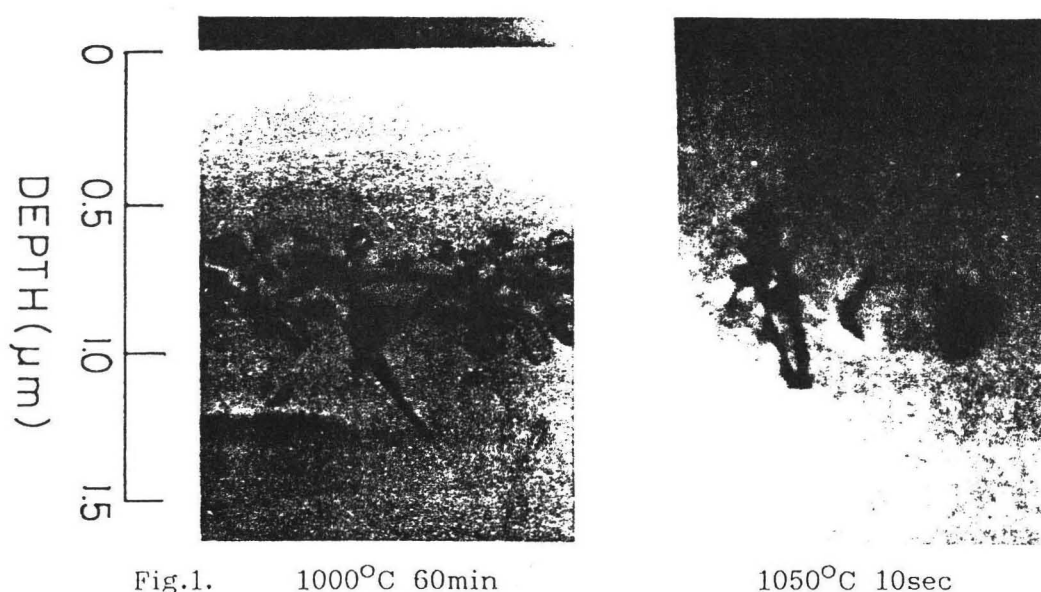


Fig.1. 1000°C 60min

1050°C 10sec

(1) T. Inada et al, J. appl. Phys. Nov. (1990)

Photochemical Valence Isomerization of Norbornadiene Derivative
Using Multifunctional Polymeric Photosensitizers

T. Kawashima, K. Inomata and T. Nishikubo

*Department of Applied Chemistry, Faculty of Engineering, Kanagawa
University, Rokkakubashi, Kanagawa-ku, Yokohama 221 JAPAN*

Polymeric photosensitizers are of interest in view of development of effective photosensitizing system in organic photochemistry and progress in solar energy storage processes using norbornadiene (NBD) - quadricyclane (QC) derivative systems. However, the efficiency of these photosensitizers was generally lower than that of the corresponding low molecular weight (LMW) photosensitizers used. Recently, we proposed (1-3) the concept of multifunctional polymeric photosensitizer having pendant substrate-attracting groups and photosensitizing groups, and it was found that the polymers containing pendant substrate-attracting groups and photosensitizing groups have higher photosensitizing efficiency than the LMW photosensitizers for photochemical isomerization of potassium cinnamate and potassium sorbate in water. Therefore, our sensitizers might also be applied to the solar energy storage process of NBD - QC derivative system. In this paper, we wish to report the efficiency of soluble polymers and insoluble polystyrene beads containing pendant nitroaryl groups as photosensitizers and quaternary onium salts as substrate-attracting groups for the photochemical valence isomerization of potassium 3-phenyl-2,5-NBD-2-carboxylate (PNC) in water or methanol.

Photosensitized isomerization of PNC was carried out in water and methanol upon the irradiation with >330 nm light. The disappearance of the absorption maximum at 290 nm of PNC was measured by UV spectrophotometer. These results indicate that the soluble and insoluble multifunctional polymeric photosensitizers containing pendant photosensitizing groups and substrate-attracting groups have higher photosensitization efficiency than the LMW photosensitizers. Furthermore, it was found that the photosensitization efficiency was strongly affected by the content of photosensitizing unit in the polymer, the concentration of photosensitizer in the reaction system and reaction medium.

- 1) T. Nishikubo et al., *Macromolecules*, 21, 1583 (1988)
- 2) T. Nishikubo et al., *Makromol. Chem.*, 190, 1471 (1989)
- 3) T. Nishikubo et al., *Macromolecules*, 22, 3827 (1989).

PRECURSOR OF THE 74 GAUSS DOUBLET IN α -SiO₂

Manabu Kitagawa, Shuji Munekuni, Hiroyuki Nisikawa,
Kaya Nagasawa*, Yoshimichi Ohki, and Yoshimasa Hama

Department of Electrical Engineering, Waseda University,
3-4-1 Ohkubo, Shinjuku-ku, Tokyo 169, Japan.

*Department of Electrical Engineering, Shonan Institute of
Technology, 1-1-25 Tsujido-Nishi-kaigan, Fujisawa, Kanagawa
251, Japan.

It has been previously reported that when γ -rays are irradiated in high doses ($>10^6$ rad), 74 gauss doublet spectra in electron-spin-resonance (ESR) can be observed in high-OH type pure silica glass. In the present report, γ -rays were irradiated on high-OH and low-OH oxygen deficient silica glass preform and optical fiber samples, and then ESR measurement was done. The 74 gauss doublet is only induced in the low-OH oxygen deficient optical fiber sample while in high-OH optical fiber and both type of silica glass preform samples, it is not. The structure responsible for the 74 gauss doublet is suggested to be E' type center, whose one of the three nearest oxygens is replaced by the impurity proton. From the data, it may be assumed that during fiber drawing, defects in low-OH oxygen deficient sample must have reacted with protons which existed in silicone cladding, and resulted to be the precursor of the 74 gauss doublet.

Manabu Kitagawa
Waseda University
Dept. of Electr. Engi., Ohki Laboratory
3-4-1 Ohkubo, Shinjuku-ku, Tokyo 169, Japan.
Tel: 03-203-4141 ext. 73-3167
Fax: 03-200-2567

ELECTROCHROMIC COPPER OXIDE FILM BY ELECTRODEPOSITION

T.Kojima, T.Yoshino, N.Baba

Tokyo Metropolitan Univ.

Many of transition metal oxides are known as the electrochromic material. Up to now, however, about copper oxides, there are few reports with EC phenomena in detail.

In this study, copper oxide film was obtained by electrodeposition method using copper-ammine complex electrolyte and its EC property and others were investigated.

To prepare the electrolyte, NH_4OH (conc.) was added to $0.005\text{M CuSO}_4 - 0.015\text{M (NH}_4)_2\text{SO}_4$ mixed solution up to $\text{pH}=9.4$. In this electrolyte, using NESA glass as a working electrode, electrodeposition was performed at a constant potential 900mV (vs.SCE) and brown thin film was obtained. In 0.1M NaF solution this film showed change in contrast by applying redox potentials; fading at 0mV and growing dark at 900mV respectively. Figure 1 shows cyclic voltammetric curve and simultaneously measured optical density at 500nm wavelength. By the XPS measurement, it is considerable that this film is mainly composed of Cu(II) oxide (shown in figure 2).

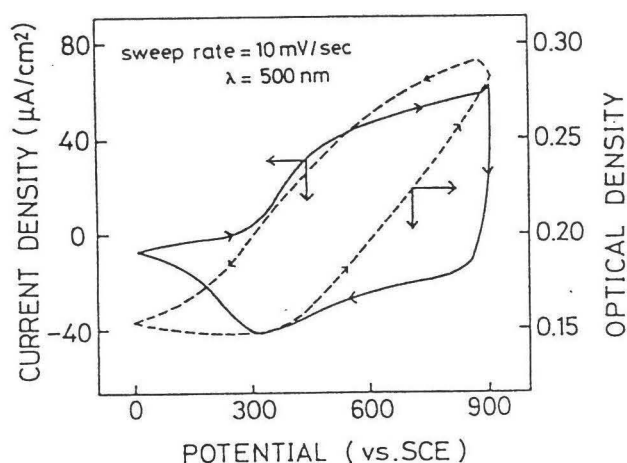


Fig.1 Cyclic voltammogram of CuO_x in 0.1M NaF solution and its change in optical density measured at 500nm

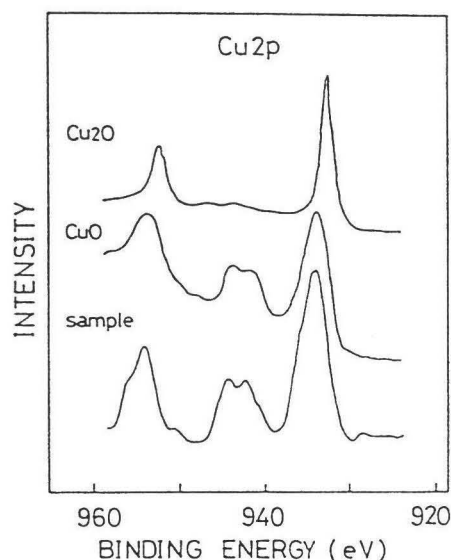


Fig.2 Cu 2p X-ray photoemission spectra

A New Fabrication Technique for Oxide/Metal Composites by Controlled-Directed- Oxidation Process

S. Kokubo¹⁾, Y. Kagawa²⁾, A. Okura³⁾

1) Graduate School Student, Tokyo Institute of Technology,
4259, Nagatsuta-cho, Midori-ku,
Yokohama-shi, Kanagawa 227, Japan

2) Institute of Industrial Science, The University of Tokyo,
7-22-1, Roppongi, Minato-ku, Tokyo 106, Japan

3) Institute of Space and Astronautical Science,
3-1-1, Yoshinodai, Sagamihara-shi, Kanagawa 229, Japan

ABSTRACT

A new fabrication process of oxides/metal composites by controlled-directed-oxidation process (CDO process) has been investigated using model aluminum alloys. Possibility of in-situ formation of $\text{Al}_2\text{O}_3/\{\text{Si}\}$ composite materials by controlled-directed-oxidation of liquid Al-Si-Mg alloys was examined. The typical composite was obtained by oxidizing an aluminum melt in dry-air at temperatures of 1400 to 1700K for 5-30h.

Microstructures of the composites were observed in detail. A method for simple modeling of the growth kinetics is discussed. The effects of additive elements on the growth mechanism of the $\text{Al}_2\text{O}_3/\{\text{Si}\}$ composite can be explained by the simple model. Application of this process for the SiC(PCS) fiber-reinforced $\text{Al}_2\text{O}_3/\{\text{Si}\}$ matrix composite is also discussed.

New Microporous Glass-Ceramics Composed of $\text{CaTi}_4(\text{PO}_4)_6$ Skeleton and Their Application to Carriers for Immobilization of Enzymes

H. MAENAMI, T. NARUSE, H. HOSONO and Y. ABE

Department of Materials Science and Engineering
Nagoya Institute of Technology, Nagoya, JAPAN

T. SUZUKI and M. TORIYAMA

Government Industrial Research Institute, Nagoya

Recently, ceramic materials have attracted much attention in the field of biotechnology. Although porous ceramics are very important as carrier materials for immobilization of enzyme, research has been so far limited to Vycor glass[®] composed of 96% SiO_2 . Since SiO_2 dissolves in alkaline solutions with $\text{pH} > 9$, application is restricted to enzymes which have optimal pH in the neutral and acidic regions. We have developed a new microporous ceramics by a controlled crystallization of glasses in the $\text{CaO-TiO}_2\text{-P}_2\text{O}_5$ system and subsequent acid leaching. Their skeleton is composed of $\text{CaTi}_4(\text{PO}_4)_6$, and the mean pore diameter and surface area are 24nm and 90m²/g, respectively. These ceramics are very durable in both acidic and alkaline solutions because of high TiO_2 content. We have examined these new porous glass-ceramics as carriers for immobilization of alkalophilic proteinase with an optimal pH in the alkaline solution, and found that the present porous glass-ceramics are superior to the conventional porous silica glass.

Preparation of Powder ACEL Device Using Alumina Dielectrics Formed by Sol-Gel Method.

M.Mori, T.Yoshino, S.Morisaki, N.Baba
Tokyo Metropolitan Univ.

A simple preparation of powder ACEL device using alumina dielectrics has been obtained by sol-gel method.

Aluminium triisopropoxide was mixed with pure water in the mole ratio of 1:100, and it was hydrolyzed at 150°C for 2 hours with stirring. It was peptised by dropping HCl, and white semitransparent alumina sol was obtained. This alumina sol was coated on NESA glass by screen printing method, after being aged at 75-85°C for several hours. The phosphor (ZnS:Cu) dispersed in alumina sol was coated on the first alumina layer and it was dried at 150°C for 2 hours. Alumina sol was again coated on this layer, and dried. Finally aluminum plate was used for reflecting back electrode.

Figure 1 shows the change in luminance-voltage characteristic of the EL device and Figure 2 shows EL spectra measured at various AC frequencies.

From this study, it was found that the alumina prepared by sol-gel method can be used for dielectrics of powder ACEL device. And it was shown that the emission of the EL device was observed from 30V, and the luminance at 200V was 40cd/cm².

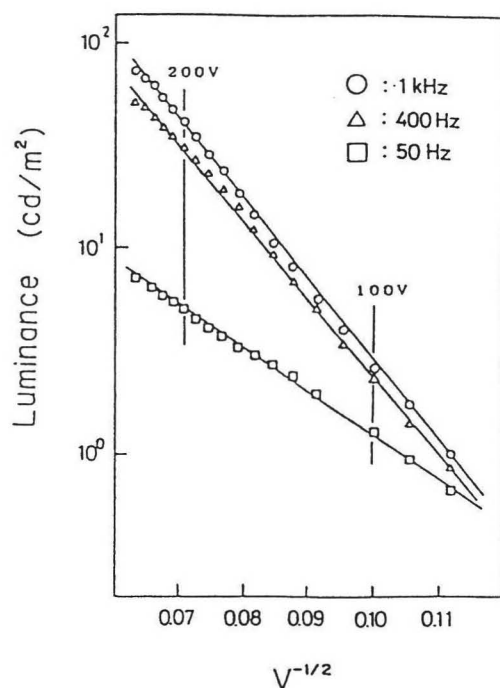


Fig. 1 Luminance vs. $V^{-1/2}$

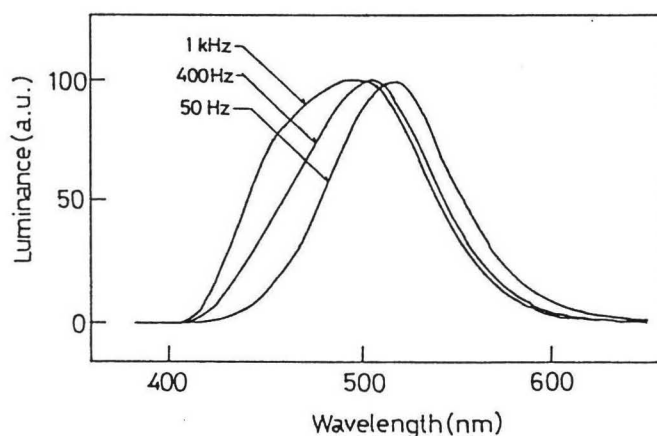


Fig. 2 EL spectra measured at various frequencies

Thermal Decomposition of $9\text{Al}_2\text{O}_3 \cdot 2\text{B}_2\text{O}_3$ Whiskers into Al_2O_3 Whiskers and Preparation of its Composites

○ Harufumi MUTOH, Kiyoshi OKADA, Nozomu OTSUKA
 Department of Inorganic Materials, Tokyo Institute of Technology
 and Toyohiko YANO
 Research Laboratory for Nuclear Reactor,
 Tokyo Institute of Technology

Recently $9\text{Al}_2\text{O}_3 \cdot 2\text{B}_2\text{O}_3$ (abbreviate to AB) whiskers, which have a similar structure with mullite, are commercially available from Shikoku Chemicals Co. These whiskers are reported to decompose into $\alpha\text{-Al}_2\text{O}_3$ and melt phase above 1440°C . Thermal decomposition reaction of these whiskers are, therefore, investigated. The AB whiskers were found to convert to $\alpha\text{-Al}_2\text{O}_3$ topotactically succeeding a whisker shape by firing above 1440°C and B_2O_3 component disappeared by vaporization. The crystallographic orientation relation between two whiskers was as follows;

$[1010]_{\text{Al}_2\text{O}_3} // [001]_{\text{AB}}$ (elongated direction)
 $(0001)_{\text{Al}_2\text{O}_3} // (120)_{\text{AB}}$ (side planes)

Four kinds of Al_2O_3 whiskers which have the different crystallographic orientations have been reported. The whiskers obtained in this study corresponded to the A2 type. During the conversion from AB to Al_2O_3 , a ring-like pattern probably caused by the defect structure was observed inside the AB whiskers as shown in Fig. 1. Since no discontinuity of the lattice image was detected except the different contrast even in high resolution electron micrographs, the reason of this ring pattern was uncertain.

Composites of Y-TZP/ Al_2O_3 whiskers were prepared by firing the compaction of mixtures of Y-TZP and AB whiskers using the conversion reaction of AB to $\alpha\text{-Al}_2\text{O}_3$ and B_2O_3 evaporation at high temperature. The composites with less than 20% Al_2O_3 composition was able to be densified by firing above 1500°C . Distinct grain growth, however, occurred in Y-TZP particles during the firing probably by the reaction with melt phase. It caused the tetragonal to monoclinic transition for zirconia and brought down heavy cracking for the composites with high Al_2O_3 content.



Fig.1 TEM micrographs of AB and Al_2O_3 whiskers.

MÖSSBAUER EFFECT OF MAGNETIC PHASES WITH ULTRA FINE STRUCTURE OF $\text{Fe}_{73.5}\text{Cu}_1\text{Nb}_3\text{Si}_{13.5}\text{B}_9$

H. Nakabayashi, M. Doi and M. Matsui

Dept. of Materials Science and Engineering, Nagoya Univ., Nagoya

Y. Yoshizawa and K. Yamauchi

Magnetic and Electronic Materials Research Laboratory, Hitachi Metals Ltd., Kumagaya

1. Purpose: Recently, a new soft magnetic material $\text{Fe}_{73.5}\text{Cu}_1\text{Nb}_3\text{Si}_{13.5}\text{B}_9$ was reported by Yoshizawa and Yamauchi. They found that the alloy had an ultra fine structure at a maximum permeability. To make clear the relation between the high magnetic permeability and magnetic phases with ultra fine structure, the magnetic properties and the process of precipitation at various annealing temperatures of $\text{Fe}_{73.5}\text{Cu}_1\text{Nb}_3\text{Si}_{13.5}\text{B}_9$ were investigated. The magnetic phases were identified by the analysis of the precise Mössbauer spectra.

2. Experimental methods: Amorphous Fe-Si-B-Cu-Nb alloy ribbons were prepared by the single roller method. Thermal annealings of these ribbons were carried out in the temperature range from 450 to 700 °C. The magnetic properties of them were measured and the precipitated phases were identified by X-ray diffraction. Using the results of X-ray experiments, the Mössbauer spectra were analyzed.

3. Results: The Mössbauer spectra of an as-rolled sample and of annealed at 500, 580 and 700 °C are shown in Fig. 1. According to the analysis, the following results are obtained. In an as-rolled sample, there exist an amorphous phase and a Fe_5SiB_2 phase. The hyperfine field of the amorphous phase are evaluated to be 215kOe. At 500 °C annealing, both of a partially ordered Fe_3Si and a Fe_3B phases slightly appear. As the annealing temperature is increased, the ordering of Fe_3Si phase is developed and the volume fraction of amorphous phase decreases. At 580 °C annealing, the permeability becomes maximum. The volume fractions of Fe_{23}B_6 and Fe_3B phases are increased rapidly by the annealing above 600 °C, where the permeability is decreased. We could say that the highest permeability state in $\text{Fe}_{73.5}\text{Cu}_1\text{Nb}_3\text{Si}_{13.5}\text{B}_9$ is composed of partial-ordered Fe_3Si (69%), Fe_3B (7%), Fe_5SiB_2 (7%) and amorphous(17%) phases.

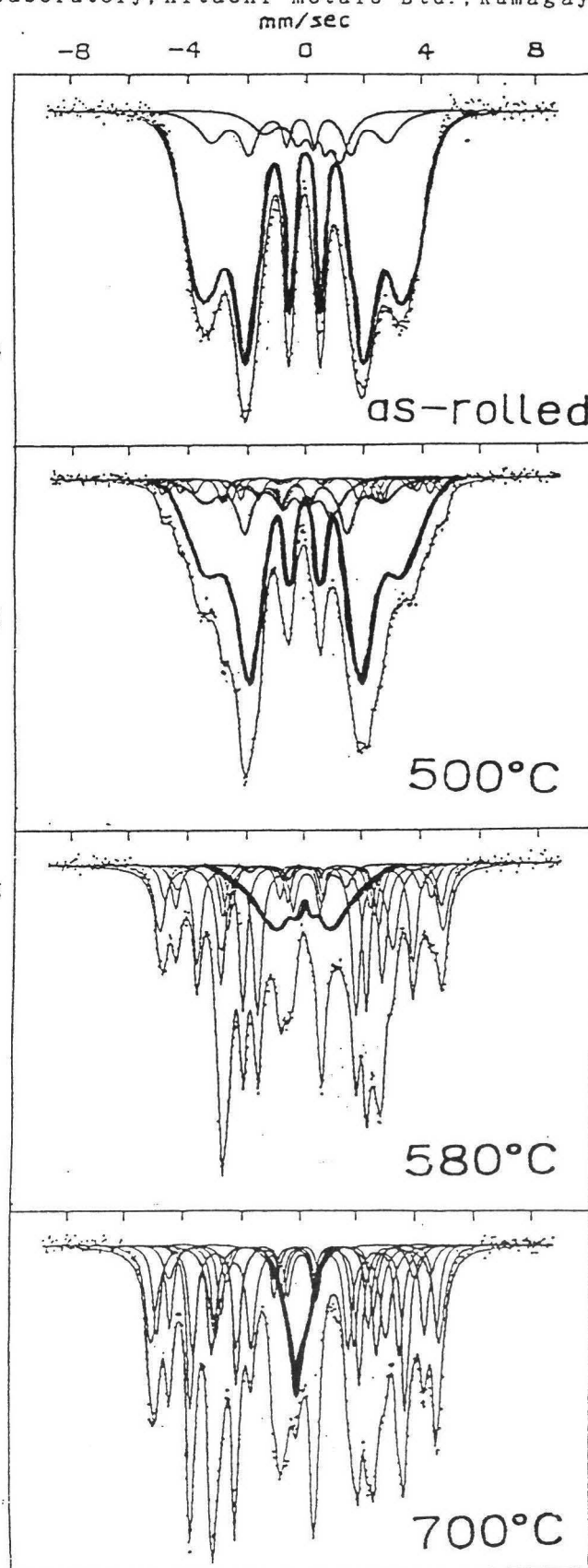


Fig. 1

Saccharide Recognition of Ultrafine Platinum Particle-Modified Concanavalin A

Naoki Toshima, Satoshi Nakagawa, and Yasukazu Saito
Department of Industrial Chemistry, Faculty of Engineering,
The University of Tokyo, Hongo, Tokyo 113 JAPAN

Biological macromolecules generally exhibit speciality in molecular recognition. Concanavalin A (Con A) is known as a lectin which can recognize saccharide. On the other hands, ultrafine metal particles show many valuable characteristics such as unusual catalyses for various reactions. Combination of the biological macromolecules with ultrafine metal particles may provide a new route for functionalization of the biological macromolecules. In the present studies, Con A is immobilized by covalent attachment onto ultrafine platinum particles, and the saccharide recognition properties of the modified Con A are investigated.

Immobilization of Concanavalin A onto Ultrafine Particles

Con A was treated with ultrafine platinum particles protected by a copolymer of methyl acrylate and N-vinyl-2-pyrrolidone. The reference reaction using poly(N-vinylpyrrolidone) as a protective polymer instead of the copolymer confirmed the formation of an amide bond between an amino group in Con A and a methyl acrylate residue in the protective copolymer.

Saccharide Recognition of Ultrafine Platinum Particle-Modified Concanavalin A

The agglutinating activity of the platinum particle-modified Con A thus prepared was examined for yeast mannan, a blanchd polymer of mannose. The agglutinating behavior of the modified Con A was similar to that of the native Con A. The inhibiting behavior by methyl α -D-mannoside and methyl α -D-glucoside for the above agglutination between Con A and yeast mannan was also similar to each other for both the ultrafine particle-modified Con A and the native Con A. The saccharide binding properties of Con A are therefore considered to be retained even after the modification by the covalent attachment with ultrafine platinum particles.

PHOTON ENERGY DEPENDENCE OF DEFECT PHOTOGENERATION IN α -SiO₂

Ryuta Nakamura, Hiroyuki Nishikawa, Kaya Nagasawa*,
Yoshimichi Ohki, and Yoshimasa Hama.

Department of Electrical Engineering, Waseda University,
3-4-1 Ohkubo, Shinjuku-ku, Tokyo 169, Japan.

*Department of Electrical Engineering, Shonan Institute of
Technology. 1-1-25 Tsujido-Nishi-kaigan, Fujisawa, Kanagawa 251,
Japan.

Photon energy dependence of defect photogeneration in α -SiO₂ is investigated. Two kinds of excimer lasers were used in this study : ArF (6.4 eV) and F₂ (7.9 eV). Irradiation was done at room temperature in nitrogen gas on four types of silicas : oxygen-surplus, oxygen-deficient (B₂ α), B₂ β , and high-OH. Induced paramagnetic defects were detected by electron spin resonance with X band at 77K. For both 6.4-eV and 7.9-eV lasers, E' centers (\equiv Si \cdot) are observed in all types of silicas. Nonbridging oxygen hole centers (\equiv Si-O \cdot) are induced only in oxygen-surplus and B₂ β type silicas for the 6.4-eV irradiation, while in all silicas for the 7.9-eV irradiation. Peroxy radicals (\equiv Si-O-O \cdot) are generated only in oxygen-surplus silicas irradiated by 7.9-eV photons. The observed photon-energy dependence suggests that the excitation process is closely related to the defect generation. Defect creation mechanisms are also discussed.

Ryuta Nakamura
Ohki Laboratory
Department of E.E., Waseda University
3-4-1 Ohkubo, Shinjuku-ku, Tokyo 169 Japan
Tel:03-203-4141 ext. 73-3167
Fax:03-200-2567

Preparation of Barium Ferrate (BaFeO_4) films by Electrochemical Method

O Masaharu NAKATSU, Seung Eul YOO, Nobuo ISHIZAWA and
Masahiro YOSHIMURA

(Research Laboratory of Engineering Materials,
Tokyo Institute of Technology)

Introduction

We have studied the preparation of Ba-Fe complex oxide films by Hydrothermal-Electrochemical method¹⁾. During the study, we found that well-crystallized BaFeO_4 film was prepared by electrochemical treatments of Fe substrates. Although BaFeO_4 was previously prepared as fine powders by a precipitation method but this was reported to be unstable, the film prepared in the present study were stable to be characterized.

Experimental

Fe plate with 99.9% purity was used as a working electrode and Pt plate as a counter electrode, respectively. Electrochemical treatments were performed in 0.25-0.5M $\text{Ba}(\text{OH})_2$ aqueous solutions for 60 min by means of galvanostatic method with the current density of 1-49 mA/cm^2 . Temperature was varied in the range of 22-200°C and pressure was 1-16 atm corresponding to the temperature. BaFeO_4 films prepared on the Fe plate were analyzed by XRD, SEM and IR.

Results and Discussion

BaFeO_4 was prepared as a film, which were directly formed on the Fe plate in $\text{Ba}(\text{OH})_2$ aqueous solutions at 22-90°C. The SEM micrograph (Fig.1.) shows the BaFeO_4 particles having the size of 0.3-0.8 μm .

The amount of BaFeO_4 increased with increasing current density. Up to 70°C, only BaFeO_4 was formed and it's amount increased with temperature. Above the temperature an unidentified phase was formed in addition to BaFeO_4 . Above 100°C, under hydrothermal conditions, another unidentified phase was started to form instead of BaFeO_4 . Above results indicate that electrochemical oxidation of FeO_2 is preferred at low temperatures below 70°C.

The formed BaFeO_4 films were stable upon exposing air probably because of well-crystallized one.

The lattice parameters of $a=7.323(1)$, $b=9.104(2)$ and $c=5.475(1)$.

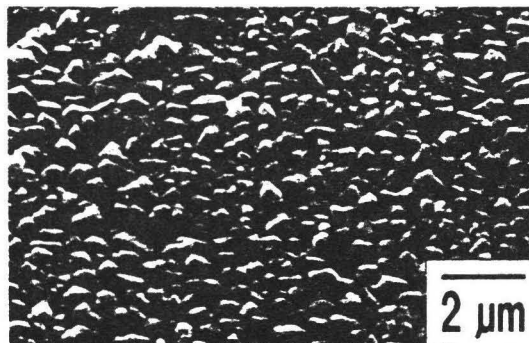


Fig.1. SEM micrograph of a surface of BaFeO_4 films prepared on a Fe substrate.

1) N.Isizawa et al., Proc. Annual Meeting of The Ceramic Society of Japan, p.506(Kobe,1990)

THE UNIVERSITY OF ELECTRO-COMMUNICATIONS

1-5-1, CHOFUGAOKA, CHOFU-SHI, TOKYO

STRONG PHOTOLUMINESCENCE FROM Si FINE PARTICLES

Y. Orihara, H. Gomyoh and F.W. Ping

Department of Communications and Systems,
The University of Electro-Communications,
Chofu-shi, Tokyo 182 Japan

Strong photoluminescence has been observed in Si fine particles prepared by both gas-evaporation and arc-discharge techniques. Measurements of the spectral distribution has shown that the luminescence consists of a single band at about $1.4\mu\text{m}$ with a broad distribution, a full width at half maximum being typically about $0.4\mu\text{m}$. According to the transmission electron microscopic study, the particle size formed by arc-discharge is widely scattered from several ten angstroms to several microns, whereas gas-evaporated Si particles show fairly uniform size in the range between 200 and 500 angstroms. Crystallographic characterization of Si particles has been made by Raman spectroscopy. Silicon particles formed by arc-discharge have shown a Raman peak at 520cm^{-1} which is a characteristic of crystalline Si. The similar Raman spectrum has been observed in gas-evaporated Si after heat-treatment at 900°C for 3 hours in argon atmosphere. The strong luminescence observed in Si fine particles has been attributed to the recombination via the surface states: A huge density of surface states is a characteristic feature of the fine particles. Optical absorption spectra of Si fine particles are now under investigation.

PREPARATION AND CHARACTERIZATION OF NOVEL 1-NYLON
BY ANIONIC RING-OPENING POLYMERIZATION
OF 2-PHENYL-1,3,4-OXADIAZOLIN-5-ONE

Yasuo SAEGUSA, Yasuhiro OZEKI, and Shigeo NAKAMURA

Department of Applied Chemistry, Faculty of Engineering,
Kanagawa University, Kanagawa-ku, Yokohama 221, JAPAN

To clarify the structure-properties relationships of polyamides, a large number of polyamides have been hitherto synthesized mainly by polycondensation and ring-opening polymerization. However, it is difficult to obtain the simplest polyamides, 1-nylons, because both the methods described above can not be used for their preparations. The only method previously reported was anionic polymerization of monoisocyanates leading to N-substituted-1-nylons. We have found that a five-membered heterocyclic urethane, 2-phenyl-1,3,4-oxadiazolin-5-one (PO), undergoes anionic ring-opening polymerization in the presence of an appropriate initiator giving 1-nylon with pendant benzamido groups. The present work is therefore concerned with the detailed study of the synthesis of a novel 1-nylon by anionic ring-opening polymerization of PO and also conversion of the resulting ring-opened polymer, N-benzamido-1-nylon, to N-amino-1-nylon by selective hydrolysis of the pendant groups.

The ring-opening polymerization of PO was carried out by bulk and solution polymerizations by using various initiators, such as alkaline metal salts of PO, alkaline metal fluorides and tertiary amines. The ring-opened polymer with the highest reduced viscosity of 0.11 dL/g was obtained by these methods with a 10 mol% of sodium salt of PO to PO. The \overline{M}_n of this polymer was 2,000. The $\overline{M}_w/\overline{M}_n$ ratio was 1.1, indicating that this ring-opened polymer has extremely narrow molecular weight distribution. Conversion of the ring-opened polymer to N-amino-1-nylon was successfully attained in reasonable yield in aqueous ethanol containing a small amount of hydrochloric acid. The IR spectrum of the hydrolyzed polymer showed complete disappearance of a strong absorption due to benzamido carbonyl groups of the ring-opened polymer, suggesting that hydrolysis of the pendant groups occurred selectively.

The ring-opened polymer dissolved easily in aliphatic and aromatic alcohols such as methanol, ethanol and m-cresol and in polar aprotic solvents such as DMAc, DMF, DMSO, HMPA and NMP, but insoluble in common organic media and water, whereas the hydrolyzed polymer was not soluble in any organic solvents but highly soluble in water. The ring-opened polymer and hydrolyzed polymer began to decompose at around 200 and 170°C, respectively, in air. The reduced viscosity of the hydrolyzed polymer in water increased drastically with the decrease in polymer concentration. The viscometric behavior agreed well with that of usual polyelectrolytes with flexible backbone. The conformation of N-amino-1-nylon in solution is, therefore, supposed not to be rigid rod-like one similar to that of α -helical poly- α -aminoacids but to have some flexibility.

Design of Polymeric Micelle Recognizable by Hepatic Parenchymal Cells and Its Application to Drug Delivery System(DDS)

Mitsuaki Goto¹, Akira Kobayashi¹, Seishirou Tobe¹, Kazukiyo Kobayashi²,
Kazuhiro Saito³, Toshihiro Akaike^{1,3}

1. Kanagawa Academy of Science and Technology, Takatsu-ku, Sakado 100-1, Kanagawa 213
2. Faculty of Agriculture, Nagoya University, Furou-cho Chikusa-ku, Nagoyashi, Aichi 464
3. Faculty of Bioscience and Biotechnology, Tokyo Institute of Tech., Midoriku, Kanagawa 227

We have synthesized and examined the properties of lactose-carrying polystyrene (PVLA), which has been found as an useful surface coating material for hepatocyte cell culture. (1) PVLA was recognized by hepatic parenchymal cells, and this highly specific recognition could be through the asialoglycoprotein receptors on the hepatocyte surface. (2,3) Another useful property of PVLA is the micellar formation in aqueous solution.(2,3) The PVLA micelle could be potential inclusion carriers of drugs in a target-specific drug delivery system.

In this study, we examined the interaction between hepatic parenchymal cells with FITC-labeled saccharide-carrying poly-styrenes *in vitro* and *ex vivo* by flow cytometry. The PVLA interact much better with the hepatic parenchymal cells than with nonparenchymal cells. On the other hand, the maltose-carrying polystyrene (PVMA) showed binding specificity to the nonparenchymal cells. Moreover, the

behavior of PVLA to form inclusion compounds was examined by differential absorption spectra. These results suggested that the PVLA could bind hydrophobic and hydrophilic compounds effectively in its hydrophobic and hydrophilic domains.

Our result suggested that the saccharide-carrying poly-styrenes may be used as a highly specific targeting drug delivery devices.

References:

- 1) K. Kobayashi, H. Sumitomo, Polym. J., 17, 567(1985)
- 2) A. Kobayashi, T. Akaike, K. Kobayashi, H. Sumitomo, Makromol. Chem. Rapid Commun., 7, 645(1986).
- 3) T. Akaike, A. Kobayashi, K. Kobayashi, H. Sumitomo, J. Bioactive Compatible Polym., 4, 51(1989)

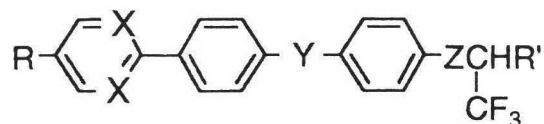
Synthesis and Properties of the Ferroelectric Liquid Crystals with a Trifluoromethyl group at the Asymmetric Center

Akira Sakaigawa and Hiroyuki Nohira

*Department of Applied Chemistry, Faculty of Engineering,
Saitama University*

Ferroelectric liquid crystals have been currently studied with great interest because of their potential applicability to a wide variety of devices, such as displays, light shutters, pyroelectric detectors, and spatial light modulations. Therefore characterization of the material and understanding of the correlation between the molecular structure and its properties are desirable. We noted the material constants such as spontaneous polarization(P_s), response time(τ), tilt angle(θ), rotational viscosity(η) and phase sequence, and discussed the correlation between the molecular structure and these constants for the materials with fluorinated asymmetric flames.

We have newly synthesized the ferroelectric liquid crystals with a trifluoromethyl group as shown by the following structure.



These materials generally possess a large spontaneous polarization and short response time, however these properties are mainly affected by the structure of the spacer group Z. For example, the materials having $-\text{CH}_2\text{O}-$ as a spacer group possess extremely large spontaneous polarization($300\text{nC}/\text{cm}^2$), while having $-\text{COCH}_2-$ group possess a two order small one. The stability of chiral smectic C phase(Sc^*) on the other hand is largely affected by R and R'. The temperature range of the Sc^* phase is varied with the length of R, while the appearing temperature of Sc^* phase is varied with R'. Similarly, the other properties are also closely related with the specific part of the molecular structure.

We have been able to obtain a numerous knowledge with respect to the relationship between the material properties and the molecular structure of ferroelectric liquid crystals for the optimal molecular design.

The Fracture Mechanics of FRP Plate with Cracks and Notches

M-24

Poster Session Dec. 13, 1990

by

Kazuhiko SATO(Tokai Univ.)

Yoshiaki YASUI(Tokai Univ.)

Somchai NORASETHASOPON(KMITL)

Hirakazu KASUYA(Tokai Univ.)

ABSTRACT

Advanced composites such as the fiber reinforced plastics(FRP) have been used for the various parts of light weight structures. The crack will arise from the parts of stress concentration in the member. The crack has broke out in the structure member which caused of the failure of the structure. The failure behavior of this crack for the structure design of FRP is very important case to study. Because, the FRP has material properties of the higher anisotropic. The problem of its behavior has not completely been resolved. In this case, the stress anlysis has need of numerical analysis to approach of the fracture mechanics which are related to the stress intensity factors, the J-integral and the energy release rate, etc. These analyses are attainable more simply by Finite Element Method(FEM).

This study was treated the stress intensity factors, the stress distribution and failure behavior of glass-fiber/epoxy(GFRP) and carbon-fiber/epoxy(CFRP) with the cracks or the notches. The analysis by using personal computer has made remarkable progress in solution of FRP failure in the past several years. Numerical analysis has been carried out on the assumption that the cracks or the notches existing perpendicularly in the load direction at both ends of FRP plate. Numerical analysis varied on the geometrical parameter of the crack or notch size dimension, the material properties, etc. The analytical results by FEM worked out the stress distribution and the stress intensity factor, and they were applied to the failure criterion.

The unidirectional composite plate has higher strength toward the fiber oriented direction. The CFRP plate has higher stress intensity factor. But the FRP plate has high stress it does not always follow that it is failure. The FEM analysis by personal computer has seen sufficiently agreement with theoretical results.

Joining of Silicon Nitride with Copper Using Filler Alloys

JWRI of Osaka Univ.

Nobuya Iwamoto

Masayoshi Kamai

Graduate Student of Osaka Univ.

○ Naoharu Satoh

1. Introduction

The increased use of silicon nitride as structural components has provided a method of joining with metals. Joining ceramics with metals has such a problem as cracking by thermal stresses which is taken place by difference of the rate of thermal expansion. Therefore, joining method which controls and decreases thermal stress is required. One method to decrease thermal stresses is joining by metals with low melting point. In welding field, Soldering technology is long-established in order to simplify joining, which is used with low melting point metals such as Pb, Sn, Zn, Bi, In, and Al etc. In order to join silicon nitride with copper, reactive-element, Ti, and low-temperature metals, was used. Then joining property was investigated.

2. Materials and Methods

Si_3N_4 (20mm in diameter, 10mm thick), and Cu (20mm diameter, 20mm thick) were polished in mirror face and cleaned in acetone. All filler alloys were prepared by vacuum high frequency melting ($<10^{-2}\text{Pa}$) and thinned under $200\mu\text{m}$. Joining condition is as follows. Joining specimen was held for 1h at fixed temperature in vacuum condition (10^{-3}Pa). Each interface of joint was analysed by E.P.M.A., and thermal cycle test was carried on. Some joined materials were examined by sharing tests.

3. Results

Some results of joining tests, thermal cycle tests, sharing tests, were in Table.

Table. Results of joining tests

No	Composition (wt%)	Temp (°C)	Joining result	Thermal cycle test (5times) (°C)	Sharing test (MPa)
1	63Ag35Cu2Ti	900	◎	400○550○700△	40
2	94Pb4Ag2Ti	400	△	—	3
3	59Pb39In2Ti	400	◎	200○280○	40
4	85In10Ag3Cu2Ti	400	○	200○280△	33
5	50Sn40Pb8Ag2Ti	400	×	—	—
6	98Sn2Ti	400	△	200△280×	—

Formability and Sinterability of Alumina-Platy Alumina Mixed Powders

Yasuhiro Takagi, Kiyosi Okada, Nozomu Otsuka

(Dept. Inorg. Mater., TIT)

Seiichi Taruta, Kunio Kitajima and Nobuo Takusagawa

(Dept. Chem. Mater. Eng., Shinshu Univ.)

The packing and sintering behavior of binary alumina-platy alumina powder mixtures were investigated by their density, open pore distribution and microstructure. The fine powders with a classified particle size of $<1\mu\text{m}$ and the coarse platy powders with a classified particle size of $6\sim7\mu\text{m}$ were used to prepare the binary mixtures with various ratios at 10% intervals, i.e., 0% fine + 100% coarse, 10% fine + 90% coarse, ... 100% fine + 0% coarse. Each sample was prepared by mixing two powders using a ball-mill with an ethanol. After dried and calcined, the powders were ground by a dry ball mill to remove large agglomerates. Compactions were made by an isostatical pressing at 98 MPa and were sintered at 1600°C . Figure 1 shows the green density and the sintered density, fired at 1600°C for 2h, for two kinds of mixed powders with the platy particles and the spherical one. Green density of both mixed powders was almost same except for a little difference around 30% fine particle sample ($W_f = 0.3$).

On the other hand, there were a considerable difference in the sintered density. The density with the platy particles in $W_f = 0.3$ to 0.9 was lower than that with the spherical particles. There was, however, little difference in the samples with $W_f = 0.0$ to 0.3 , in which packing structure was constructed with the framework of coarse particles. It was concluded that the sinterability of platy particles was inferior to that of spherical particles because of a wide flat plane corresponding to infinitely large curvature.

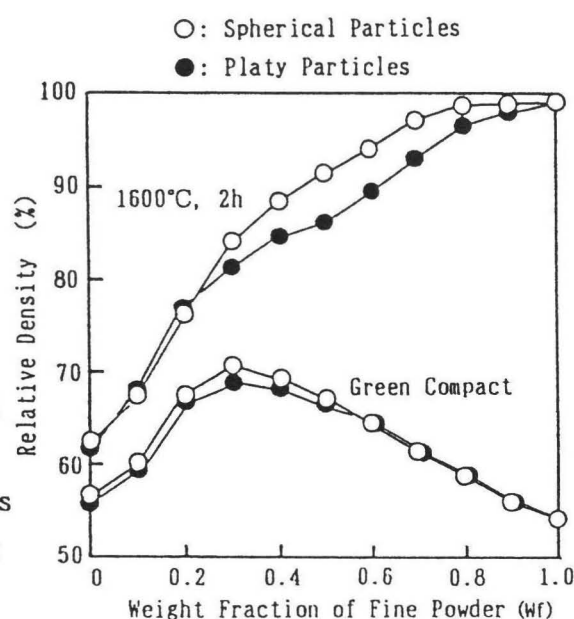


Figure 1 Density of Green and Sintered Compacts

Fabrication and Evaluation of Natural Mullite/SiC Nanocomposites by Pressureless Reaction-sintering

Hiroshi Takada and Koichi Niihara

The Institute of Scientific and Industrial Research,
Osaka University
8-1 Mihogaoka, Ibaraki 567, Osaka, Japan

Mullite has been expected as a high-temperature structure material because of its excellent thermal stability, chemical inertness and high creep and thermal resistances. Conventional mullite ceramics fabricated from natural kaolin and Al_2O_3 (natural mullite), however, have some problems such as poor room-temperature toughness and strength, and rapid strength degradation at high temperatures because of the existence of glass phases at the grain boundaries. To resolve these problems, therefore, the researches of mullite ceramics was focused on the development of high purity ceramics and/or their composites. Our present research concept is different from these trends and the purpose is to improve the mechanical properties of natural mullite containing relatively large amount of impurity by dispersing the nano-size SiC particles both at the grain boundaries and within the matrix grains.

The natural kaolin and Al_2O_3 powders were selected for the starting materials for the mullite matrix. The natural mullite/SiC nanocomposites were fabricated by pressureless reaction-sintering the mixtures of natural kaolin, Al_2O_3 and SiC powders at 1700°C . Homogeneous dispersions were made by the wet and/or dry ball milling techniques. The micro- and nanostructure were observed by optical microscopy, SEM and TEM.

The structure analyses revealed that SiC particles larger than $0.2\mu\text{m}$ were dispersed at the grain boundaries, while the SiC particles less than $0.1\mu\text{m}$ were located not only at the grain boundaries but also within the mullite matrix grains. As shown in Fig.1, the fracture strength of natural mullite ceramics were strongly improved by these nano-size SiC dispersions: 170MPa to 490MPa. The low toughness of natural mullite, $1.2\text{MPa}\cdot\text{m}^{1/2}$, was also improved to $3.3\text{MPa}\cdot\text{m}^{1/2}$. These high toughness and strength are almost comparable to those for advanced high-purity mullite ceramics and their composites. Furthermore, the high temperature strength was also improved remarkably: 770MPa at 1000°C . The final emphasis was placed on the understanding of effects of nano-size SiC dispersions on mechanical properties of natural mullite.

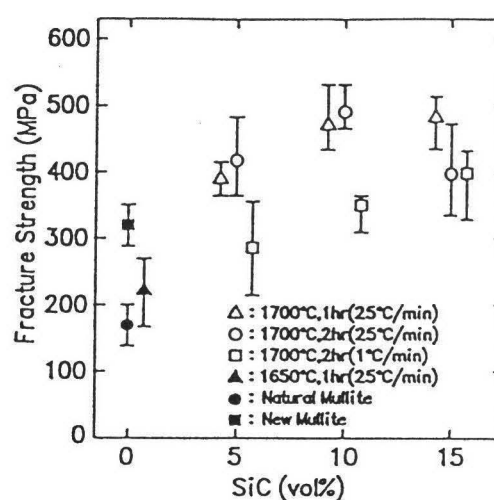


Fig.1 Effect of SiC dispersion on fracture strength for natural mullite/SiC nanocomposites.

Susceptibility of Cobalt(II)-Alginate Complex Films to Moisture

Hirofumi YAJIMA*¹, Toshiyuki MIYAMOTO*¹, Kei TAKAHASHI*¹, Ryuichi ENDO*¹
and Setsuko FURUYA*²

Co(II)-alginate complex film (ACF) prepared by soaking sodium alginate (Alg-Na) film in the solution of Co(II) salt is hydrochromic. In order to gain better information on the susceptibility of ACF to moisture and to explore the practicability of ACF for use as a humidity sensor, the effects of relative humidity (RH), thickness (D) of the film, and molecular weight (M_v) of Alg-Na on the hydrochromism of ACF were studied in the processes of adsorption and release of water. The ACF exhibited a blue shift of the maximum absorption band from 560 nm to 520 nm, accompanied by some hypochromism in the transient process, with the increase in the moisture content of the ACF (Fig. 1). The responsivity of hydrochromism of the ACF was increased with increasing the degree of the change in RH and with decreasing the D and M_v values. On the other hand, the study of the removal process of moisture from the ACF showed that the water molecules coordinated to Co^{2+} in the ACF were very difficult to release. The above results suggest that thin filmization and a considerable elevation of the rate of release of the coordinated water molecules are required to achieve enough practicability of ACF for use as a humidity sensor.

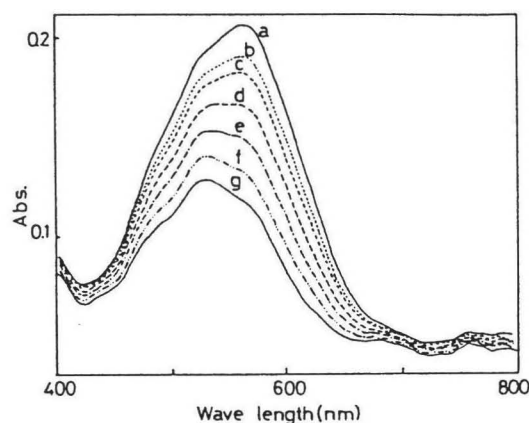


Fig. 1 Transient absorption spectra of ACF (3 cm \times 1 cm \times 13 μ m) for the environmental change of RH from 0% to 65%, where ACF was prepared from Alg-Na with M_v of 9.7×10^4 . Time (min): a, 0; b, 5; c, 10; d, 20; e, 30; f, 40; g, 50.

*1 Department of Applied Chemistry, Faculty of Science, Science University of Tokyo (1-3 Kagurazaka, Shinjuku-ku, Tokyo, 162 Japan)

*2 Research Institute for Polymers and Textiles (1-1-4 Higashi, Tsukuba, 305 Japan)

Synthesis and Characterization of Mullite Whiskers

○ Akihiro TANAKA, Kiyoshi OKADA and Nozomu OTSUKA

Department of Inorganic Materials, Tokyo Institute of Technology

Mullite, $\text{Al}_{4+2x}\text{Si}_{2-2x}\text{O}_{10-x}$, whiskers were synthesized by the chemical reaction between a mullite composition xerogel and AlF_3 . They are fired at $900\sim 1600^\circ\text{C}$ in a certain airtight container and/or an atmosphere controlled furnace. Two types of powders were prepared. The powder A was without AlF_3 and fired with AlF_3 powders in the container. The powder B was mixing AlF_3 in it. Fig. 1 shows the relation between an average whisker length and the firing temperature. The whiskers from the powder B were apparently longer than those from the powder A. They became longer as higher the firing temperature and were around $10\mu\text{m}$ in length when fired at 1600°C . Fig. 2 shows the relation between an average aspect ratio of whiskers and the firing temperature. They decreased as higher the firing temperature from around 25 at 1100°C to 10 at 1600°C . Longer duration at firing temperature was found to be effective to obtain longer whiskers. These whiskers were found to be elongated to the c-axis and the side planes were $\{110\}$ plane of a form by a TEM observation. Since no droplet was found on the tip of whiskers, these whiskers were concluded to be grown by the VS(vapor-solid) mechanism. Clear lattice image continued up to the edge of the whiskers in high resolution electronmicrographs and no defect structure was observed. Chemical composition of the whiskers was evaluated from XRD data and also from analytical TEM measurement. The whiskers prepared under 1200°C were found to be very much Al_2O_3 rich composition than stable mullite solid solution range while those above 1200°C were Al_2O_3 rich limit of solid solution range.

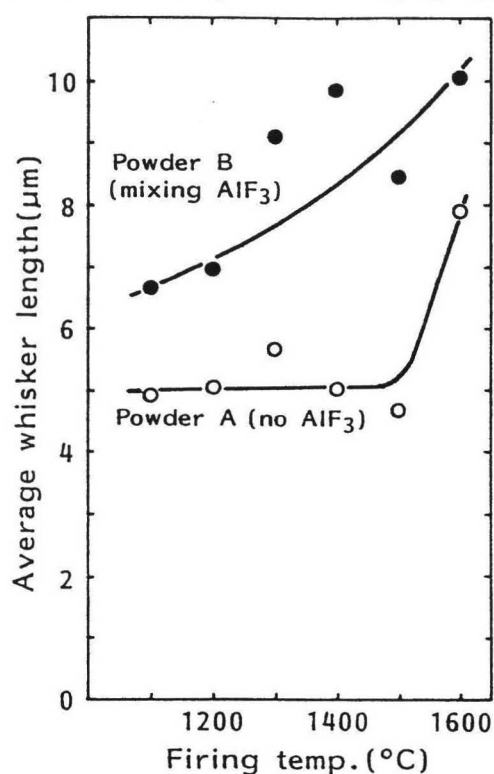


Fig.1 Average whisker length vs firing temp.

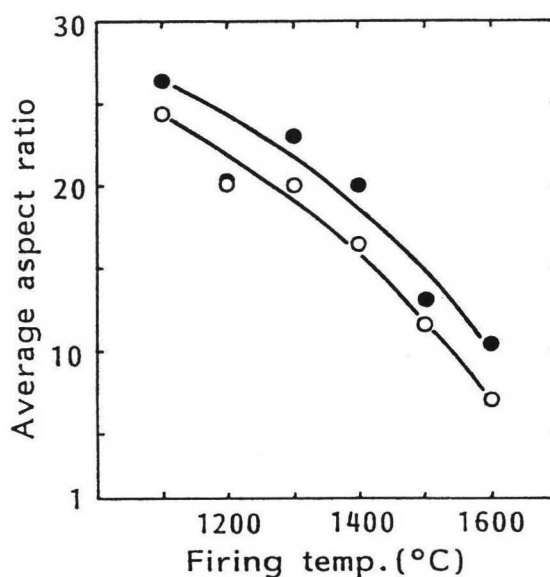


Fig.2 Average aspect ratio vs firing temp.

The Synthesis of High-purity Ceramics by Alkoxy-based Preparation

JWRI of Osaka Univ. Nobuya Iwamoto
Masayoshi Kamai
Graduate Student of Osaka Univ. ○ Masamichi Tanida

1. Introduction

Ceramics are comparably stable materials in body fluid, and expected to be artificial bone or teeth. To examine the degree of the affinity with body cell, high-purity specimens are required.

In present work, to obtain high-purity ceramics, alkoxy-based preparation method was applied. The properties of these specimens were investigated.

2. Experimental Method

Alkoxy-based preparation and normal sintering method were applied in order to obtain BaTiO_3 bulk specimens. The outline of former is as follows; Barium metal reacts with iso-propanol at 80°C in dried N_2 gas. Then, Barium iso-propoxide was formed. This one and Titanium tetra-propoxide and some additives were dissolved in iso-propanol. In the stirred solution, drops of deionized distilled water brought about hydrolysis reaction. The BaTiO_3 was precipitated from the solution. The hydrated oxide dried in air at 50°C was crushed. The high-purity submicron BaTiO_3 powder was prepared. In addition, the method can obtain bulks directly was also tried. The outline of latter is as follows; BaCO_3 and TiO_2 powder were stirred with ethanol in a ball mill for 24hrs. Then, it was dried in air at 50°C . Both of these powder were formed to be pellet and sintered in air at 1400°C for 2.2hrs.

3. Result

The experiment suggests that the specimens by alkoxy-based preparation method has remarkable better properties such as density, hardness, etc. It due to that powder was very formable and no gas generates in sintering reaction.

Table ; Results of knoop hardness

Sample	Condition	Knoop hardness	Remarks
BT	$1400^\circ\text{C}/2.2\text{hr.}$	70 (60.4 ~ 77.4)	non-additives
BTSG	$1400^\circ\text{C}/2.2\text{hr.}$	830 (658.1 ~ 990.9)	sol-gel powder
BT5S	$1400^\circ\text{C}/2.2\text{hr.}$	680 (665.5 ~ 690.7)	5 at.% SiO_2
BT3S	$1400^\circ\text{C}/2.2\text{hr.}$	330 (297.5 ~ 409.1)	3 at.% SiO_2
0.95BT5S	$1400^\circ\text{C}/2.2\text{hr.}$	430 (429.6 ~ 433.8)	Ba:Ti=0.95:1
0.90BT5S	$1400^\circ\text{C}/2.2\text{hr.}$	360 (327.6 ~ 429.6)	Ba:Ti=0.90:1

(load; 50 ~ 100g load time 15sec.)

NEW WAY TO PRODUCE TITANIUM BY ELECTRON BEAM REMELTING

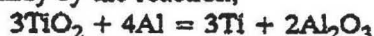
Toshifumi Yahata

Institute of Industrial Science, University of Tokyo

Titanium is conventionally produced by a chloride based technique "Kroll-method". A chlorination in this process is rather dangerous and its cost is high. Reduction of TiCl_4 by Mg is a key reaction and the electro-winning of Mg is the most energy consuming step. We propose a new process. We have developed a less expensive process to produce titanium by the combination of Aluminothermic Reduction(ATR) and the deoxidation by melting in the Electron Beam Remelting Furnace.

1.ATR

We can produce Ti-Al alloy by the reaction,



in an atmosphere of argon at 1700°C . This reaction lasted for about twenty minutes. As shown in figure 1, when Al/TiO₂ molar ratio was 1.3 (which is the stoichiometric ratio), the produced alloy contained 6wt% oxygen. And when the ratio was 2.2, the oxygen content was about 1wt%. Since the oxygen content required for the commercial product of titanium is 0.2wt%, the deoxidising process is necessary.

2.Deoxidation of Titanium by Electron Beam Remelting

The Electron Beam Furnace can treat at very high temperature and clean vacuum. But when we melted only pure titanium, oxygen in titanium concentrated because of evaporation of titanium. In short, we can't deoxidise it as an oxygen gas.

Figure 2 is a result after we treated Ti-Al alloy containing 10wt% aluminum and 10wt% oxygen. As long as aluminum existed in titanium, oxygen content decreased. Oxygen in titanium was removed as an aluminum oxide gas. A possible gas species is AlO , Al_2O , AlO_2 or Al_2O_2 . In order to determine the gas species, we assume that a thermodynamic equilibrium on the surface is attained. From the amount of evaporation we can calculate that the surface temperature is 2150K and that the activity of aluminum at 2150K is 0.003 when its molar ratio is 0.1. From these values we can presume that we deoxidised titanium as an Al_2O gas.

To investigate a deoxidation limit, we treated titanium containing 0.13wt% oxygen while adding aluminum. When the aluminum content increased to about 6wt%, the oxygen content decreased to 0.05wt%.

Conclusion;

- (1)We can produce Ti-Al alloy containing 1wt% oxygen by ATR, and this reaction lasts for about twenty minutes.
- (2)By Electron-Beam Remelting, we can deoxidise Ti-Al alloy as an Al_2O gas. And when the aluminum content is 6wt%, the oxygen content decrease to 0.05wt%.

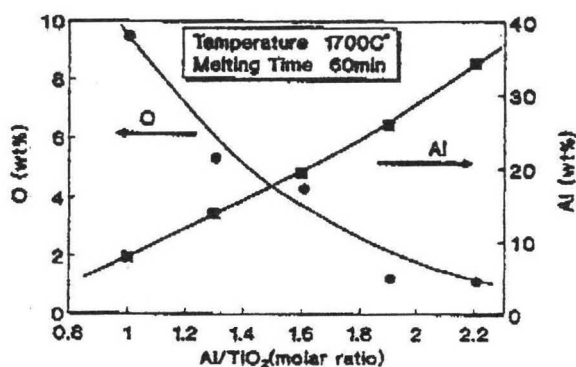


Fig.1 Oxygen and Aluminum content vs. Al/TiO_2 molar ratio

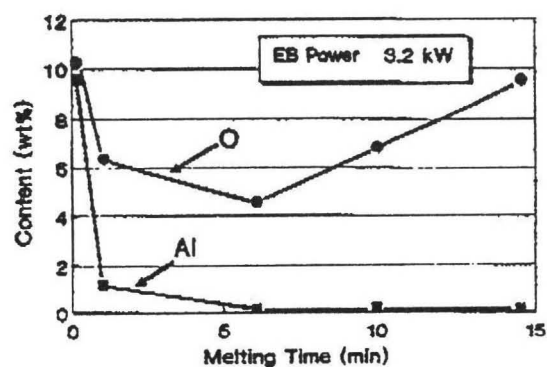


Fig.2 Oxygen and Aluminum content as a function of Melting Time

DECOMPOSITION OF ALPHA PHASE IN Ti-40%Al ALLOY

Yoko YAMABE and Makoto KIKUCHI

Department of Metallurgical Engineering
Tokyo Institute of Technology, Tokyo 152, Japan

A lamellar microstructure, consisted of γ -TiAl and α_2 -Ti₃Al alternate lamellae, is an important microstructural constituent in gamma titanium aluminides. Mechanisms of its formation have not yet fully been established. In this paper, the decomposition process of a high temperature alpha phase was investigated using a eutectoid composition with Ti-40 at%Al binary alloy.

The binary titanium aluminum alloy with 40 at% Al was first homogenized at 1250°C, where a disordered hcp alpha phase is stable. The homogenized specimens were directly quenched in a two phase region between 900 and 1100°C, where the ordered α_2 with a structure of DO₁₉ and the ordered gamma with a structure of L1₀ are stable. The microstructure was observed by optical as well as electron microscopy.

Ordering of the alpha phase into the α_2 phase took first place, followed by gamma plates formation in the ordered α_2 phase. The gamma plates nucleated preferentially at the grain boundary and grew into grain interior on a unique basal plane of the α_2 phase, as a habit plane. This precipitation process produced the gamma/ α_2 lamellar microstructure. The lamellar microstructure formed by this mechanism is termed as the primary gamma/ α_2 lamellar structure in order to distinguish the gamma/ α_2 lamellae produced by discontinuous coarsening.

The orientation relationship between the α_2 matrix and the gamma precipitate strictly obeyed the Blackburn orientation relationship. Six variants, which were predicted by a geometrical consideration, were confirmed to exist experimentally. Relative orientation relations between adjacent gamma plates were confined to only four types. Each type contained two different atomic arrangements due to the ordered structure of the gamma phase.

This formation mechanism of the gamma/ α_2 lamellar microstructure can successfully explain most microstructural features of the gamma/ α_2 lamellae observed in titanium aluminides with higher aluminum concentrations by other investigators.

Hydrothermal synthesis of LiTaO_3 Thin Film on Ta Substrate

○ Hidemasa YAMAGUCHI, Nobuo ISHIZAWA, Masahiro YOSHIMURA
Research Laboratory of Engineering Materials, Tokyo
Institute of Technology

【Introduction】

New formation techniques for the films of complex oxides called as hydrothermal and/or hydrothermal-electrochemical methods have been developed in our groups. We could previously prepare LiNbO_3 thick films by hydrothermal-electrochemical method (Room Temperature \sim 200 $^{\circ}\text{C}$). But those films were not dense, because sparking was needed in the formation process. In the present study, LiTaO_3 thin films were prepared by hydrothermal synthesis at higher temperature (300 \sim 400 $^{\circ}\text{C}$).

【Experimental】

A Ta metal plate and a LiOH aqueous solution of fixed concentration (0.01M \sim 5M) were sealed in an Au capsule. This capsule was hydrothermally treated at 300 $^{\circ}\text{C}$ \sim 400 $^{\circ}\text{C}$ under 30 \sim 60MPa in a test tube type vessel filled up with distilled water. At 200 $^{\circ}\text{C}$ the Ta plate was directly treated in the solution in an autoclave. The constituent phases of the films were analyzed by an X-ray diffractometer equipped with a thin film attachment, where the gracing angle was fixed at 0.5 $^{\circ}$.

【Results and Discussion】

Well-crystallized polycrystalline LiTaO_3 thin films were formed on the surface of Ta plate (Fig.1) by the simple hydrothermal method under the limited conditions of above 300 $^{\circ}\text{C}$ in 0.03 \sim 0.07M LiOH solutions. IN low concentration LiOH solution (0.01M), or below 200 $^{\circ}\text{C}$ no apparent films were formed even under the applied voltage of 15 V. Above results clearly indicate the temperature (above 300 $^{\circ}\text{C}$) are effective to make Ta oxides and react with Li components in the solution.

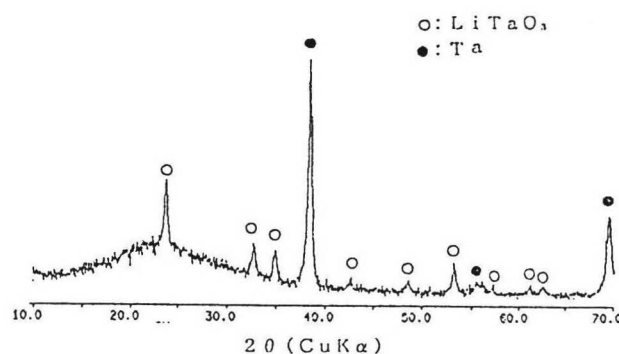


Fig.1. XRD pattern of a LiTaO_3 film formed in 0.05M LiOH at 300 $^{\circ}\text{C}$ under 30MPa for 60min.

New molecular design method for noncentrosymmetric crystal structure

Lambda (Λ) shape molecules for frequency doubling

H.Yamamoto, S.Katogi, T.Watanabe, H.Sato, S.Miyata, T.Hosomi*

Chemical and Biological Science and Technology, Tokyo University
of Agriculture and Technology, 2-24-16, Nakamachi, Koganei-shi,
Tokyo 184 Japan

* Sumitomo Bakelite Co.,Ltd., 495, Akiba-cho, Totsuka-ku,
Yokohama-shi, Kanagawa 245 Japan

Recently, organic materials have much attention for nonlinear optical applications such as frequency doubler and electro-optic device because of their large second-order nonlinearities[1,2]. For the efficient SHG, the organic molecules must possess a large second-order hyperpolarizability β and also must crystallize into the lack of inversion center. We investigated a new molecular design method for noncentrosymmetric crystal structure. Molecular-orbital calculation by MOPAC AM1 method demonstrated that the conformations of the methanediimine derivatives, such as N,N'-bis-(p-nitrophenyl)-methanediimine (p-NMDA), became lambda (Λ) shape. The Λ shape molecules seem to form noncentrosymmetric crystals because they easily stack along one direction.

The intramolecular charge-transfer contribution to the nonlinear polarizabilities of Λ shape molecules has almost a two-dimensional character, therefore the predominant β component is not β_{yyy} but β_{yxx} .

Almost all methanediimines synthesized in our laboratory form noncentrosymmetric structures and show SHG activities in the powder form. As the results of crystal structure analyses, we have found the Λ shape molecules stacking along one direction, which means all the molecular dipole moments align parallel to the crystal axis. And it has been found that the packing density of Λ shape molecules increased when they were stacking. This is close to an optimum orientation for bulk phase-matched nonlinearity, as reported by Zyss et al[3]. According to the oriented gas model, therefore, the largest β tensor effectively contributes to the phase-matchable nonlinear optical coefficient, for example d_{yxx} . This molecular concept leads easily the design of the phase-matchable SHG materials.

- [1] D.J.Williams, ed., Nonlinear optical properties of organic and polymeric materials, ACS Sym. Ser. 233(Am.Chem.Soc., Washington, 1983)
- [2] D.S.Chemla and J.Zyss, ed., Nonlinear optical properties of organic molecules and crystals. Vols.1,2 (Academic Press. Inc. Orlando, 1987)
- [3] J.Zyss and J.L.Oudar, Phys.Rev. A26, 2016 and 2028(1982)

Effect of the substrate on diamond synthesis in gas phase

Yo-ichi YAZAKI, Hisako HIRAI^A, Hiroyuki IKAWA, Osamu FUKUNAGA

Faculty of Engineering, Tokyo Institute of Technology, Meguro, Tokyo

^A Research Laboratory of Engineering Materials, T.I.T, Yokohama

We synthesized diamond on to the four substrate materials; Silicon(Si), Aluminium Nitride(AlN), cubic Boron Nitride(cBN) and Pyrolytic Boron Nitride(P-BN) by microwave plasma CVD method. [only Si is a single crystal and others are polycrystals] Before deposition, each substrate is polished by $6,3,1\mu\text{m}$ diamond subsequently. Depositing condition is as follows: substrate temperature 860°C , methane concentration 0.6%, flow rate 100SCCM, total pressure 40torr, time 5, 15, 30min and 1hour. In order to observe the essential effect of substrate on synthesized diamond, we analyze nucleation density of diamond before growing to the film. Synthesized diamond is observed scanning electron microscope, and its quality is estimated by Raman spectra.

Results obtained as follows: On Si, AlN and P-BN, diamond film is formed after about 1 hour reaction, but on cBN, more than 3 hours reaction is necessary to grow to the film.(Fig.1) Diamond nucleation density on Si substrate is largest and that on cBN is smallest.(Fig.2) Raman spectrum of diamond on each substrate appears near 1333cm^{-1} , and full width of half maximum of diamond on AlN or cBN or P-BN (FWHM $9\text{-}10\text{cm}^{-1}$) is smaller than that on Si (FWHM 20cm^{-1}).

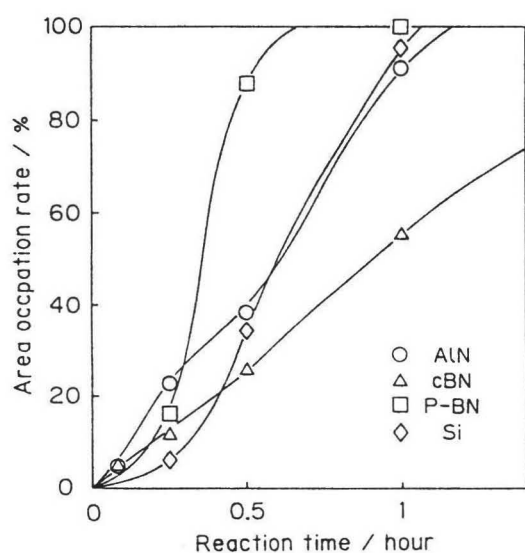


Fig.1 Area occupation rate of diamond on substrates

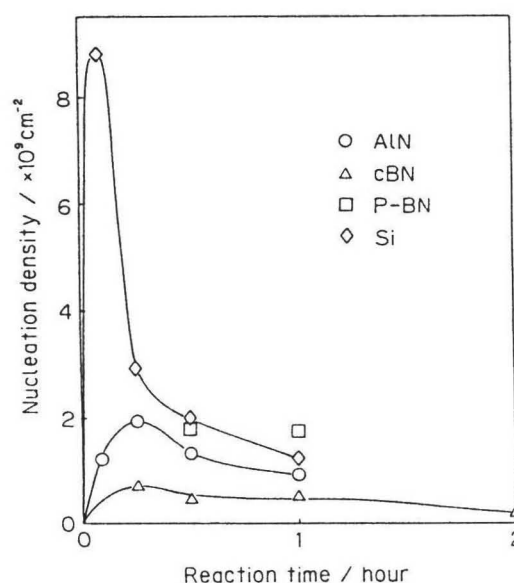


Fig.2 Nucleation density of diamond on substrate

Enhancement of the Magneto-optical Rotation of Fe Films due to Ion implantation

K. Aoyagi

Faculty of engineering, Yokohama National University,
Hodogaya-ku, Yokohama 240, Japan

Enhancement of magneto-optical rotation is required for disk materials of magneto-optical recording systems. In order to seek new magneto-optical materials, we have studied the surface modification due to ion implantation technique, because the magneto-optical effects are influenced by the characteristics of thin surface layers of the films. We have reported that the specific Faraday rotation of 3d-transition metal films is enhanced by ion implantation at low doses for any kind of ion.¹⁾ Particularly, Tb⁺ implanted Fe films show the enhancement of the specific Faraday rotation up to 30%. On the other hand, Fe⁺ implanted Fe films also show the similar effect without compositional changes. Such self-ion implantation is expected to cause only non-equilibrium disorder in the target films. This experimental result indicates that the magneto-optical effect is strongly influenced by the structural changes due to the high energy ion bombardment. Electrical resistance, ferromagnetic resonance (FMR) and TEM studies confirm the structural changes at the low dose region. It should be noted that at this doses, the optical constants n and κ exhibit minima. The specific Faraday rotation depends on the optical constants and the complex off-diagonal components of the conductivity tensor. In the case of self-ion implantation, the off-diagonal components are not influenced, but only the diagonal components, the optical constants, change by implantation, and their changes induce the enhancement of the Faraday rotation. To examine the result due to the change of off-diagonal components, we have tried to form Fe₁₆N₂ thin films by nitrogen implantation and measure its Faraday rotation by using a pulse magnetic field up to 4.3T. The Fe₁₆N₂ thin film is a metastable state compound and it has high saturation magnetization of 2.8T.²⁾ This compound is expected to exhibit considerable Faraday rotation due to its high saturation magnetization. The formation of Fe₁₆N₂ in the Fe films was confirmed by the saturation of the Faraday rotation at its saturation magnetic field.

- [1] Y. Gondō, K. Aoyagi and H. Kogure, J. Appl. Phys. 69 (1991),
to be published.
- [2] T. K. Kim and M. Takahashi, Appl. Phys. Lett., 20, 492 (1972).

Ag/Cu multilayered films prepared by different vapor deposition methods

Katsuki HAZAMA, Jun'ichi KOZAKI, Koji HACHIYAMA and Osamu NITTONO

Department of Metallurgy, Tokyo Institute of Technology

Multilayered films with artificial periods have been prepared by various methods. It is considered that the preparation conditions including the deposition method can affect the internal structure of multilayered films, especially the microstructure around the interface between two constituent layers. Therefore, we are interested in the characteristics of multilayered films prepared by different deposition methods.

We prepared Ag/Cu multilayered films by two different methods:

a) vacuum evaporation method: The base vacuum system was in the range of 10^{-8} Torr and the vacuum during deposition was kept below 2×10^{-6} Torr. Silver and copper were evaporated separately from two alumina-coated crucibles. The deposition rate of each element and the deposited amount are monitored by a quartz oscillating thickness sensor. The deposition rate was 0.2 nm/sec. The deposited amount of each silver or copper layer was controlled within an accuracy better than 0.2 nm, being less than the thickness of one atomic layer. The substrates were cooled down to -140°C .

b) dc-sputtering method: The base pressure was below 1.8×10^{-6} Torr and sputtering Ar gas pressure was 9.0×10^{-4} Torr. The deposition rate proved to be a function of target current. The applied voltage and the target current were 700 ~ 800 V and 100 ~ 200 mA respectively. Under these conditions, the deposition rate was about 0.05 nm/sec. The substrate temperature was less than 50°C .

In both cases, films were prepared on glass substrates.

The structures of multilayered films were investigated by using X-ray diffraction. By the both methods, every profile had a clear first-order peak at the low-angle part. The values calculated from observed peaks were comparable with designed periods. In addition, at the middle-angle part, there were some splitting peaks, and they were not identified with the reflection peaks due to silver or copper, however, for the samples of large periods, splitting peaks were very different from each other in both the peak positions and the intensities.

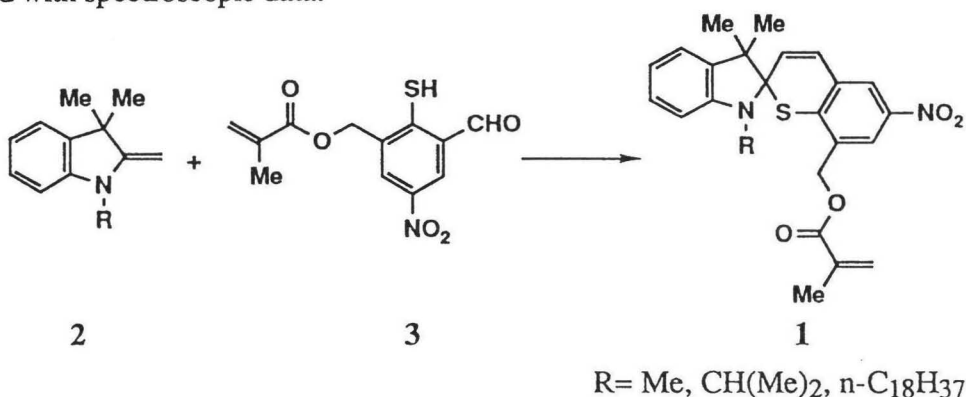
The results of computer simulation confirmed that the different profiles between the two methods reflect a difference in lattice spacing for each layer.

A. MIYASHITA, M. HIRANO, and H. NOHIRA

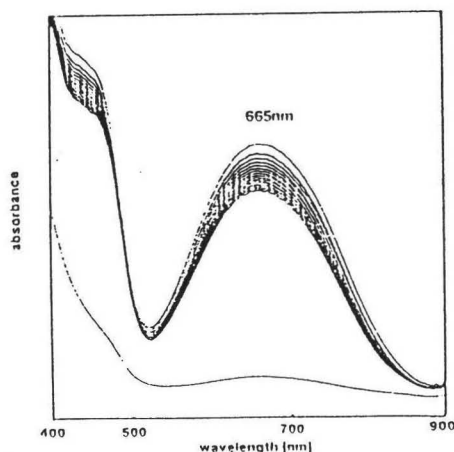
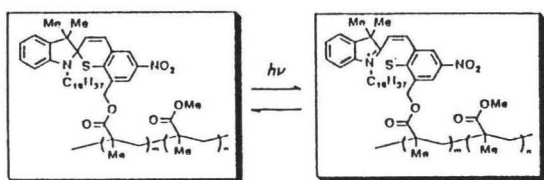
 Department of Applied Chemistry, Faculty of Engineering, Saitama University,
 255 Shimo-ohkubo, Urawa 338

Much attention has been currently focused on the photochromic spiropyranes because of their potential utilities for photo-information memory devices. However, the colored forms of spiropyranes are usually thermodynamically unstable so that they convert to stabler colorless forms in a few minutes spontaneously.

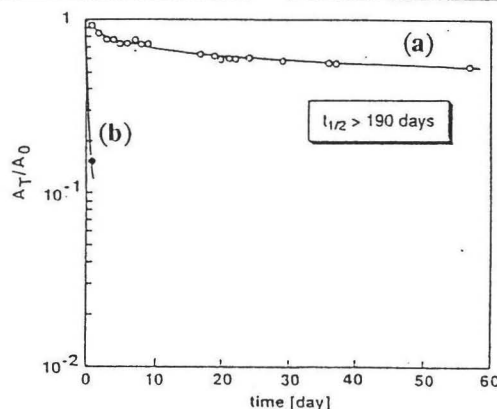
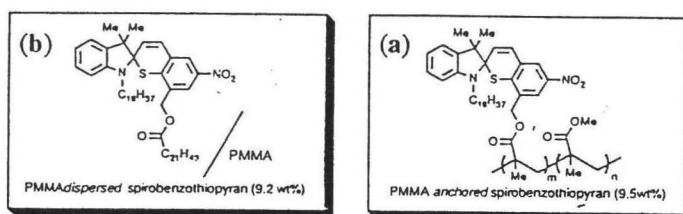
Spiropyran 1 were newly prepared by the reaction of 3,3-dimethyl-2-methyleneindoline (2) with 3-methacryloxymethyl-5-nitrothiosalicylaldehyde 3 in refluxing 2-butanone and mostly characterized with spectroscopic data.



By the copolymerization of 1 with MMA or styrene, photochromic copolymers have been afforded in good yield. Especially, the metastable colored form of the N-octadecyl spirobenzothiopyran with MMA copolymer has the absorption maxima at 665 nm and the half-life is more than 190 days at room temperature in dark.



Electronic spectra of N-octadecyl spirobenzothiopyran-MMA copolymer



Thermal bleaching of colored spiropyran-MMA copolymer (a) and spiropyran composite in PMMA (b)

Characterization of Defect and Relation between Defect Size
Distribution and Fracture Strength in Y-TZP Ceramics

Jin-Young Kim, Zenji Kato, Nozomu Uchida, Keizo Uematsu,
Katsuichi Saito

(Nagaoka University of Technology)

To understand the defect-strength relation for high-strength Y-TZP ceramics, internal defects with size down to 1 μm are characterized with an transmission optical microscope in a high density Y-TZP ceramics and are corelated to the fracture strength. The specimens are prepared by sintering at 1500 $^{\circ}\text{C}$ for 2h and by post-HIPing at 1300-1500 $^{\circ}\text{C}$, 100MPa for 2h. Populations of defects decrease significantly by HIP treatment and with increasing HIP temperature, but there are small but distinct populations of large defects in the size range of tens of micrometer. Fracture toughness of each specimen determined by SEPB method is almost constant and about 4.5 $\text{MN}\cdot\text{m}^{-3/2}$. Fracture strength measured by 3-point bending increases significantly by HIP treatment and with increasing HIP temperature. Influence of defect size distribution on fracture strength will be also discussed.

Difference in High Temperature Creep Behaviors
Between As-Cast TiAl and Homogenized TiAl

Myunghoe KOO, Takashi MATSUO and Makoto KIKUCHI

Department of Metallurgical Engineering,
Tokyo Institute of Technology, Tokyo 152, Japan

Compared with a microstructure of a homogenized TiAl having a gamma single phase, the microstructural features of an as-cast TiAl is characterized by mixed structure of two regions; a lamellar colony and a gamma phase region. The lamellar colonies consist of thin plates of Ti_3Al and TiAl plates with a very high dislocation density. In spite of the above large difference in the microstructures, the creep behavior of the as-cast TiAl has not been studied in detail. In this study, the difference in creep rate-time (or strain) curves between the as-cast TiAl and the homogenized TiAl were investigated by correlating with the difference in dislocation substructures formed during creep deformation.

Constant stress creep tests were carried out at 1123K in the stress range of 69 to 245MPa and the dislocation substructures of the creep interrupted specimens and the ruptured ones were examined.

Both of the as-cast TiAl and the homogenized one showed extended accelerating creep stage occupying more than 80 % of the rupture life. And there were not large differences in creep rate during accelerating stage between the as-cast TiAl and the homogenizing one.

All over the transient stage, however, the as-cast TiAl showed about eightfold larger creep rate than the homogenized one, and this larger creep rate of an as-cast TiAl continued up to the onset of the accelerating stage. The strain at the time of minimum creep rate of an as-cast TiAl was about tenfold larger than that of a homogenized TiAl.

During the accelerating stages in both of as-cast TiAl and a homogenized one, proceeding of the subgrains was observed, and there were no marked difference in the development of subgrains.

During the transient creep stage in the as-cast TiAl, the dislocation density in the lamellar regions decreased drastically, and the hardness also decreased dramatically. This softening phenomenon during the transient stage, unlike in the homogenized one, could not be correlated to the decrease in the creep rate during transient stage.

Consequently, the decrease in creep rate during transient stage was explained by the annihilation of excessive dislocations in the lamellar regions.

Electrical Properties of $\text{ZrO}_2\text{-TiO}_2\text{-Y}_2\text{O}_3$ System

Hitoshi NAITO and Haruo ARASHI

Research Institute for Scientific Measurements, Tohoku University
1-1, 2-Chome, Katahira, Aoba-ku, SENDAI 980, JAPAN

Mixed electronic-ionic conductors have many applications such as electrodes and membrane for gas separation. If $\text{ZrO}_2\text{-TiO}_2\text{-Y}_2\text{O}_3$ system shows mixed conduction, it is applicable to electrode of SOFC because of its thermal stability and good adherency to solid electrolyte such as yttria stabilized zirconia(YSZ). To assure its possibility, its fundamental studies, especially electrical properties, are required. In this study the sintered specimens were prepared at 1750°C in air by means of solid-state reaction. The temperature dependence of total conductivity in this system shows an anomalous behavior as shown in Fig. 1. To clarify this conduction mechanism, the ionic transport number was measured by EMF method in a concentration cell. The result indicated that this system exhibited only ionic conduction as shown in Fig. 2. If this system exhibits electronic conduction, it is expected that titanium takes two valence states of $4+$ and $3+$. The valence states of titanium in this system were determined by XPS. The results indicated that only Ti^{4+} was present in this system. When these specimens were treated up to 1400°C under strongly reducing condition, their color changed from white to pale gray. This suggests that titanium in the reduced specimens is present in both $4+$ and $3+$ valence states and exhibits electronic conduction. To investigate oxygen partial pressure dependence of conductivity, conductivity measurements under reducing atmosphere are in progress.

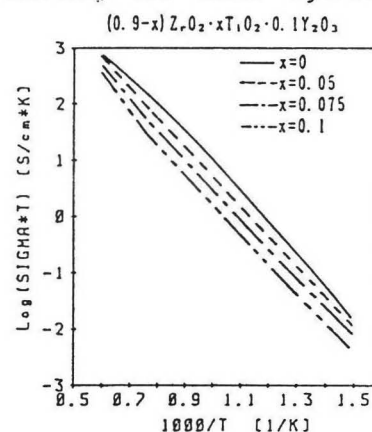


Fig. 1 Temperature dependence of total conductivity in $\text{ZrO}_2\text{-TiO}_2\text{-Y}_2\text{O}_3$ system

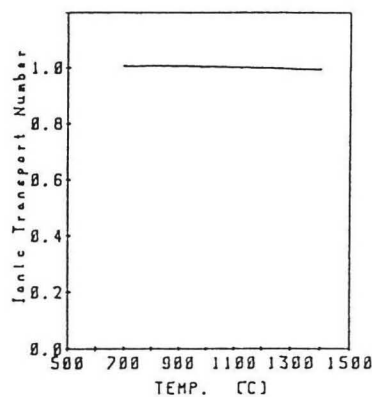


Fig. 2 Temperature dependence of ionic transport number of $0.8\text{ZrO}_2\text{-}0.1\text{TiO}_2\text{-}0.1\text{Y}_2\text{O}_3$

SOLID SOLUTION STRENGTHENING DUE TO CHROMIUM AND MOLYBDENUM IN HIGH TEMPERATURE CREEP
IN AN AUSTENITIC SINGLE PHASE ALLOY
-EFFECT OF DISLOCATION SUBSTRUCTURE FORMATION-

Kaname NAKAJIMA, Takashi MATSUO and Makoto KIKUCHI

Department of Metallurgical Engineering
Tokyo Institute of Technology, Tokyo 152, Japan

In austenitic heat resisting steels, dispersion strengthening due to carbides is the most beneficial strengthening method to increase the high temperature creep resistance, and a morphology of carbide precipitation strongly depends on the dislocation substructures formed during creep, because the dislocation substructure operates as the precipitation site of carbides.

Such dislocation substructures with the uniform distribution and high density are available to obtain the high precipitation density of carbides with a high creep resistance, such high precipitation density of carbides yields further high dislocation density during creep. It has been understood that the solid solution strengthener such as chromium and molybdenum affects the dislocation substructures formed in austenitic single phase alloys during creep, but the any basic study on the effect of solid solution strengthener on dislocation substructure formed in austenitic single phase has not been examined.

On the other hand, under the conditions of higher temperatures and lower stresses, the creep resistance of an austenitic heat resisting steel would be determined by the intrinsic strength of the austenite matrix, because of instability of the carbide dispersion strengthening. To confirm the intrinsic strength of the austenite matrix after long term exposure at high temperature, the stress dependence of solid solution strengthening must be examined.

In the austenitic single phase steels, the subgrain formation which leads to decrease in creep resistance, restricted at the higher stresses and the higher temperatures, because the stacking fault energy in the austenitic steels is substantially lower than that in the nickel base alloys. From this reason, the approach on the correlation between the stress dependence of solid solution strengthening and the dislocation substructures should be conducted by using the materials such as the nickel base alloys.

In this study, the change in dislocation substructures formed during high temperature creep with the additions of the solid solution strengthener, chromium and molybdenum and their stress dependence were investigated over a wide stress range, and were correlated with the changes in the creep resistance and the internal stress with the additions of chromium and molybdenum by carrying out the constant stress creep tests at 14.7 ~ 68.6 MPa at 1,173 K for Ni-10 wt pct Cr, Ni-30 wt pct Cr and Ni-10Cr-5 wt pct Mo alloys.

About one order of the magnitude decreases in minimum creep rate by the additions of 20 wt pct chromium and 5 wt pct molybdenum were obtained at 68.6 MPa, and the decreasing rate of minimum creep rate due to a chromium and molybdenum decreased with decreasing the stress levels.

The dislocation substructures in a Ni-10Cr alloy turned to the more uniform distribution and higher density of dislocations by the additions of chromium and molybdenum, particularly at the higher stresses, the evolution of subgrains occurred in a Ni-10Cr alloy was suppressed by the additions of chromium and molybdenum. In a Ni-10Cr alloy, both of the increasing rates of the dislocation density within subgrains and the internal stress with stress became smaller at the higher stresses, corresponding to the evolution of subgrains. By the additions of chromium and molybdenum to a Ni-10Cr alloy, however, the increasing rates of the dislocation density and the internal stress with stress remained unchanged at the higher stresses.

Consequently, the larger solid solution strengthening effects due to chromium and molybdenum at the higher stresses would be attributed to the retarding effects of chromium and molybdenum against the evolution of subgrains.

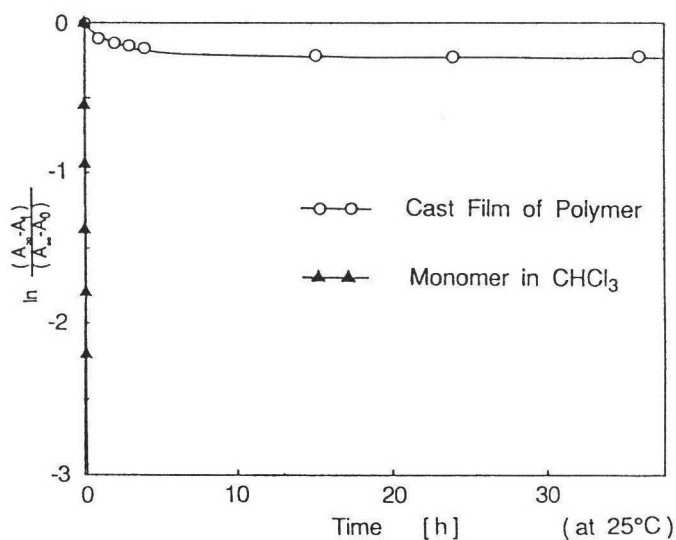
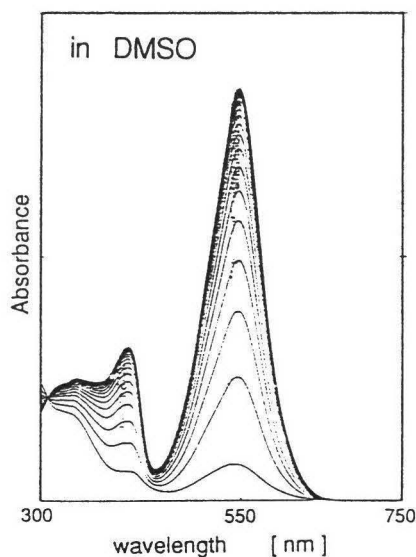
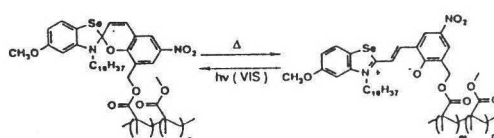
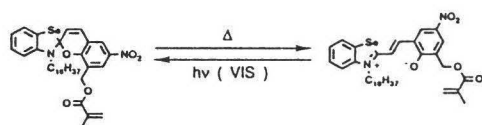
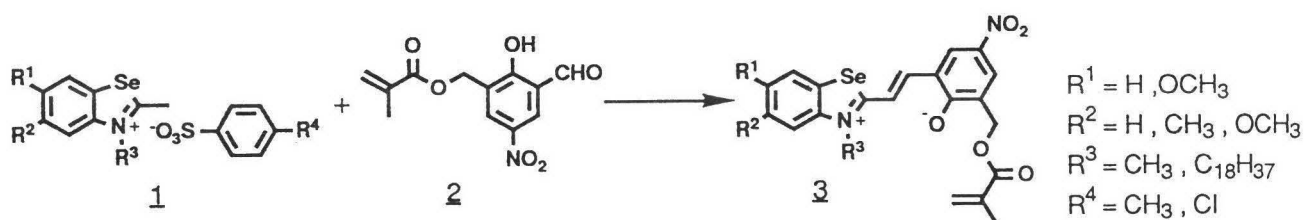
Synthesis of New Reverse-photochromic Spirobenzo-selenazolinobenzopyran Polymers

A. MIYASHITA, S. NAKANQ, and H. NOHIRA

Department of Applied Chemistry, Faculty of Engineering, Saitama University,
255 Shimo-ohkubo, Urawa 338

Recently, various photochromic compounds are extensively re-investigated from the viewpoint of application to photo-information memory devices. We have studied new photochromic polymers contained various spiropyrans as side chain. Here, we demonstrate about synthesis of new reverse-photochromic spirobenzoselenazolinobenzopyran polymers and their photochromic properties.

Spirobenzoselenazolinobenzopyrans are usually colored form (ring-opened PMC form), and show reverse-photochromism. Ring-opened spirobenzoselenazolinobenzopyrans having a methacryloxymethyl group **3** were prepared by the reaction of 3-alkyl-2-methylbenzoselenazolenium benzenesulfonate **1** with 3-methacryloxymethyl-5-nitrosalicylaldehyde **2**. UV-Vis spectrum of **3** [$R^1, R^2=H, R^3=C_{18}H_{37}$ on exposure to Vis light ($>500\text{nm}$) in DMSO] is shown in Figure. Reverse-photochromic polymers were obtained as purple solid by the copolymerization of **3** with MMA. On exposure to Vis light ($>500\text{nm}$), the color of these polymers (cast film) changed from purple to colorless and then, those colorless states were kept after a little initial coloration for a long time at room temperature ($\tau_{1/2} = >80\text{days}$).



CHLORINE- AND OXYGEN-RELATED PARAMAGNETIC CENTERS IN
VUV-IRRADIATED HIGH-PURITY SILICAS

Hiroyuki Nishikawa, Ryuta Nakamura, Kaya Nagasawa*,
Yoshimichi Ohki, and Yoshimasa Hama

Department of Electrical Engineering, Waseda University,
3-4-1 Ohkubo, Shinjuku-ku, Tokyo 169, Japan.

*Department of Electrical Engineering, Shonan Institute of
Technology, 1-1-25 Tsujido-Nishi-kaigan, Fujisawa,
Kanagawa 251, Japan.

Impurity related paramagnetic defects in VUV-irradiated silica glasses are investigated by the electron spin resonance (ESR) technique. ESR measurements were performed at 77K and X band ($\nu \approx 9.2\text{GHz}$). Various types of silicas were exposed to the unfocused beam of F_2 excimer laser (7.9 eV, 157nm) at room temperature through an optical path purged with N_2 gas. We observed, for the first time, chlorine- and oxygen-related species which are stable at room temperature, together with fundamental defect centers such as E' center, nonbridging oxygen hole center, and peroxy radical. The chlorine-related radical exhibits a hyperfine structure. A signal centered around $g \approx 2.02$ is probably due to excess oxygen. Isochronal annealing experiments show that both of the chlorine- and oxygen-related species grow up to 100-200 °C.

Deformation behavior in dispersion strengthened

Al-8mass%Fe alloy at high temperatures

*Yoshinobu SAKURAI

Abstract

An Al-8mass%Fe alloy prepared by a single roller technique has uniformly dispersed fine second phase particles and fine grains. The alloy containing about 20 volume percent of the second phases is typical dispersion strengthened material for using at high temperature condition. These fine grains and particles are effective strengthening factors for room temperature mechanical properties. While, in high temperature ranges over $1/2 T_m$, the influence of these fine structures to the deformation mechanism is not clear. In this study, compression test and relaxation test are performed at temperatures up to 450°C and at strain rates from $5 \times 10^{-5} \text{s}^{-1}$ to $5 \times 10^{-2} \text{s}^{-1}$ for Al-8mass%Fe and Zr-containing alloys to measure flow stress and internal stress. The relation between flow stress at about 5% strain and strain rate can be expressed by the power law equation. The flow stress increases with increasing strain rate and decreasing temperature. The stress exponents decrease from 12 (300°C) to 7 (450°C) and the apparent activation energies are much greater than that of aluminum lattice diffusion. There are no differences between two alloys in these phenomena. The internal stress of Al-8mass%Fe alloy obtained by relaxation test decreases with increasing temperature and shows no strain rate dependence. Logarithm effective stress (flow stress - internal stress) vs logarithm strain rate shows a linear relationship, and the stress exponents are $3.9 \sim 4.5$. The activation energy for deformation is 83kJ/mol . These results suggest that alternative diffusion mechanisms should be considered, which drives lower activation energy than that of lattice diffusion. The internal stress of Zr-containing alloy heat-treated at 520°C for 1h is higher than that of Al-8mass%Fe alloy up to 350°C . This results from precipitation of metastable L_{12} Al_3Zr phase, however the difference diminishes at 400°C .

*:Graduate Student, Tokyo Institute of Technology (Meguro-ku, Tokyo).

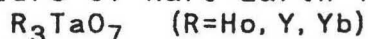
Deformation behavior in dispersion strengthened Al-8mass%Fe alloy at high temperatures

*Yoshinobu SAKURAI

Abstract

An Al-8mass%Fe alloy prepared by a single roller technique has uniformly dispersed fine second phase particles and fine grains. The alloy containing about 20 volume percent of the second phases is typical dispersion strengthened material for using at high temperature condition. These fine grains and particles are effective strengthening factors for room temperature mechanical properties. While, in high temperature ranges over $1/2 T_m$, the influence of these fine structures to the deformation mechanism is not clear. In this study, compression test and relaxation test are performed at temperatures up to 450°C and at strain rates from $5 \times 10^{-5} \text{s}^{-1}$ to $5 \times 10^{-2} \text{s}^{-1}$ for Al-8mass%Fe and Zr-containing alloys to measure flow stress and internal stress. The relation between flow stress at about 5% strain and strain rate can be expressed by the power law equation. The flow stress increases with increasing strain rate and decreasing temperature. The stress exponents decrease from 12 (300°C) to 7 (450°C) and the apparent activation energies are much greater than that of aluminum lattice diffusion. There are no differences between two alloys in these phenomena. The internal stress of Al-8mass%Fe alloy obtained by relaxation test decreases with increasing temperature and shows no strain rate dependence. Logarithm effective stress (flow stress - internal stress) vs logarithm strain rate shows a linear relationship, and the stress exponents are 3.9~4.5. The activation energy for deformation is 83kJ/mol. These results suggest that alternative diffusion mechanisms should be considered, which drives lower activation energy than that of lattice diffusion. The internal stress of Zr-containing alloy heat-treated at 520°C for 1h is higher than that of Al-8mass%Fe alloy up to 350°C. This results from precipitation of metastable L_{12} Al_3Zr phase, however the difference diminishes at 400°C.

Superstructure of Rare-Earth Tantalum Oxides



O Taisuke Tanaka, Yasunori Tabira, Nobuo Ishizawa

Fumiyuki Marumo, Masahiro Yoshimura

Research Laboratory of Engineering Materials,

Tokyo Institute of Technology

[Introduction]

Rare-Earth Tantalum Oxides R_3TaO_7 ($R=Ho, Y, Yb$) have defect fluorite-type structure. The diffuse scattering was found in diffraction pattern of Y_3TaO_7 ¹⁾. We observed the microstruture of R_3TaO_7 ($R=Ho, Y, Yb$) by TEM (transmission electron microscopy) to study the origin of those diffuse scattering.

[Experimental]

Single crystals of R_3TaO_7 (75mol% Y_2O_3 - Ta_2O_5) were grown by means of the floating zone method. Crystals were crushed in mortar and dispersed in methyl alcohol. Thin fragment floating in the alcohol were put on microgrids for electron microscopy.

The electron diffraction patterns were taken with the JEM-2000ex electron microscope. The electron microscopic images were also taken with the H1250 electron microscope.

[Results and Discussion]

Figure 1 shows the electron diffraction patterns of Ho_3TaO_7 at a) $[1\bar{1}0]$ b) $[11\bar{2}]$ and c) $[33\bar{2}]$ incidences. Diffuse circle were observed between the fundamental reflections of the fluorite-type structure. Similar diffuse circles were observed in patterns from Y_3TaO_7 and Yb_3TaO_7 . Figure 2 illustrates the loci of diffuse circles. From Fig. 2, it is found that the diffuse circles are divided into two types: one has its plane-normal parallel to $\langle 233 \rangle$ and the other parallel to $\langle 211 \rangle$.

A distorted lattice image was observed by the high resolution electron microscopy.

1) J. G. Allpress and H. J. Rossel., J. Solid State Chem., 27 105 1979

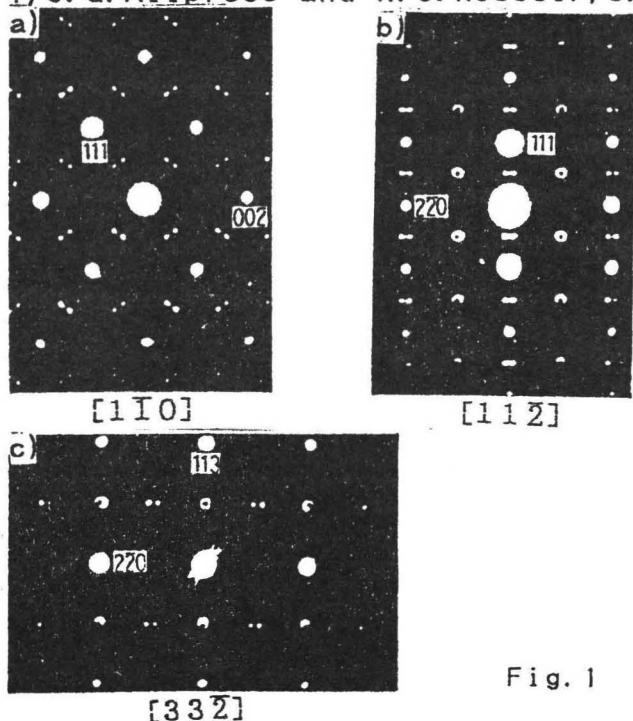


Fig. 1

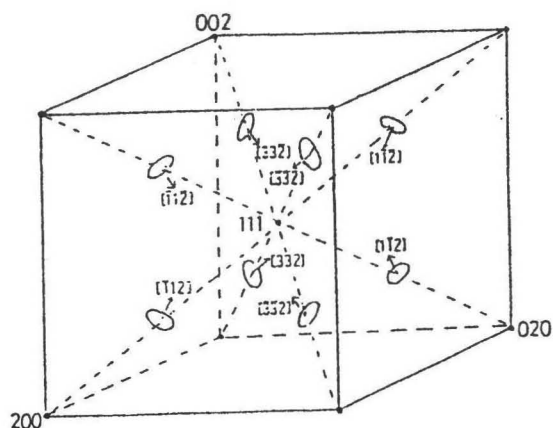
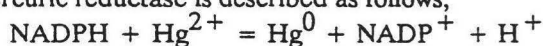


Fig. 2

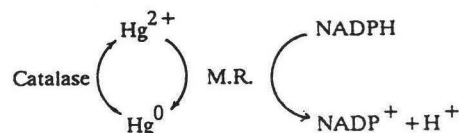
Mercuric Sensor with Immobilized Mercuric Reductase on Porous Glass

Motohiro Uo, Masahiko Numata^{*}, Eiichi Tamiya^{**}, Isao Karube^{**}, Akio Makishima

The porous glass is useful for career of enzymes and microbes because of its chemical and thermal durability and controllability of micro-structure. In this investigation, the mercuric reductase (NADPH-Hg(II) oxido-reductase) and catalase were immobilized on porous glass and mercuric sensor was prepared. The reaction of mercuric reductase is described as follows;



The enzymatic cycling reaction with mercuric reductase and catalase is used for high-sensitive measurement of mercuric ion(II). As Scheme 1, reduced mercury(0) is reoxidized to mercuric ion(II) by catalase and reduced by mercuric reductase again. Thus, with this enzymatic cycling reaction, higher amount of NADPH is oxidized than in the case of without catalase.



Scheme 1 The enzymatic cycling reaction

[Materials and Methods] Porous glass were prepared from chlorine containing $10\text{Na}_2\text{O}-50\text{B}_2\text{O}_3-40\text{Si}_2\text{O}$ system by heat treatment and leaching with hot water and enzymes were immobilized on the arylamino derivative of porous glasses. The mercuric reductase was purified from E.coli transformant. Concentration of NADPH was determined by measurement of fluorescence intensity.(Excitation = 340nm, Emission = 470nm) The diagram of flow system is shown in Fig.1.

[Results] The relationship between the decrease of fluorescence intensity and concentration of mercuric ion(II) is shown in Fig.2. In the case of only immobilizing mercuric reductase, linear relation was found in the range of Hg concentration from $0.3\ \mu\text{M}$ to $5\ \mu\text{M}$ and the lower limit of mercuric measuring was found to $0.3\ \mu\text{M}$ (60ppb). In the case of enzymatic cycling reaction, the lower limit advanced up to $0.1\ \mu\text{M}$ (20ppb).

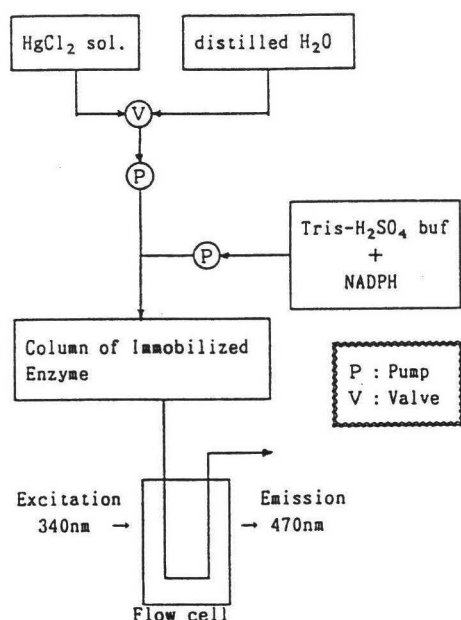


Fig.1 Schematic diagram of mercuric sensor

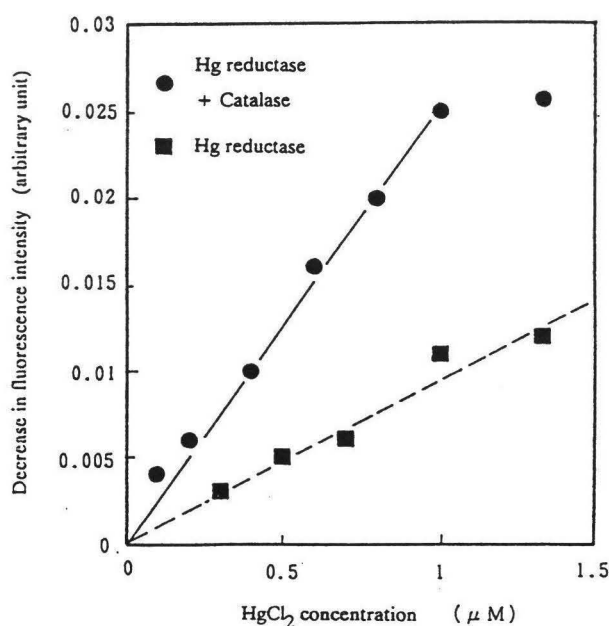


Fig.2 Relationship between HgCl_2 concentration and decrease in fluorescence intensity

Department of Materials Science, Faculty of Engineering, University of Tokyo

^{*} Central Research Lab. Dowa Mining Co.,Ltd.

^{**} Research Center for Advanced Science and Technology (RCAST), University of Tokyo

A Theoretical Estimation of Ceramic Strength at High Temperatures

Jian-ren Zeng and Koichi Niihara
ISIR, Osaka University

Grain boundaries exist in all polycrystalline ceramics. The grain boundary phase is, in the liquid phase sintering, a glass which promotes densification during sintering, but enhances creep or causes slow-crack-growth failure when the ceramic is stressed at a temperature above the glass transition temperature of the grain boundary phase. Therefore, it is of paramount importance to understand the delayed fracture behavior since most structural ceramics are designed for uses at temperatures above the glass transition temperature of the intergranular glass phase (the highest glass transition temperature of oxide glass is considered to be that of silica of about 1200 °C).

In the existing models describing the high temperature failure of ceramics containing small amounts of a glass phase, the growth of voids from preexisting cavities of nano-order size or from the cavities newly nucleated ahead a crack is assumed to be an important step for the sub-critical crack propagation. However, neither assumption is convincing, because the assumption of preexisting cavities lacks theoretical ground and experimental confirmation, while that of cavity nucleation because of stress concentration due to grain boundary sliding is contrary to the viscous flow of the glass phase.

Therefore, based on the theory of liquid adhesive, we propose an alternative fracture model for ceramics with a viscous grain boundary. Different from the existing models, the numerous grain boundaries present at the free surface of a ceramic is considered as a cavity network. The grain boundary sliding is supposed to be inhibited by the geometrical restrictions of the grain boundaries, then the applied stress has to overcome the capillary force generated at the free surface in order to cause grain boundary separation. The existence of a maximum in the capillary force leads to the possibility of predicting the theoretical strength of a ceramic at high temperatures. This theoretical strength can be basically evaluated from the thickness and surface energy of the intergranular glass phase and the contact angle between the glass phase and the matrix grains. We applied this new theory to silicon nitride ceramics and obtained a fairly good agreement between the calculated high-temperature safe-operating stress and the experimental stress in literature.

Preparation of wollastonite powder by co-precipitation method

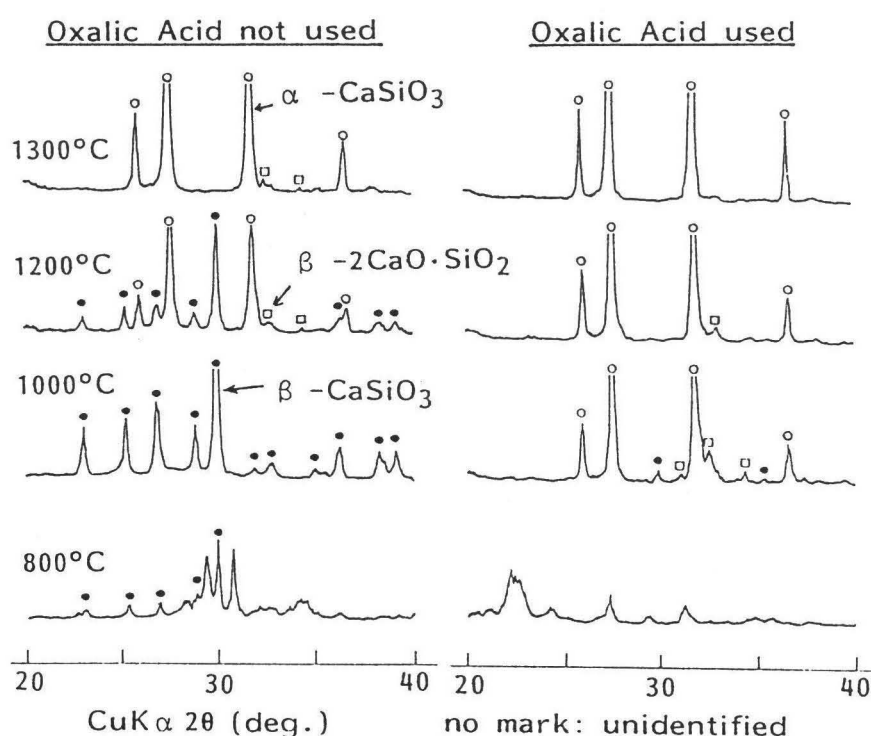
○ Shigeo Hayashi, Kiyoshi Okada, Nozomu Otsuka

Faculty of Engineering, Tokyo Institute of Technology

Wollastonite, CaSiO_3 , is used as the filler of paper or resin, the additive to porcelain, and the raw material of high-frequency ceramic insulator. Since high temperature firing is necessary for its synthesis by the conventional solid-state reaction, it is desirable to develop another kind of synthesis methods. The validity of the co-precipitation method in the synthesis of wollastonite was, therefore, examined by changing the co-precipitation conditions.

Equimolar ratio of calcium nitrate and tetraethyl orthosilicate were dissolved in ethyl alcohol. After 2 hours mixing, co-precipitates were prepared by two different way; (1) adding 25% ammonium hydroxide and (2) adding the solution of oxalic acid before the method (1). These two co-precipitates were dried, and calcined at 500°C . Their thermal properties were measured by a DTA, and crystalline phase change was measured by an XRD. Synthesized wollastonite powders were observed by a SEM, and the particle size distributions were measured by a laser scattering method.

In the powder (1), $\beta\text{-CaSiO}_3$ appeared at 800°C , and transformed to $\alpha\text{-CaSiO}_3$ at about 1200°C . On the other hand, α -phase appeared at 1000°C instead of β -phase in the powder (2). Both powders have very fine primary particles under $1\mu\text{m}$ in diameter, but tend to form agglomerates in several microns.



X-ray diffraction patterns of samples

Design and Evaluation of Materials for Controlling the Differentiation of Hepatocytes

Akira Kobayashi¹, Yuka Takei¹, Seishiro Tobe¹, Mitsuaki Goto¹, Takuji Sekine², Aki. Masumoto³, Noboru. Yamamoto³, Kazukiyo Kobayashi⁴, Toshihiro Akaike^{1,5}

1. Kanagawa Academy of Science and Technology, Takatsu-ku, Kanagawa 213

2. Tokyo University of Agr. and Tech. , Koganei-shi, Tokyo 184

3. Kitazato University, Sagamihara-shi, Kanagawa 228

4. Nagoya University, Nagoya-shi, Aichi 464

5. Tokyo Institute of Tech., Midori-ku, Kanagawa 227

We have been actively examining the interaction between oligosaccharide-carrying styrene homopolymer (PVLA) and hepatocytes in an attempt to create an hybrid artificial liver.(1) The lactose moiety on the PVLA mimics the function of an asialoglyco-protein and interacts with the receptor on the surface of the hepatocyte results in stimulating the cell cultured on this substratum to retain liver-specific functions.(2) The factors that cause the hepatocytes to maintain their differentiated functions have been unknown. In this study, the effects of the coated PVLA concentration on the ³H-thymidine uptake, the morphology and the liver specific functions of the attached hepatocytes were examined.

The isolated hepatocytes were precultured on polymer coated plates for 20hrs to allow maximum attachment of the hepatocytes to the substratum followed by incubation with ³H-thymidine for 17hrs. The

uptake of ^3H -thymidine during this period was assumed to be the level of DNA synthesis of the hepatocytes after attachment. The DNA synthesis of hepatocytes after attachment to culture plates coated with different concentrations of PVLA were examined.

Our results suggest that DNA synthesis in cultured hepatocytes is correlated to the cell-shape which could be controlled by the concentration of PVLA substratum. Since PVLA at low concentrations take on spread shapes and at high concentration take on micelle-forms on the polystyrene culture dishes(3), it is possible that hepatocytes recognized the delicate structure of these coated surfaces and adhere in forms which mimics the shapes of PVLA on the culture dishes. Our results also suggest that the PVLA could potentiate the control in the differentiation and dedifferentiation of hepatocytes.

References:

- 1) A. Kobayashi, T. Akaike, K. Kobayashi, H. Sumitomo, Makromol. Chem. Rapid Commun., 7, 645(1986)
- 2) T. Akaike, A. Kobayashi, K. Kobayashi, H. Sumitomo, J. Bioactive Biocompatible Polym., 4, 51(1989)
- 3) T. Takayama, K. Kobayashi, T. Matsuda, T. Akaike, Seitai Zairyou, 8, No.3, pp.122-128(1990)

Mn-Substituted Giant Magnetostrictive RFe_2 and Its Application.

T. Kobayashi, T. Funayama, I. Sakai, and M. Sahashi

R & D Center, Toshiba Corporation, Komukai, Kawasaki 210, Japan

Intermetallic compounds with a cubic laves phase structure of the type RFe_2 ($R=Tb, Dy$) exhibit high magnetostriction of the order 10^{-3} , but suffer from greatly degraded magnetostriction at low temperature due to spin reorientation from $[111]$ to $[100]$.

We have investigated the effects of transition metals on the magnetocrystalline anisotropy of RFe_2 in $Dy(Fe_{1-y}M_y)_2$ and $Tb_xDy_{1-x}(Fe_{1-y}M_y)_2$ ($M=Ni, Co, Mn$).

In Mn substituted RFe_2 , and especially in samples of $Tb_{0.5}Dy_{0.5}(Fe_{0.9}Mn_{0.1})_2$, a maximum magnetostriction of over 10^{-3} has been observed with an applied field of only 2kOe. It has been also found that Mn substitution suppresses the spin reorientation phenomenon observed with free Mn, and which causes drastic deterioration of its magnetostriction. Detailed study has revealed that Mn located in the transition metal sites, which form a tetrahedron, strongly affects the magnetocrystalline anisotropy through spin frustration due to antiferromagnetic coupling of Mn and ferromagnetic coupling of Fe.

This effect results in the low magnetocrystalline anisotropy and the observed suppression of spin reorientation in $Tb_{0.5}Dy_{0.5}(Fe_{0.9}Mn_{0.1})_2$.

This newly developed material is not limited to applications such as various small, high-power actuators to replace piezoelectric materials PZT, but should also lead to new devices such as positioners, and acoustic transducers.

One example of an application is the micropositioning system using $Tb_{0.5}Dy_{0.5}(Fe_{0.9}Mn_{0.1})_2$ which has been developed. Displacement can be controlled to within the order of 10 nanometers.

PHOTOELECTROCHEMICAL INFORMATION RECORDING USING THE NEWLY-FOUND
HYBRID PROCESS OF AZOBENZENE SYSTEM

Zhong-Fan Liu, Kazuhito Hashimoto, and Akira Fujishima
Department of Synthetic Chemistry, Faculty of Engineering,
The University of Tokyo, Hongo, Tokyo 113

Photoelectrochemical behavior of azo compounds in LB films was studied. A novel clockwise hybrid phenomenon was obtained due to two experimental observations: the first is that the cis isomer of the azo molecule used is more easily reduced to a hydrazo species than the trans isomer; the second is that the hydrazo molecule subsequently produced is exclusively oxidized to the trans isomer. On the basis of this unique hybrid effect, a new "photon-mode" information storage system is proposed.

In this storage system, the hydra molecule is used as the "storage state" for information instead of the thermally unstable cis isomer. Two kinds of recording schemes, either "optical writing" or "electrochemical writing", are available. For the "optical writing", a high-density storage is obtained using a fine-beam laser to induce a local trans to cis isomerization, followed by switching the potential of the entire storage film to a region where the cis isomer is reduced but not the trans isomer. A high-density "electrochemical writing" is, on the other hand, obtained by controlling the reduction area of cis state film after a uniform UV irradiation of the entire film. This becomes possible, using a sharp glass-coated probe as the counter electrode, with the distance between the probe and the storage film-modified electrode being controlled. A submicron level of recording is expected for both recording modes, and especially for the "electrochemical writing", over 10^{12} bits/cm² of storage density is principally possible even without utilizing the frequency domain of light. For reading out of information, an optical method is available. Since the information-recording process consists of two reaction steps, i.e., the photochemical isomerization and the electrochemical reduction, the optical readout operation will not destroy the information stored.

Moreover, the "3-state" feature of the present system may allow a multi-function memory to be realized since the metastable cis state can be used for "short-term" storage, and the hydra state for "long-term" storage.

IMPROVEMENTS OF MECHANICAL PROPERTIES FOR $\text{Al}_2\text{O}_3/\text{SiC}$ NANOCOMPOSITE

Atsushi Nakahira and Koichi Niihara
 Institute of Scientific and Industrial Research,
 Osaka University
 8-1 Mihogaoka, Ibaraki, 567, Osaka, Japan.

Al_2O_3 ceramic is a promising material as structural applications due to the good wear resistance, good chemical inertness, good sinterability and low cost. However its wide uses have been limited by relatively low fracture toughness and strength, poor thermal shock and creep resistances and relatively low reliability. Therefore, many attempts have been made to resolve these problems by developing microstructures and/or by dispersing the second phases. But the significant improvements of mechanical properties were not achieved yet. For these couple years, thus, we have been attempting to improve the mechanical properties by dispersing the nano-size SiC particles into the matrix Al_2O_3 grains.

$\text{Al}_2\text{O}_3/\text{SiC}$ nanocomposites were successfully prepared by the conventional sintering technique. The key conditions to fabricate the nanocomposites by sintering are to select the finer starting powders to make the homogeneous dispersions of SiC into Al_2O_3 and choose the optimum sintering temperatures. Transmission electron microscopic observations of this Al_2O_3 composites indicated that the nanometer-size SiC particles were predominantly within Al_2O_3 matrix grains when the volume fraction of dispersion was less than 33vol%. The striking finding in this $\text{Al}_2\text{O}_3/\text{SiC}$ nanocomposites is that the fracture strength of monolithic Al_2O_3 was approximately 3 times increased by the nanometer-scale particulate reinforcement: 390MPa to 1050MPa as shown in Fig.1. This extremely high fracture strength was also kept even up to 1200 C. Furthermore, the high fracture strength was improved to approximately 1550MPa by annealing the $\text{Al}_2\text{O}_3/\text{SiC}$ nanocomposite in Air or Ar atmosphere at 1000 to 1300C for 1hr. Weibull modulus of $\text{Al}_2\text{O}_3/\text{SiC}$ nanocomposite was also greatly increased by this annealing treatment. The roles of nano-size SiC dispersions were made clear by investigating the relation between the nanostructure within the Al_2O_3 matrix grains and the mechanical properties.

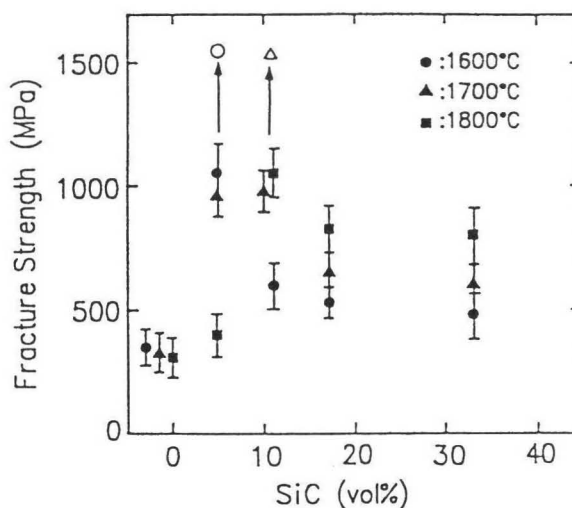


Fig.1 Effects of SiC content on fracture strength for $\text{Al}_2\text{O}_3/\text{SiC}$ nanocomposite.

Electroluminescent Behavior of 2,5-Distyrylpyrazine Derivatives

Masao Nohara, Masaki Hasegawa, Chishio Hosokawa,* Hiroshi Tokailin,* and Tadashi Kusumoto*

Department of Synthetic Chemistry, Faculty of Engineering, The University of Tokyo

*IDEMITSU KOSAN Co., Ltd., Central Research Laboratories, Material Physics Laboratory

2,5-Distyrylpyrazine (DSP) is one of the most famous monomers for the four-center type photopolymerization, which proceeds by repeating the [2+2] photocyclodimerization in the crystalline state.

In the course of study on the photoreaction of DSP derivative crystals, we found a new series of promising compounds for electroluminescent (EL) devices, such as 2,5-bis[2-(1-naphthyl)vinyl]pyrazine (BNVP) and 2,5-bis[2-(1-pyrenyl)vinyl]pyrazine (BPVP). All these EL crystals were photostable, and photostable property was reasonably explained by their crystal structure.

Light emission was observed on these compounds under the forward dc bias with the positive voltage on the ITO electrode. The EL cell composed with BNVP, emitted visible yellow luminance attained to high brightness level (360 cd/m^2) at the current of 68.7 mA/cm^2 . The luminous efficiency was estimated to be 0.16 lm/W . The luminance and the current increased to 932 cd/m^2 and 213 mA/cm^2 , respectively with increasing applied voltage at to 12 V. In the case of BPVP, the luminance attained to 1005 cd/m^2 and visible orange lights were observed at the 9.5 V. By the measurement of the current-voltage (I-V) characteristics, the current was found to be proportional to V^2 in the low voltage range below 2 V and proportional to V^9 in the range between 2 V and 12 V. The luminance was found to be proportional to I in high current range above 3 mA/cm^2 . In the low current range between 0.09 and 3 mA/cm^2 , the luminance was proportional to $I^{1.3}$.

Mechanical Properties and Microstructure of Boride Based Composite Ceramics.

Toray Industries Inc. Tomohiko Ogata, Hiroshi Kuwajima

1. Introduction

Recently TiB_2 or ZrB_2 based ceramics are drawing attention as the electrode and heating materials¹⁾ that offer both high melting point and same electric conductivity as some metals. Furthermore, those materials are expected as cutting tools and engineering materials²⁾ for high temperature use because of their high hardness and high heat conductivity.

For the present study, some mechanical properties and microstructure on densified bodies by hot pressing are reported.

2. Experimental Procedure

Boride powders (TiB_2 and ZrB_2), some carbide powders (SiC , B_4C , TiC and ZrC) and SiC whisker were obtained from H.C.Starck Berlin, Japan New Metals Co. Ltd. and Tokai Carbon Co. Ltd., respectively.

Boride raw powders containing carbides and SiC whisker were mixed at pre-determined proportion, and then they were milled in ethyl alcohol. Finally the crushed powders, after had been dried by rotary evaporator, were sintered by hot pressing.

The test specimens were cut from as-sintered material, and then density, bend strength, Vickers' hardness and fracture toughness were measured. And then secondary electron microscope (SEM) and transmission electron microscope (TEM) observation were examined on their microstructure.

3. Results and Discussion

The sintered body was porous and consisted of extremely large grains in case of boride single composition. The addition of carbides enhanced densification and inhibited grain growth of boride materials.

Above all, TiB_2/TiC composite shows excellent mechanical properties, and the grain boundary layer which suggested eutectic phase³⁾ were observed by TEM.

Furthermore, TiB_2/TiC system containing 10, 20 and 30vol% SiC whisker were prepared in order to enhance strength. In these cases it needed slightly higher temperature than that of without SiC whisker composition to densify. As a result, high densified microstructure without micropores was obtained.

Maximum strength exhibits 1140MPa at the composition of 56vol% TiB_2 /24vol% TiC /20vol% SiC whisker.

The result of SEM observation, needle-like shape of whisker couldn't be found in the microstructure. It would have been changed to complicated form⁴⁾ by boundary reaction during sintering. The mechanism of strengthening seemed to be mainly crack deflection since whisker pull-out were not observed.

1) R.Jinbou et al., Yogyo-Kyokai-Shi, 94 (1986) p224-228

2) K.Mannami et al., ibid., 94 (1986) p214-223

3) E.Nold et al., Fresenius Z Anal Chem., (1989) 333: 492-497

4) A.Kamiya et al., J. Mater. Sci. Lett., 8 (1989) 566-568

ホウ化物系複合セラミックスの微細組織と機械的性質

東レ株式会社 高分子研究所 尾形知彦、桑島宏

1. 緒言

近年、ホウ化物系セラミックスが注目され始めている。ホウ化物は高融点材料であり、金属なみの電気伝導性を有することから電極材料、発熱体などの用途¹⁾が開かれ、また高硬度で熱伝導性が優れていることから切削工具をはじめとする高温構造物材料²⁾として期待されている。本研究では、 ZrB_2 、 TiB_2 について炭化物の複合化により緻密なホットプレス焼結体を得、機械的性質やSEMによる微細組織観察を行った結果について報告する。

2. 実験方法

原料として、 ZrB_2 、 TiB_2 粉末 (H. C. スタルク製) および複合化するSiC、TiC、 B_4C 、ZrC粉末 (日本新金属製) とSiCウイスキー (東海カーボン製) を用いた。原料のホウ化物粉末、炭化物粉末およびSiCウイスキーを所定の割合で調合し、エタノール中ボールミルにて粉碎後、ロータリエバポレータにて減圧乾燥して複合粉末を得る。混合粉末は、真空ホットプレスにより焼結する。得られた焼結体について、密度、曲げ強度、ビッカース硬度、破壊靱性 (MI法) を測定した。また組織観察には、SEMおよびTEMを用いて行った。

3. 結果と考察

ZrB_2 、 TiB_2 のホウ化物単相の焼結では多孔質となり、粒径も極めて大きい、種々の炭化物を複合することによって、ほぼ気孔のない緻密でかつ微細粒子からなる焼結体組織が得られた。とりわけ TiB_2 /TiC系は、機械的性質の優れた値を示し、TEMによる組織観察では、中間化合物³⁾と思われる粒界相の存在が確認された。この系について、さらにSiCウイスキーをそれぞれ10、20、30体積%複合したものを調整し、強度の向上をはかった。ウイスキーを用いることによって、緻密化のために焼結温度は無添加の場合に比べ若干高い温度を要したが、ミクロポアのない高密度焼結体を得られた。56vol% TiB_2 /24vol% TiC/20vol% SiCウイスキー組成の時、最高強度1140MPaを得た。

SEMによる組織観察の結果、ウイスキー複合系の焼結体組織の中には、もともとの形状である針状ウイスキーがほとんど見当たらず、高温での焼結中にマトリックスとの界面反応によって変形し、柱状化や球状化が起こった⁴⁾と思われる。このためウイスキーの引抜きも観察されなかったが、強化は主としてクラック偏向によると考えられる。

1) R.Jinbou et al., *Yogyo-Kyokai-Shi*, 94 (1986) p224-228

2) K.Mannami et al., *ibid.*, 94 (1986) p214-223

3) E.Nold et al., *Fresenius Z Anal Chem.*, (1989) 333: 492-497

4) A.Kamiya et al., *J. Mater. Sci. Lett.*, 8 (1989) 566-568

**The mechanism of molecular recognition by β -Cyclodextrin
- Application of molecular dynamics simulation to the design of
molecular recognition materials-**

H. Okazaki, T. Yamashita, T. Yasukawa, and T. Akaike

Kanagawa Academy of Science and Technology, KSP 100-1 Sakado
Takatsu-ku Kawasaki-shi Kanagawa-ken. 213 Japan

The chemistry of complex formation between Cyclodextrin(CD) and guest molecules have been well studied. Understanding how this complex is formed is applicable to basic studies of artificial receptors or enzymes. We studied the dynamic processes, and relative changes in binding free energy during the complex formation between β -cyclodextrin (CD) and D- or L-methyl mandelate(MMA) in gas phase and in aqueous solution by means of molecular dynamics simulation and thermodynamic perturbation method.

Molecular dynamics simulations were carried out with NPT ensemble on 169 atoms and about 400 water atoms, at 1 bar, 300 K with 10 psec for equilibration and 10 psec for data collection. The time dependent potential energies of both CD:D-MMA and CD:L-MMA complex did not show meaningful difference between gas phase and aqueous solution. By calculating atom-atom interactions between CD and D(L)-MMA, it was found that oxygen atoms attached to C4 and C6 on each glucose subunit of CD make stronger attractive interaction with the hydrogen atom of the hydroxyl group and carbon atom of the carboxyl group of MMA than other oxygens on CD. While, oxygen atom of hydroxyl group and oxygen atom of carboxyl group on MMA make strong repulsive interactions with oxygen atoms attached to C4 and C6 of CD.

The calculated difference in the free energy of CD:D-MMA complex and CD:L-MMA complex was -2.60 Kcal/mol in the gas phase and -9.43 kcal/mol in the aqueous solution. The resultant free energy in the aqueous solution was much larger than in the gas phase. This showed that CD had greater ability in distinguishing between D-MMA and L-MMA in aqueous solution than in gas phase due to hydrophobic effects.

PREPARATION OF NITROGEN-CONTAINING CELLULOSE DERIVATIVES
AND THEIR ADSORPTION BEHAVIOR OF HEAVY METAL IONS

Shigeo NAKAMURA, Masato AMANO, and Yasuo SAEGUSA

Department of Applied Chemistry, Faculty of Engineering,
Kanagawa University, Kanagawa-ku, Yokohama 221, JAPAN

Nitrogen-containing cellulose derivatives such as aminoalkylcelluloses (AmACs), hydrazinodeoxycellulose (HDC) and carboxyalkylhydrazinodeoxycelluloses (α - and β -CAHDCs) were prepared from 6-chlorodeoxycellulose (CDC) and their adsorption behavior of heavy metal ions from dilute aqueous solutions were studied in detail.

CDC with degree of substitution of 1 was directly prepared from cellulose using methanesulfonyl chloride in N,N-dimethylformamide (DMF)-chloral-pyridine. AmACs with different methylene length of diamine moieties were synthesized by the reaction of CDC with diamines such as ethylenediamine, tetramethylenediamine, hexamethylenediamine and octamethylenediamine in dimethyl sulfoxide (DMSO). HDC was obtained by reacting CDC with an excess amount of hydrazine hydrate. α - and β -CAHDCs were prepared by reacting CDC with α - and β -hydrazinopropionic acids in DMF or DMSO.

Adsorption of heavy metal ions was carried out by putting finely pulverized adsorbent powder into an aqueous solution containing 1 mmol/L of CuCl_2 , MnCl_2 , CoCl_2 and NiCl_2 , filtering the adsorbent after stirring for a predetermined period at ambient temperature and determining metal ions remaining in the solution.

Adsorption of heavy metal ions on AmACs occurred rapidly in weakly acidic solutions and increased with increasing pH. No adsorption, however, occurred in strongly acidic solutions. The amount of adsorbed ions decreased with increasing methylene length of diamine moieties of AmACs, and AmAC from ethylenediamine was most effective.

α -CAHDC adsorbed heavy metal ions more effectively than β -CAHDC. HDC scarcely adsorbed heavy metal ions in the pH range of 1 to 2, where α - and β -CAHDCs were effective. However, the adsorption of metal ions on HDC increased rapidly with increasing pH and HDC was more effective than α -CAHDC in weakly acidic solutions.

When these adsorbents were immersed in the solutions containing two metal ions, Cu^{2+} were selectively adsorbed. Irving-Williams order is obeyed in these adsorbent/heavy metal ion systems. The effectiveness of adsorption of Cu^{2+} was in the order of $\text{AmAC} \geq \text{HDC} > \alpha\text{-CAHDC} > \beta\text{-CAHDC}$, and AmAC from ethylenediamine was most effective and selective.

The metal ions adsorbed on AmAC from ethylenediamine were completely desorbed by treating with 0.1 M hydrochloric acid at room temperature for 2 h. After desorption of metal ions, these adsorbents effectively readsorbed metal ions.

Evaluation of the Zirconia Form as a Heating Element

Tsunenobu Saeki
Sinagawa Refractories Co. Ltd

It is well known that the partially stabilized zirconia form has oxygen ion lattice defects, and shows ion conductivity at high temperature. Therefore, it is utilized as a oxygen sensor and solid electrolyte in various fields.

The application of the zirconia form to the heating element was so many tried since ten years ago. However some important problems such as thermal spalling were pointed out, and zirconia heating element was not established.

We newly developed zirconia form as a high temperature heating element, and in order to evaluate the yttria doped zirconia form as a heating element, the electric resistance, heating properties by flowing current and the physical properties of the sintered body were investigated. This zirconia form shows stability as a a high temperature heating element, and a little physical change after heating test up to 2000°C by flowing current.

THE PROPERTIES OF R_3T COMPOUNDS
AS HEAT REGENERATOR MATRIX USED IN SMALL SIZE HELIUM REFRIGERATOR

Y. Tokai, A. Takahashi, and M. Sahashi
Toshiba R&D center, Kawasaki, Japan.

Conventional small refrigerators can refrigerate down to 10 or 20 K from room temperature, 300 K, and they are used as cooling units in cryopumps, MRI systems, and infrared sensors. The performance of the heat regenerator, one component of the refrigerator, governs cooling performance.

The lower limit on cooling is mainly due to the lack of specific heat at low temperatures. The specific heat of conventional regenerator matrixes, Pb and Cu, is dominated by lattice contribution to specific heat, which falls rapidly with decreasing temperature, since it is proportional to T^3 .

In looking for a larger specific heat at low temperature, the excess heat capacity due to entropy changes in magnetic ordering has been studied in rare earth compounds.

Some R_3T compounds (R :rare earth, T :Ni,Co), especially Er_3Ni , have a large excess heat capacity. The specific heat of Er_3Ni is comparable to that of Pb above 15 K and is far greater than Pb below 15 K.

We have succeeded in making spherical grains of Er_3Ni 0.2 to 0.3 mm in size. These spherical grains are durable enough to withstands thousands of hours of operation, while crushed grains of the same composition break down gradually given the same operating conditions.

The lowest temperature, in the 2 K range, was obtained by using the grains in a 2-stage GM-cycle refrigerator.

EPOXY MOLDING COUPOUND FOR ADVANCED SEMI-CONDUCTOR DEVICES

Stress Redution Technology with Silicone polymer

TAKASHI TSUCHIYA

Silicone-Electronics Materials Reserch center

Shin-Etsu Chemical Co.,LTD

1. Intoroduction

Epoxy resin is widely used in IC and LSI encapsulant. Plastic Encapsulation of large semi-conductor chips has resulted in increased stress-related failure. In an effort to minimize the stress problems, we have tried to lower a modulus by modifying the epoxy resin. As a result, Ultra low stress molding compound have been developed.

2. Reducing Stress Technology

An internal stress can be generally expressed by using the following equation.

E:modulus of elasticity of molding compound

Stress $\rho = K \int E \cdot \alpha \cdot dT$ α :coefficient of thermal expansion of molding compound

T:temperature K:constant

As gathered from the equation given above, it is necessary to decrease both the modulus of elasticity and the coefficient of thermal expansion of the molding compound to reduce stress.

2-1. Reducing the Modulus of Elasticity

A silicone polymer forms a two-phase structure(sea-island structure) in the epoxy matrix. Applying silicone, therefore, permits achievement of a lower modulus of elasticity without lowering the glass transition temperature(Fig.1)

2-2. Morphology Control

To disperse a silicone polymer in the epoxy matrix, the Block copolymer A of formula (1) can be obtained by reaction between the alkenyl group contained epoxy resin and the $\equiv\text{SiH}$ group contained organopolysiloxane, it is possible to controlled domain size of silicone polymer in the matrix to the submicron level by using Block copolymer A.

As shown in Figure 2, Stress characterstics are significantly dependent upon the domain size.

Block copolymer A

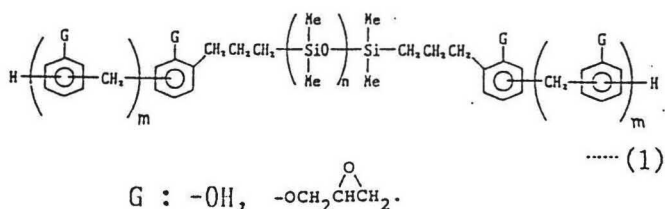
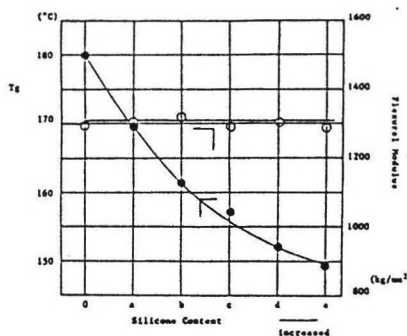
Fig. 1 T_g and Flexural Modulus VS Silicone Content

Fig. 2

